



CIVIL ENGINEERING STUDIES  
Illinois Center for Transportation Series No. 09-031  
UILU-ENG-2009-2001  
ISSN: 0197-9191

# DETERMINATION OF USABLE RESIDUAL ASPHALT BINDER IN RAP

Prepared By

**Imad L. Al-Qadi**  
**Samuel H. Carpenter**  
**Geoff Roberts**  
**Hasan Ozer**  
**Qazi Aurangzeb**

University of Illinois at Urbana-Champaign

**Mostafa Elseifi**  
Louisiana State University

**James Trepanier**  
Illinois Department of Transportation

Research Report ICT-09-031

**ICT-R27-11**  
**Determination of Usable Residual Asphalt Binder in RAP**

Illinois Center for Transportation

January 2009

# TECHNICAL REPORT DOCUMENTATION PAGE

1. Report No. FHWA-ICT-09-031		2. Government Accession No.		3. Recipient's Catalog No.	
4. Title and Subtitle Determination of Usable Residual Asphalt Binder in RAP				5. Report Date January 2009	
				6. Performing Organization Code	
7. Author(s) Imad L. Al-Qadi, Samuel H. Carpenter, Geoffrey L. Roberts, Hasan Ozer, Qazi Aurangzeb, Mostafa A. Elseifi, and James Trepanier				8. Performing Organization Report No. ICT-09-031 UILU-ENG-2009-2001	
				10. Work Unit (TR AIS)	
University of Illinois at Urbana-Champaign Department of Civil and Environmental Engineering 205 North Mathews Ave, MC 250 Urbana, Illinois 61801				11. Contract or Grant No. ICT-R27-11	
				13. Type of Report and Period Covered	
				14. Sponsoring Agency Code	
12. Sponsoring Agency Name and Address Illinois Department of Transportation Bureau of Material and Physical Research 126 East Ash Street Springfield, IL 62704					
15. Supplementary Notes Study was conducted in cooperation with the U.S. Department of Transportation, Federal Highway Administration					
16. Abstract <p>For current recycled mix designs, the Illinois Department of Transportation (IDOT) assumes 100% contribution of working binder from Recycled Asphalt Pavement (RAP) materials when added to Hot Mix Asphalt (HMA). However, it is unclear if this assumption is correct and whether some binder may potentially be acting as "black rock," and not participating in the blending process with the new binder. Furthermore, it is also unclear whether binder modifications should be considered in the mix design for recycled HMA. The goal of this research was to determine if the current IDOT mix design practice required modification with respect to the use of RAP.</p> <p>A set of mixtures was prepared using RAP in accordance with current practice. Additional sets were prepared using recovered binder and recovered aggregate to simulate the effect of RAP binder blending with virgin binder. Mixes containing 0, 20, and 40%RAP were prepared and the dynamic modulus testing results of these mixtures were compared to illustrate the effect of RAP on HMA. Tests on recovered, virgin, and blended binders were also conducted using the Dynamic Shear rheometer (DSR).</p> <p>This study found that up to 20% RAP in HMA does not require a change in binder grade. However, at 40% RAP in HMA, a binder grade bump at high temperature and possibly at low temperature is needed; more tests are required to verify the need for low temperature binder grade bumping. In addition, this study recommends RAP fractionation in the preparation of laboratory specimens.</p>					
17. Key Words Recycled Asphalt Pavement (RAP), Working Binder, Dynamic Modulus			18. Distribution Statement No restrictions. This document is available to the public through the National Technical Information Service, Springfield, Virginia 22161.		
19. Security Classif. (of this report) Unclassified		20. Security Classif. (of this page) Unclassified		21. No. of Pages	22. Price

## **ACKNOWLEDGMENT, DISCLAIMER, MANUFACTURERS' NAMES**

This publication is based on the results of ICT-R27-11, **Determination of Usable Residual Asphalt Binder in RAP**. ICT-R27-11 was conducted in cooperation with the Illinois Center for Transportation; the Illinois Department of Transportation, Division of Highways; and the U.S. Department of Transportation, Federal Highway Administration.

The contents of this report reflect the view of the authors, who are responsible for the facts and the accuracy of the data presented herein. The contents do not necessarily reflect the official views or policies of the Illinois Center for Transportation, the Illinois Department of Transportation, or the Federal Highway Administration. This report does not constitute a standard, specification, or regulation.

Trademark or manufacturers' names appear in this report only because they are considered essential to the object of this document and do not constitute an endorsement of product by the Federal Highway Administration, the Illinois Department of Transportation, or the Illinois Center for Transportation.

The input from the members of the Technical Review Panel (TRP) was extremely useful in the completion of this project and the interpretation of the results. The authors are grateful for their support. Members of the Technical Review Panel are the following:

Marvin Traylor, Illinois Asphalt Pavement Association  
Melvin Kirchler, Illinois Department of Transportation  
William Pine, Heritage Research  
Laura Shanley, Illinois Department of Transportation  
Tim Murphy, Murphy Pavement Technology  
Derek Parish, Illinois Department of Transportation  
Tom Zehr, Illinois Department of Transportation  
Amy Schutzbach, Illinois Department of Transportation  
Steve Gillen, Illinois Tollway

## EXECUTIVE SUMMARY

For current recycled mix designs, the Illinois Department of Transportation (IDOT) assumes 100% contribution of working binder from Recycled Asphalt Pavement (RAP) materials when added to Hot Mix Asphalt (HMA) mixes. However, it is unclear if this assumption is correct and whether some binder may potentially be acting as “black rock” and not participating in a blending process with the new binder. Furthermore, it is also unclear whether binder modifications should be considered in mix design for recycled HMA. The goal of this research was to determine if the current IDOT mix design practice required modification with respect to the use of RAP.

An innovative test program was developed to determine the amount of working binder occurring in HMA mixes containing RAP. A set of mixtures for testing purposes was prepared using RAP in a normal recycling manner. Additional sets were also prepared using recovered binder and recovered aggregate to simulate the effect of RAP binder blending with virgin binder. Blends of 0, 20, and 40 percent were prepared and the dynamic modulus of these mixtures was compared to illustrate the effect of RAP blending percentages. Tests on recovered, virgin, and blended binders were also conducted using the Dynamic Shear rheometer (DSR).

Limited fracture testing was conducted to determine how RAP percentages affect the thermal cracking properties of the HMA. Finally, scanning electron microscopy (SEM) was performed to determine if the blending effects of the virgin and RAP binder could be observed after the mixing process.

The dynamic modulus measurements did not provide a clear indication of the amount of working binder in RAP. This was due to selective absorption effects and changing aggregate structure which obscured the effect of the stiff binder. However, it was determined that from a mix design standpoint, the addition of RAP did not require any additional binder to achieve densities similar to HMA containing no RAP. The dynamic modulus testing showed that the stiff binder effect could be offset by modification of the binder grade.

The limited fracture energy testing at low temperatures found that the presence of RAP decreased the fracture energy of the HMA samples and thus indicated a lower thermal cracking resistance. The fracture testing also showed that the modification of binder type did not offset the RAP effect as was seen in the dynamic modulus testing. Finally, the SEM method was not able to visually identify binder blending locations, but a promising method was developed for future work.

This study recommends RAP fractionation in the preparation of laboratory specimens. When up to 20% RAP is used in HMA, binder grade does not need to be changed. The total amount of binder in the RAP should be considered as part of the binder content. The use of a PG 58-28 binder instead of a PG 64-22 binder, also known as “double bumping,” with 40% RAP content in HMA appeared to increase the level of binder blending. The addition of a softer binder allowed for the mixes to offset the increase in stiffness due to the presence of 40% RAP in the HMA. This study found that up to 20% RAP in HMA does not require a change in binder grade. However, at 40% RAP in HMA, double bumping the binder grade appears to be needed. Although preliminary tests suggested the potential need for low temperature binder grade bumping, more tests are required to verify that.

# CONTENTS

<b>TECHNICAL REPORT DOCUMENTATION PAGE .....</b>	<b>i</b>
<b>ACKNOWLEDGMENT, DISCLAIMER, MANUFACTURERS' NAMES .....</b>	<b>ii</b>
<b>EXECUTIVE SUMMARY .....</b>	<b>iii</b>
<b>CHAPTER 1 INTRODUCTION .....</b>	<b>1</b>
1. 1 BACKGROUND .....	1
1. 2 RESEARCH OBJECTIVES .....	2
1. 3 RESEARCH METHODOLOGY AND SCOPE .....	2
<b>CHAPTER 2 EXPERIMENTAL PROGRAM.....</b>	<b>4</b>
2. 1 MATERIALS .....	4
2.1.1 Binder and Aggregate Recovery .....	5
2.1.2 Rotovapor Extraction Method .....	6
2. 3 SPECIMEN SETS .....	8
2. 4 SPECIMEN PREPARATION.....	9
2.4.1 Laboratory Blending and RAP .....	9
2.4.2 Mixture Design .....	10
2.4.2.1 Aggregate Blend and Gradation.....	11
2.4.2.2 Mixture Design and Volumetrics.....	12
2.4.2.3 Blended Gradation Check .....	14
2.4.2.4 Test Specimens.....	17
2. 5 SPECIMEN CHARACTERIZATION .....	17
2.5.1 Dynamic Modulus Testing .....	17
2.5.2 Stripping Evaluation .....	19
2.5.3 Environmental Scanning Electron Microscope Approach .....	19
2.5.4 Fracture Characterization.....	20
<b>CHAPTER 3 RESULTS AND ANALYSIS .....</b>	<b>22</b>
3. 1 DYNAMIC MODULUS TEST RESULTS.....	22
3.1.1 District 1 HMA with 20% RAP Scenario .....	22
3.1.2 District 1 Mix with 40% RAP scenario .....	24
3.1.3 Comparison of District 1- 0, 20, and 40% RAP Cases .....	26
3.1.4 Statistics and Goodness of Dynamic Modulus Data .....	27
3.1.5 District 4 Mix 20% RAP Scenario .....	27
3.1.6 District 4 Mix with 40% RAP Scenario.....	30
3.1.7 Comparison of District 4 HMA with 0, 20, and 40% RAP .....	31
3.1.8 Statistics of HMA Dynamic Modulus Data (District 4) .....	33
3.1.9 Comparison of Mixes Prepared with PG58-28 and PG64-22.....	33
3.1.10 Statistical Analysis of HMA Dynamic Modulus Results .....	35
3.1.11 Application of Hirsch Model to RAP Mixture Volumetrics.....	39
3. 2 RESIDUAL BINDER EVALUATION.....	41
3. 3 EVALUATION OF STRIPPING SUSCEPTIBILITY .....	43
3. 4 RAP PARTICLE-MASTIC BONDING AND BLENDING: ESEM ANALYSIS .....	46
3. 5 FRACTURE ENERGY ANALYSIS.....	55
<b>CHAPTER 4 SUMMARY AND CONCLUSIONS.....</b>	<b>59</b>

<b>CHAPTER 5 RECOMMENDATIONS .....</b>	<b>62</b>
<b>REFERENCES.....</b>	<b>63</b>
<b>APPENDIX A BATCHING EXAMPLES FOR MIXES WITH RAP .....</b>	<b>A-1</b>
<b>APPENDIX B MIXTURE DESIGN .....</b>	<b>A-6</b>
<b>APPENDIX C COMPLEX MODULUS TEST DATA STATISTICS .....</b>	<b>A-17</b>
<b>APPENDIX D MOISTURE SUSCEPTIBILITY TESTING DATA .....</b>	<b>A-28</b>

# CHAPTER 1 INTRODUCTION

## 1. 1 BACKGROUND

In recent years the use of reclaimed asphalt pavement (RAP) in new hot-mix asphalt (HMA) pavement construction has become more widespread. The use of RAP is desirable to both contactors and agencies due to the recognized cost savings in a recycling operation. Cost savings increase as higher RAP percentages are being used. However, physical changes due to the addition of high RAP percentages can pose a challenging mix design problem and significantly affect the HMA performance. One potential physical change between a virgin HMA pavement and a HMA pavement containing RAP materials is the modulus increase of the latter. The increased modulus is mainly due to the effect of the RAP's binder. The increased dynamic modulus may be affected by the increased amount of RAP material passing the #200 sieve. The binder in RAP materials is significantly stiffer than the binder in virgin HMA (Kemp and Predoehl 1981). In addition to the standard aging during construction and normal service life, the binder tends to exhibit an increase in modulus when the pavement is excessively damaged, especially due to cracking, because of the relatively higher exposure to the environment (Smiljanic et al. 1993). Once a pavement is reclaimed, RAP aging continues during the stockpiling process due to air exposure and further oxidation (McMillian and Palsat 1985). As part of this study, a literature review was published in March 2007 as *Reclaimed Asphalt Pavement – A Literature Review* (Al-Qadi et al. 2007), ([www.ict.uiuc.edu](http://www.ict.uiuc.edu)).

Once a specific RAP material is selected for use in HMA, the effect of high stiffness binder on HMA properties must also be taken into account. The designer must first determine the amount of RAP materials to be used in the HMA. It has been found that low percentages of RAP in the mix (up to 20% by mix total weight) had little to no effect on the blend of virgin and RAP binder (Kennedy et al. 1998). However, when an intermediate or high amount of RAP is used, the effect of the RAP binder on the mix properties becomes significant and ultimately may even require changing the grade of the binder added to the mix.

To determine the effect of the RAP binder on the overall mix binder properties, it is crucial to first determine the amount of blending that occurs between the RAP and virgin binder. Assuming that full blending occurs, it becomes necessary to modify the PG grade of the virgin binder to account for the possibility of high RAP binder stiffness; especially at higher RAP percentages. However, if no blending occurs, (i.e. the binder is behaving as a "black rock"), it is unnecessary for the designer to alter the PG grade of the virgin binder; hence, there is no "credit" for the RAP binder. This behavior would require the designer to add more virgin binder in order to achieve a proper mix design, ultimately decreasing the cost effectiveness of the recycling operation.

Currently, the Illinois Department of Transportation (IDOT) assumes that full blending occurs. Depending on the actual amount of blending in the mix versus the assumed amount, the resultant mix could differ compared to that of HMA with virgin materials. This would result from using the wrong PG grade or too little/much asphalt binder in the mix, and poor quality HMA may be produced. Thus, an accurate determination of the binder blending is required to ensure quality pavements containing RAP materials.

Previous research has investigated the amount of blending that occurs between RAP and virgin binder. The NCHRP 9-12 study (McDaniel et al., 2000) found that at 10% RAP, the black rock (0% blending), total blending (100%), and actual practice were not significantly different. Conversely, when mixes contain 40% RAP, the black rock case was significantly different from the actual practice and total blending case. This indicates that

partial blending of binder occurs and may need to be accounted for when 40% RAP is used. Some degree of blending is likely occurring in mixes with 10% RAP; but the effect is not as significant because of the low binder amount. Hence, no special considerations are needed for mixes with 10% RAP.

A study conducted by Huang et al. (2005) found that when heated RAP was mixed with only virgin aggregates and no virgin binder was added, 11% mixing occurred only due to mechanical mixing. However, this study only used RAP material that passed the No. 4 sieve, and virgin materials retained on the No. 4 sieve. It should also be noted that the study allowed for longer than standard mixing time and above standard temperatures as well. These conditions make it unlikely that 11% blending can be assumed. In the same study, Huang et al. (2005) investigated the amount of blending that occurred with RAP during mixing with virgin binder and aggregates. Extractions were performed on the mixed materials and it was found that the binder at the outer edges of the RAP material was softer than the binder closer to the aggregates. This indicates that blending begins at the outer edges of the RAP particles and moves inward, but because of time and condition dependency, blending was not even and thus incomplete.

It is evident that complete binder blending may not occur; but the actual binder blending is not known either. One approach that may be useful in investigating the amount of RAP's binder blending is capturing images of the mix using the Scanning Electron Microscope (SEM). The SEM allows the evaluation of the mixture structure at the micro-level, which may provide indications of binder blending mechanisms. Therefore, the SEM was used in the study to investigate the surface morphology of HMA. The use of the SEM may depict a visible difference between the RAP and virgin binders. The SEM images may be firstly used to observe if blending is occurring and secondly to determine if interactions may occur at a microscopic level between virgin and RAP materials.

## **1. 2 RESEARCH OBJECTIVES**

The objective of this research was to demonstrate the ability to characterize the amount of binder contribution of RAP materials during the mixing process. The desired outcome of the research was to develop a procedure to determine the amount of blending occurring in a recycled mix that could be readily implemented into the mix design procedure. In addition, the research project would define the effect of RAP on HMA properties.

## **1. 3 RESEARCH METHODOLOGY AND SCOPE**

In order to determine the amount of working RAP binder in a mix and the contribution of RAP to overall mixture behavior, an experimental program was developed. The experimental program was designed to allow the amount of working RAP binder to be easily determined by comparing mixes containing normally added RAP to those specifically prepared with a prescribed amount of working stiff RAP binder combined with the virgin binder. The HMA dynamic modulus was then used to evaluate the effect of blending.

In this study, mixtures containing 0, 20%, and 40% RAP added to the HMA were considered. Six different job mix formulae (JMF) were designed for the various blends of RAP. These mixes were prepared in accordance with the current IDOT specifications using aggregates from two IDOT districts and two RAP sources, each at 0%, 20% and 40% content in the HMA. Specimens, prepared with recovered RAP materials (binder and aggregate) to evaluate the effect of stiff binder/virgin binder combinations, were compared to actual practice mixtures. The HMA designs with 20% and 40% RAP included four various sets of specimens whereas the HMA design with 0% RAP had only one set of specimens:

- Set 1 - Actual RAP used with the assumption of 100% binder mobilization (current IDOT assumption)
- Set 2 - Recovered aggregates and no recovered binder used to replicate 0% binder mobilization (black rock assumption)
- Set 3 - Recovered aggregates and recovered binder used to replicate 50% binder mobilization
- Set 4 - Recovered aggregates and recovered binder used to replicate 100% binder mobilization

Of the four sets, only the first set used actual RAP materials. The remaining three sets, treated as specimens for comparison, used recovered aggregates and binders utilizing an extraction process. These sets were designed to simulate various scenarios of precisely controlled blending of recovered RAP binder and virgin binder. The sets were used for comparison with actual practice mixes where the amount of working binder is unknown.

The first aim of the research was to investigate the effect of RAP on the mixture design process, involving mixing and compaction. The impact of RAP on this process has important practical implications. The current practice of increased amounts of RAP in the mixtures raises many questions regarding the batching and mixing processes. Residual or working binder evaluation is of utmost importance because the current practice assumes 100% working binder for mix design purposes. This research study focused on the mix design with special attention to the working binder assumption. The effect of increasing RAP on the mix design procedure was also investigated. The same procedures were conducted on the materials provided by both districts with their different JMFs in order to verify the consistency of the findings.

The second aspect of the experimental methodology involved dynamic modulus tests to differentiate between the stiffness of various mixtures. The HMA dynamic modulus test, using repeated compressive loads on cylindrical specimens, is currently used to determine HMA modulus for design and research purposes. It provides a suitable testing and analysis environment to investigate the effect of mixture components at various temperatures and frequencies. It was thought that the stiffening effect of RAP binder would be manifested clearly in the dynamic modulus results. Dynamic modulus testing results would allow differentiation between specimens prepared with precisely controlled blends of RAP binder and virgin binder and those prepared in accordance with actual practice (unknown blending).

In addition to the HMA dynamic modulus testing, binder complex shear modulus was also examined. The complex shear modulus,  $G^*$ , of the virgin, recovered, and blended binders were determined using a Dynamic Shear Rheometer (DSR). Extracted binders from the RAP sources used in this study were tested as well as blends with virgin PG 64-22 binder at 20% and 40% RAP binder. Virgin PG 64-22 grade binder was also tested to provide baseline data for comparisons of binder properties.

The amount of blending and interaction between the RAP and virgin materials was examined using a SEM at the microscopic level with the intent of showing the interaction of virgin and RAP materials. There are currently two types of SEM used: conventional SEM and environmental SEM (ESEM). The primary difference is that the conventional SEM requires a completely desiccated sample, a high working vacuum, and a metal coating for non-conductive specimens (such as HMA), while an ESEM can be used in "wet mode" to allow a non-conducting hydrated specimen to be placed directly into the instrument without additional preparation. However, if the observed non-conducting specimen is large, the resolution obtained from ESEM may not be as high as that obtained from conventional SEM. The image of the SEM or ESEM is from the surface or near surface since various energy

level electron beams can penetrate different depths depending on specimen type. Moreover, the resolution of the SEM or ESEM is dependent upon the combination of accelerating voltage, spot size, vapor pressure (when ESEM is used), and working distance.

Limited fracture energy tests of the evaluated HMA were conducted. The fracture energy tests were conducted to investigate the cause of “cracking” observed in SEM images. The results of fracture energy tests can provide a general idea about the effects of RAP on the thermal cracking potential of the tested HMA. The fracture energy was measured using both the Direct Compact Tension (DCT) test and the Semi Circular Bending (SCB) test. The tests were conducted using the one material source with 0%, 20%, and 40% RAP.

The final HMA characteristic evaluated was the stripping potential of HMA. This allows the determination of the effect of RAP on the HMA stripping susceptibility either positively or negatively. The stripping potential was measured in accordance with the Illinois modified AASHTO T-283-02 test.

The experimental program is presented in section 2, while the test analysis and results are presented in section 3. The summary and conclusions of this study can be found in section 4. Section 5 contains the recommendations that result from this study.

## **CHAPTER 2 EXPERIMENTAL PROGRAM**

The materials used in this investigation were provided by IDOT. Two aggregate types and two RAP sources were utilized in the study. The virgin aggregates were collected from sources from Districts 1 and 4. The binder used in this project was collected from one source by District 1. Two binder grades, PG 64-22 and PG 58-28, were used in this study. The PG 58-28 grade binder was used for mixing with selected HMA specimens containing 40% RAP to illustrate the impact of “double grade bumping” of the binder when a high percentage of RAP is used. Double grade bumping as defined here is accomplished by reducing both the high and low temperature grades available in the Performance Graded (PG) Binder System.

### **2. 1 MATERIALS**

Five aggregate sizes were obtained from District 1: 032CM16, 038FM20, 037FM02, 004MF01, and 017CM16. Four sizes were obtained from Thornton; while the 037FM02 was obtained from Edwardsburg. The 017CM16 served as the RAP material; while the other aggregates were virgin materials. The primary rock present in the RAP material was dolomite.

Four aggregates were collected from District 4: 032CM13, 038FM21, 037FM01, and 017CM13. The 004MF01, provided by District 1, was also used in the District 4 mixes due to the difficulty of obtaining this aggregate. 032CM13 and 038FM21 materials were collected from the Riverstone Group Inc. source; 037FM01 was collected from the Otter Creek S & G source; and 017CM13, the RAP source, was obtained from W.L. Miller. All of the aggregates from all sources were fractionated prior to mixing. The virgin aggregate and RAP materials were fractionated in an effort to ensure the quality control of specimen preparation. The District 4 RAP materials required processing in order to break down the agglomerations that were found in the materials provided.

The asphalt binder provided from District 1 was used in both District 1 and District 4 specimen preparations. The source of this binder was BP Amoco in Whiting, IN. The binder grades, as provided, are PG 64-22 and PG 58-28.

Aggregate bulk specific gravities,  $G_{sb}$ , were determined for each RAP fraction by IDOT's Bureau of Materials and Physical Research. Asphalt extractions were performed on each fraction of the RAP to determine the asphalt content of that fraction. These extractions were performed using the reflux method, while the rotovapor method was used for the extraction of binder and reclaiming aggregates that were used for mixing specimen sets. Average asphalt contents were determined from weighted averages of the fractioned aggregate weights. A summary of the asphalt content of each fraction is presented in Figure 1. This graph also shows the average asphalt content considered in the mix designs of the HMA containing RAP.

### 2.1.1 Binder and Aggregate Recovery

The testing program requires combining RAP and new aggregates to achieve RAP binder blending percentages of 0, 50, and 100. To obtain these blending percentages, the binder was extracted from the RAP materials in accordance with the procedure outlined in the SHRP Extraction Method AASHTO TP2. The products of the extraction process were clean recovered aggregates and clean recovered binder. This extraction method was chosen because it is reported to cause minimal aging to the recovered binder during the extraction process. Therefore, the process should not have a significant impact on the measured HMA dynamic modulus values. A detailed overview of the extraction process can be found in Section 2.1.2. Although this extraction process can also be used to determine the asphalt content of the mix, the asphalt contents as obtained by IDOT laboratories, using the reflux method, were used for HMA design.

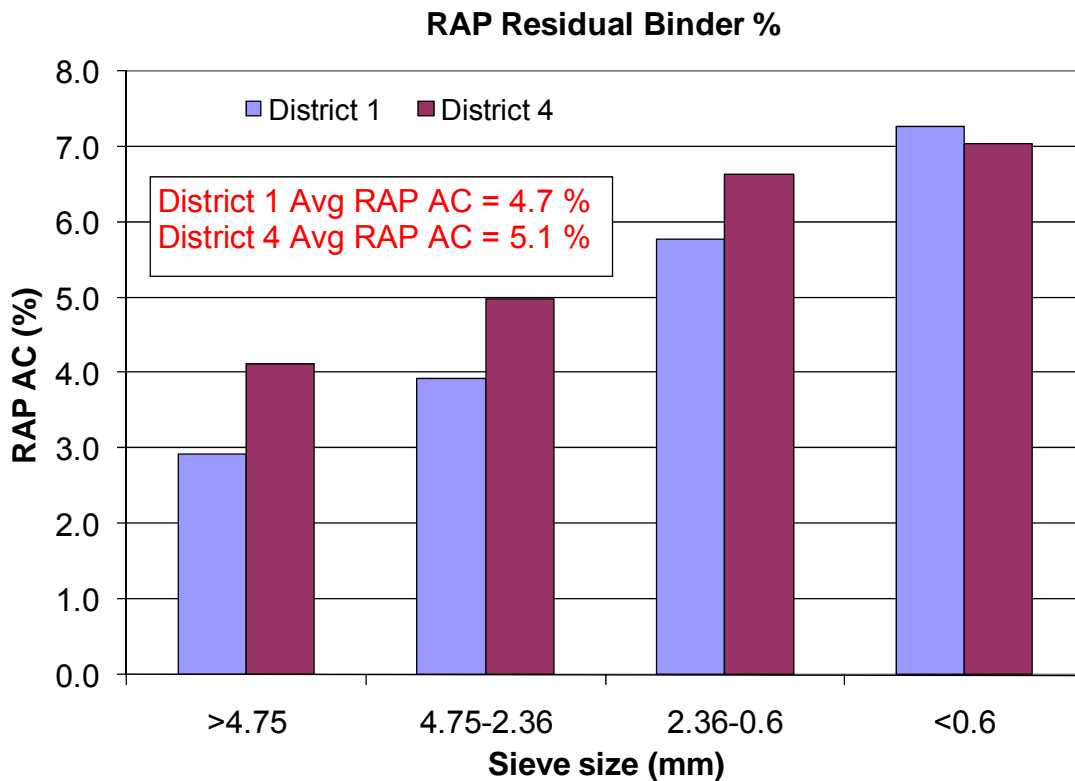


Figure 1. Asphalt contents of RAP fractions.



Figure 2. Rotovapor extraction apparatus.

### 2.1.2 Rotovapor Extraction Method

The AASHTO TP2 standard for binder extraction and recovery was followed. This standard uses a rotovapor extraction process. Other common methods include reflux or abson extraction. The rotovapor extraction apparatus was assembled at the Advanced Transportation Research and Engineering Laboratory (ATREL), where all extractions were conducted. Figure 2 illustrates the extraction apparatus; while Figure 3 shows a sample being centrifuged to remove fines during the recovery process.



Figure 3. Placing asphalt/solvent solution into centrifuge to remove fines.

The current standard does not cover certain issues related to successfully recovering the binder and aggregate for reuse, such as how to remove the recovered binder from the flask, so that it can be used in the HMA preparation process later. After the recovered binder had been centrifuged to remove fine materials, it was heated to 345 °F (174 °C) to remove all solvent and then nitrogen coated for 30 min, in accordance with the standard. The collection flask was then removed and placed into the oven. The flask was inverted to allow the binder to run out and into a binder tin, as shown in Figure 4. The recovered binder was placed into the oven at a temperature of 302 °F (150 °C) for 15 min and the temperature was then raised to 347 °F (175 °C) for an additional 10 min. After the

combined 25 min, the flask and collected recovered binder were removed from the oven. The time and temperature of the removal of the recovered binder were chosen to allow for the maximum amount of binder to be collected while keeping additional binder aging to a minimum.



Figure 4. Binder draining from collection flask in oven.

The project researchers developed the following method to preserve as much of the original gradation and quality of the recovered aggregate materials as possible. Once the extraction vessel was drained of the last solvent wash, the extraction vessel was disassembled and the clean recovered aggregates were placed into an enamel coated pan. The vessel was then allowed to air dry and the components of the vessel were then brushed clean with a soft bristled paint brush, as can be seen in Figure 5. This process prevents pan rusting and keeps the aggregates clean. During the extraction vessel cleaning, water was used to wash the internal surfaces, which left the aggregates covered with water in the pan.



Figure 5. Brushing the extraction vessel clean of fine material.

The desire to preserve the amount of fines in the recovered aggregates led to a two step process: The first step was to remove fines from the filter. This was done by removing the filter from the extraction setup and placing it in the oven at 248 °F (120 °C) for a period

of approximately 2 hrs in order to dry the filter of extraction solvent. Once the filter was dry, it was removed from the oven. The filter was then opened and the fines from the filter were placed with the rest of the recovered aggregates. Care was taken as to ensure that no plastic shavings from the filter fell into the recovered aggregates. After the outside of the filter was removed, the filter itself was tapped with a hammer to free as many fines as possible from the filter paper. The collected fines were then added to the other recovered aggregates.

The second step to preserve the fines was to clean the flasks of any fines that settled during the extraction process. Generally the only flask that contained any fines was the first flask in the setup. The fines were removed by cleaning the flask with extraction solvent and pouring the solution into the pan containing the recovered aggregates.

As a result of the cleaning process, the recovered aggregates and fines were immersed in water. The recovered aggregates were placed in the oven overnight at a temperature of 176 °F (80 °C) to dry. The next day the aggregates were removed from the oven and covered with alcohol. The addition of alcohol to the recovered aggregates removed any residual solvents that may have soaked into the aggregates during the procedure. Water was once again added to the recovered aggregates to ensure an equal covering of all of the aggregates. The recovered aggregates were once again placed in the oven overnight at 176 °F (80 °C) to allow the aggregates to dry. Figure 6 shows the RAP materials and the recovered aggregates after extraction.



Figure 6. RAP material before (left) and after (right) extraction.

After the recovered aggregates were placed in the oven overnight for the second time, they were collected and fractionated. Once the recovered aggregates were put through this recovery process they were handled similarly to the other aggregates.

### 2.3 SPECIMEN SETS

Specimens were prepared with different RAP contents to allow investigation of the amount of residual binder blending, or working, from RAP particles. The proportion of residual binder and virgin binder in HMA is expected to affect mixture volumetrics and mechanical properties. In order to quantify this effect, mixtures with 0, 20, and 40% RAP materials were designed. In addition to the specimens with varying percentages of RAP, control specimens were also prepared using recovered RAP materials (aggregate and binder). The control specimens were prepared with various ratios of recovered RAP binder

to virgin binder. This would isolate the recovered RAP binder variable in a mixture and allowed investigating the effect of recovered RAP binder on complex modulus. The same procedure was repeated using District 4 materials. In total six job mix formulae (JMF) were prepared.

Table 1 shows District 1 specimen sets. Specimen sets used in this project can be grouped into two categories. The first are JMF with actual RAP and virgin materials (aggregate and binder) and the second set are JMF with recovered aggregates and binder from RAP materials in addition to virgin aggregates and binder. The first group of specimens (Set 1) is actual practice specimens and included only virgin materials and stockpile RAP materials. Working binder in this set is unknown and has yet to be determined. The second group (Sets 2, 3, and 4) are the control specimens and are further divided into three categories that provide various blending ratios of virgin and residual binders. The difference among these three specimen sets is the proportion of recovered RAP binder to total binder content of the mix. These specimens were designed to simulate the presence of varying proportions of mobilized RAP binder in an actual HMA with RAP materials. For example, Set 2 represents a 0% working binder scenario where RAP binder is not “working” as binder in the mix. Set 4 represents a scenario where 100% RAP binder is blended with virgin binder to produce a composite binder in the mixture. The same sets were also repeated with the materials obtained from District 4 in Illinois. The specifics of laboratory mixture preparation with RAP are discussed in more detail in the following sections.

Table 1. Mixture Sets Used in the Study

RAP %	Specimen ID	Binder	RAP to Total binder (%)	Notes
0	D1-SET 1-00	Virgin	NA	
20	D1-SET 1-20	Virgin	Unknown	Actual field practice
	D1-SET 2-20	Virgin	0	0% working binder
	D1-SET 3-20	Virgin and recovered	8	50% working binder
	D1-SET 4-20	Virgin and recovered	16	100% working binder
40	D1-SET 1-40	Virgin	Unknown	Actual field practice
	D1-SET 2-40	Virgin	0	0% working binder
	D1-SET 3-40	Virgin and recovered	16	50% working binder
	D1-SET 4-40	Virgin and recovered	32	100% working binder

## 2. 4 SPECIMEN PREPARATION

### 2.4.1 Laboratory Blending and RAP

Unlike other virgin materials in a mixture, RAP aggregates contain binder; some amount of which needs to be considered in binder content calculations. Field practice assumes 100% of RAP binder is working in the HMA to form a composite binder blend. However, it is unlikely that the RAP binder absorbed into the pores will be released to mix with virgin binder, and then be reabsorbed by aggregates. It is more likely that the majority

of effective RAP binder is the portion that mixes with the virgin binder. Because no existing procedure measures absorbed binder, the current IDOT assumption, 100% RAP binder is working in the mix, was adopted in this study. Based on the amount of working binder in the RAP and the proportion of RAP in the mixture, one can calculate the virgin binder needs to be added to the mixture for a given optimum binder content. An example of mixture calculations is given in APPENDIX A to illustrate the proportion of residual and virgin binder for each set of mixtures.

RAP stockpiles have inherent variability since they can be obtained from different pavement layers and/or multiple source locations. They can be also contaminated with fabrics, joint sealants, and grids. This inherent variability and contamination can have detrimental effects if mixture preparation with RAP is not handled carefully. Another source of variability can come from agglomeration of RAP particles to each other. In addition, residual binder content of different sizes of RAP can vary significantly.

To address these variability issues, the research followed the practice of fractionating the RAP. This procedure requires separating the RAP aggregates into various sizes. This process can be difficult because RAP particles are usually agglomerated. Heating (no more than 100°F) is required to break down the agglomerates before fractionating. The gradation obtained from this process is called an “apparent gradation” and is very different than the gradation of the recovered aggregates. The following steps were applied to RAP during this process:

1. Scoop out representative samples from each bag;
2. Take the weight of the sample;
3. Heat in the oven at 100 °F (37.8 °C) no more than 2 hrs;
4. Break down agglomerates (some may remain);
5. Fractionate the material into various sizes (+12.5 mm, +9.5 mm, +4.75 mm, +2.36 mm, +0.600 mm, and -0.600 mm);
6. Reheat +9.5 mm material if there is any;
7. Break down agglomerates again;
8. Sieve again and add the materials obtained in this step to those obtained in Step 5;
9. Record retained aggregates on each sieve and calculate their percentages (this is the apparent gradation);
10. Repeat Steps 1 to 9 for at least three representative samples to determine the average apparent gradation.

This procedure is repeated to generate as much material as is needed for each sieve size. Apparent gradation of Districts 1 and 4 RAP is shown in Table 2. The gradation analysis presented in Table 2 is an average of eight samples. A comparison of recovered aggregate gradation is also shown in the table. The increased amount of the larger fractions and decreased fines, as indicated by the apparent gradation, compared to the recovered aggregate gradation suggested that fine material (smaller than 2.36 mm) remained on the surface of the larger RAP aggregates (larger than 2.36 mm). This is an important observation that can affect mixture aggregate structure if these fine particles are not released during the mechanical mixing process. Apparent gradation can be used in batching materials, but should not be used for a job mix formula calculation.

#### **2.4.2 Mixture Design**

Six JMF's were prepared with varying percentages (0, 20, and 40%) of RAP using both Districts 1 and 4 materials. The IDOT gyratory mixture design procedure was followed to prepare the mix formulae. Optimum binder content and other volumetric properties were determined for each mix design. The mixture formula is an N50 mixture design with 4.0%

air voids. Set 1 mixture designs were prepared with virgin materials (aggregate and binder) and RAP aggregates (see Table 1).

Table 2. Apparent Gradation of Districts 1 and 4 RAP Aggregates

<b>Fraction (mm)</b>	<b>DISTRICT 1 APPARENT GRADATION (% Retained)</b>	<b>DISTRICT 1 RECOVERED AGGREGATE (% Retained)</b>	<b>DISTRICT 4 APPARENT GRADATION (% Retained)</b>	<b>DISTRICT 4 RECOVERED AGGREGATE (% Retained)</b>
<b>+9.5</b>	0	0	4.7	1.2
<b>+4.75</b>	34.7	26.5	40.8	27.4
<b>+2.36</b>	26.0	24.2	25.9	24.1
<b>+0.600</b>	24.9	23.3	21.9	17.8
<b>-0.600</b>	14.3	26.0	6.7	30.1

Studying the material behavior during the mixture design is a critical step in developing an understanding of RAP behavior during the mixing process. Mixtures with varying blend percentages were prepared using the two material sources. This allows examining the impact of varying RAP percentages on the volumetric properties of mixtures, and particularly the optimum binder content. It is also crucial to know how much of the RAP binder is working in order to properly adjust the amount of virgin binder that needs to be added. Current IDOT practice for RAP mixtures assumes 100% working RAP binder. The validity of this assumption was also investigated by preparing similar mixtures with varying RAP amounts and similar aggregate gradations. The aggregate gradations used in this research were similar; except for the amount of fines passing the # 200 sieve. For HMA with the District 1 material, the amount passing the #200 sieve were as follows: 4.5%, 5.8%, and 7.1% for mixes with 0%, 20%, and 40% RAP, respectively. Similarly, for mixes with District 4 materials, the percent passing the # 200 sieve were as follows: 2.9%, 4.1%, and 6.0% for the mixes with 0%, 20%, and 40% RAP, respectively. Detailed information regarding the mixture design is described herein.

#### 2.4.2.1 Aggregate Blend and Gradation

Design gradations were chosen so that a comparable aggregate structure was obtained with each design excluding the amount of material passing the #200 sieve as was explained above. Figure 7 shows design aggregate gradation for HMA with 0, 20, and 40% RAP using District 1 materials. Figure 8 shows design aggregate gradation for 0, 20, and 40% RAP using District 4 materials. These aggregate gradation charts show that the target aggregate structure is very close for gradations with varying RAP percentage contents. An example of RAP contribution to an aggregate batch is given in Table 3.

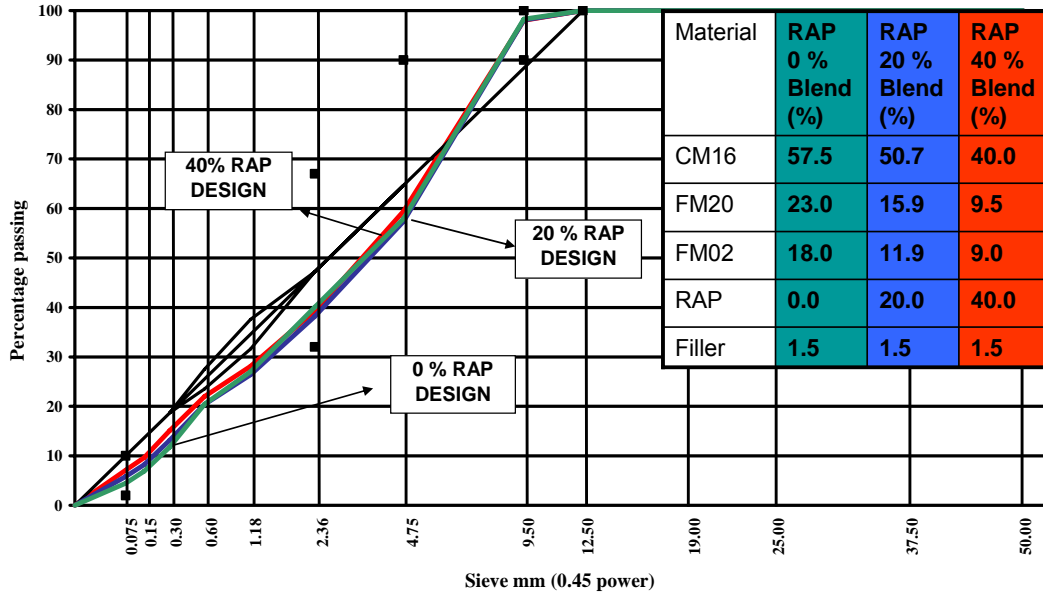


Figure 7. District 1 0, 20, and 40 % RAP blend gradation.

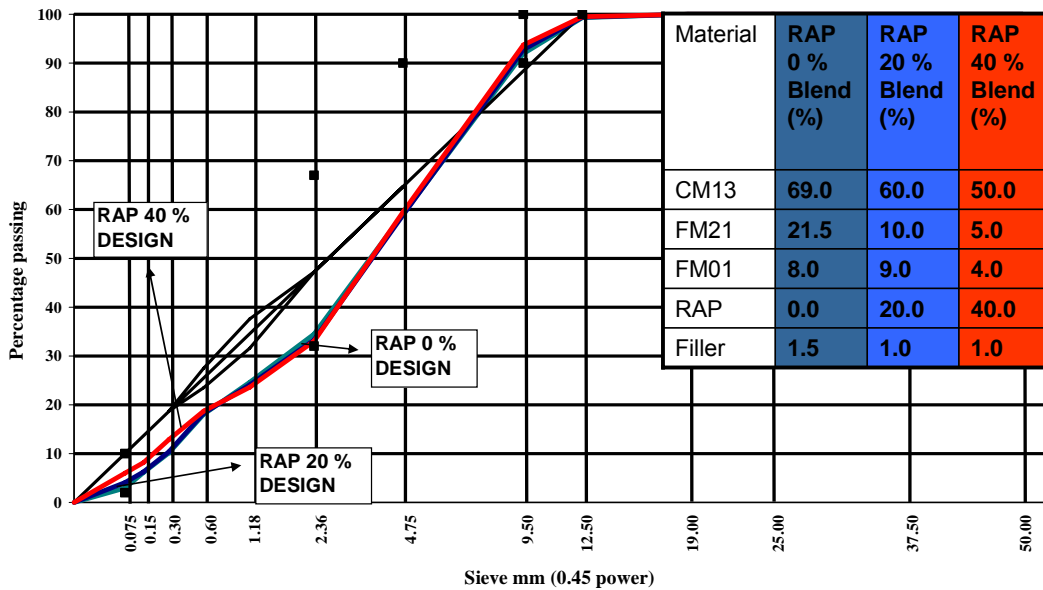


Figure 8. District 4 aggregate gradation for HMA with 0, 20, and 40% RAP.

#### 2.4.2.2 Mixture Design and Volumetrics

Optimum binder content of each HMA design was obtained from a volumetric analysis at various trial binder contents. The binder content that yields required air voids (4.0% at 50 gyrations) was selected to be the optimum binder content. The optimum binder content was physically measured in accordance with AASHTO T166. The binder content for HMA with RAP includes the existing RAP binder. Figure 9 shows the density curves with number of gyrations for Districts 1 and 4 mixtures with RAP.

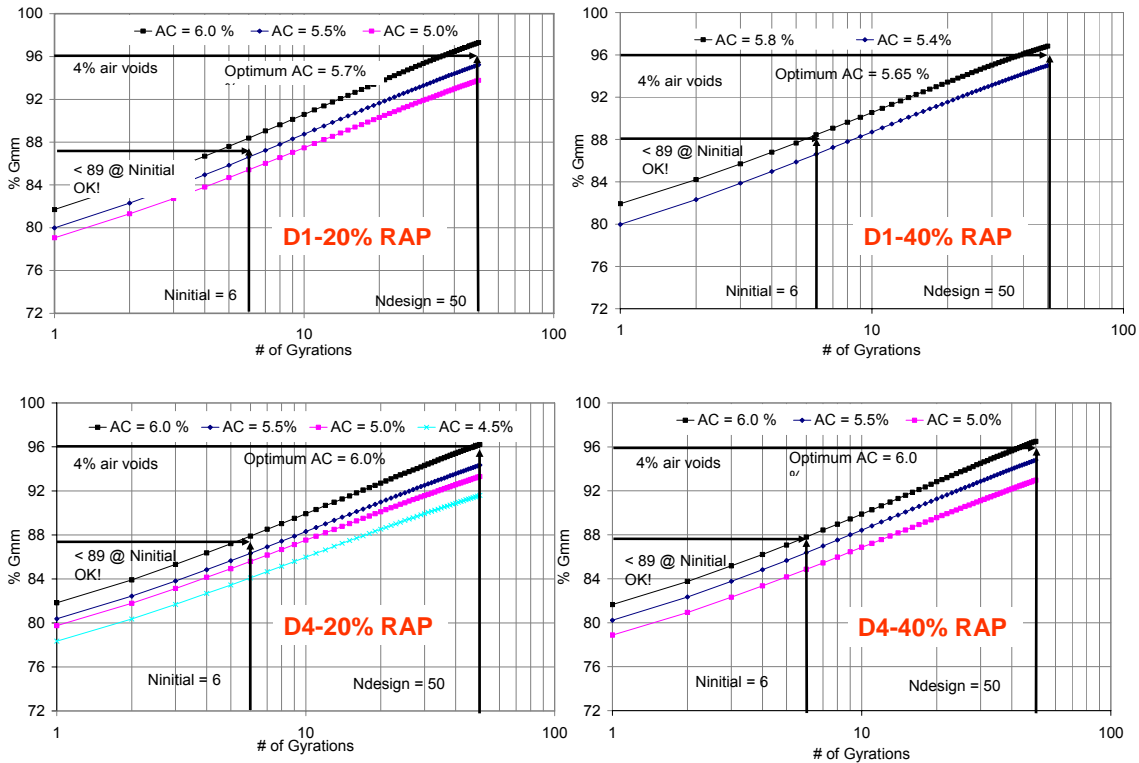


Figure 9. Optimum binder content determination for Districts 1 and 4 HMA with RAP.

A summary of each mixture design is shown in Tables 4 and 5 for Districts 1 and 4 materials, respectively (details and statistics of the samples prepared for the designs are presented in APPENDIX B). The volumetric calculations of mixes with RAP were performed based on the bulk specific gravity ( $G_{sb}$ ) of RAP aggregates. Typical values approved by IDOT were used for Districts 1 and 4 RAP aggregates (2.660 and 2.630, respectively). The use of an accurate bulk specific gravity of the RAP for VMA calculations is crucial. Substituting effective specific gravity ( $G_{se}$ ) for the  $G_{sb}$  will result in overestimating combined bulk specific gravity and thus an overestimation of VMA (Murphy, 2008). As shown in Tables 4 and 5, optimum binder content does not vary significantly with increasing RAP content. This result provides insight into the mechanism mixing and compaction process when RAP material is present. It is important to recall that 100% working RAP binder was assumed in the mix design process. Thus, it can be concluded that the 100% working binder hypothesis is acceptable from a mix design point of view since equivalent compactability was achieved regardless of RAP content. While it cannot be stated that 100% blending is occurring, the RAP binder still contributes to filling voids. In addition, a potential lubricating effect of RAP materials could facilitate compaction and lessen the need for additional binder. The VMA values of the mixes with 40% RAP using both Districts 1 and 4 materials were below the VMA minimum requirement by 0.3%.

Table 3. RAP Contribution to Aggregate Batch Having 20% District 1 RAP in the Mix

Batch weight (g)	4700	
RAP weight (g)	940	
Fractions Used	% of Total RAP	Weight Fraction (g)
+4.75 mm	34.7	327
+2.36 mm	26.0	244
+0.600 mm	24.9	234
-0.600 mm	14.3	135
Total	100	940

Table 4. District 1 Mixture Design with Various RAP Percentages

	Optimum AC (%)	Total needed binder (g)*	Virgin binder (g)	Recovered binder (g)	G <sub>mb</sub> @ optimum AC	G <sub>mm</sub> @ optimum AC	VMA @ optimum AC
0 % RAP	5.9	294	294	0	2.398	2.502	15.1
20 % RAP	5.7	281	237	0	2.397	2.496	15.0
40 % RAP	5.65	276	188	0	2.421	2.519	14.1
20 % Recovered Aggregate	5.7	284	284 (Set 2)	0 (Set 2)	2.395	2.499	15.1
			262 (Set 3)	22 (Set 3)			
			240 (Set 4)	44 (Set 4)			
40 % Recovered Aggregate	5.55	276	276 (Set 2)	0 (Set 2)	2.410	2.505	14.4
			232 (Set 3)	44 (Set 3)			
			188 (Set 4)	88 (Set 4)			

\* Total binder content for a 4,700 g aggregate batch (Total binder = Virgin binder + % 100 of RAP binder)

#### 2.4.2.3 Blended Gradation Check

Using RAP materials in HMA can cause significant variability due to differences in batching (apparent gradation) and gradation used in design, as was depicted in Table 2. It is important to check actual blend gradation against the design blend. Several design specimens were randomly selected and burned in the ignition oven in order to reclaim the aggregates. Washed aggregate gradation was then performed on these materials. Figure 10 shows the comparison of the design blend and actual sample blend for the District 1 mix with 20% RAP. Similarly, Figure 11 shows the comparison of the design blend and actual sample blend for the District 1 mix with 40% RAP. Figures 12 and 13 demonstrate the comparison of the design and actual sample blend for District 4 mixes with 20% and 40% RAP, respectively. The design and actual blends are in good agreement, which justifies the specimen preparation approach followed in this study. The variation in gradations, shown in Figures 10 and 11, could be related to the degradation of the coarse aggregate in the mix.

Table 5. District 4 Mixture Design with Various RAP Percentages

	Optimum AC (%)	Total needed binder (g)*	Virgin binder (g)	Recovered binder (g)	G <sub>mb</sub> @ optimum AC	G <sub>mm</sub> @ optimum AC	VMA @ optimum AC
0 % RAP	5.9	295	295	0	2.429	2.524	13.7
20 % RAP	6.0	297	249	0	2.409	2.508	14.1
40 % RAP	6.0	294	198	0	2.406	2.506	14.2
20 % Recovered Aggregate	5.9	295	295 (Set 2)	0 (Set 2)	2.394	2.496	14.6
			271 (Set 3)	24 (Set 3)			
			247 (Set 4)	48 (Set 4)			
40 % Recovered Aggregate	5.9	295	295 (Set 2)	0 (Set 2)	2.391	2.490	14.6
			247 (Set 3)	48 (Set 3)			
			199 (Set 4)	96 (Set 4)			

\* Total binder content for a 4,700 g aggregate batch (Total binder = Virgin binder + % 100 of RAP binder)

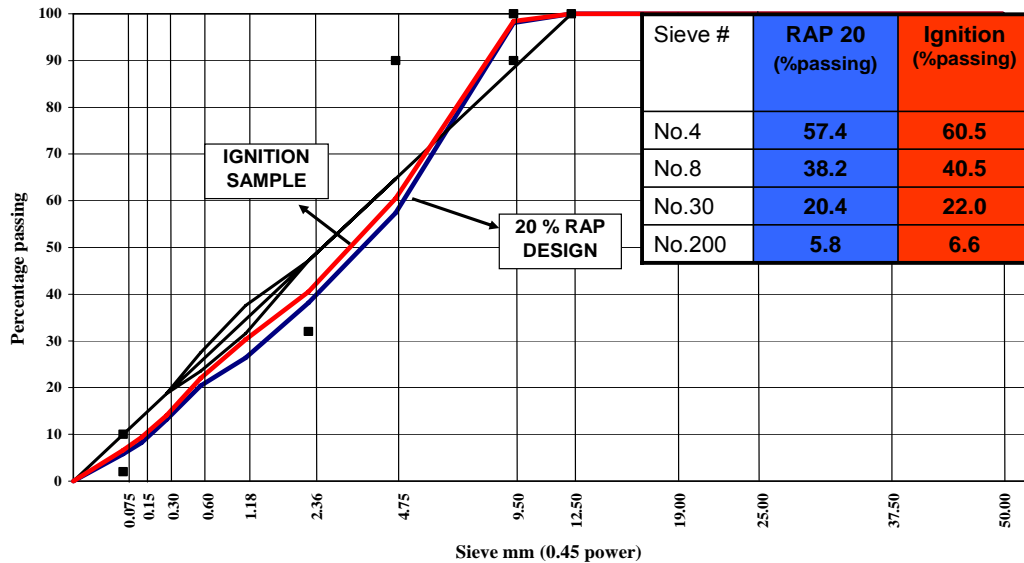


Figure 10. Blend check of District 1 design with 20% RAP.

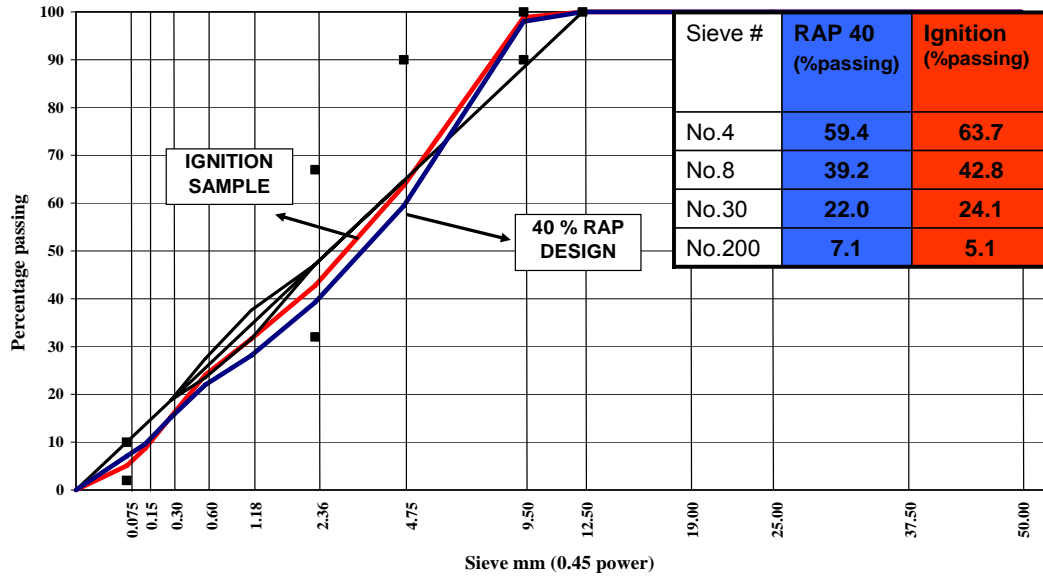


Figure 11. Blend check of District 1 design with 40% RAP.

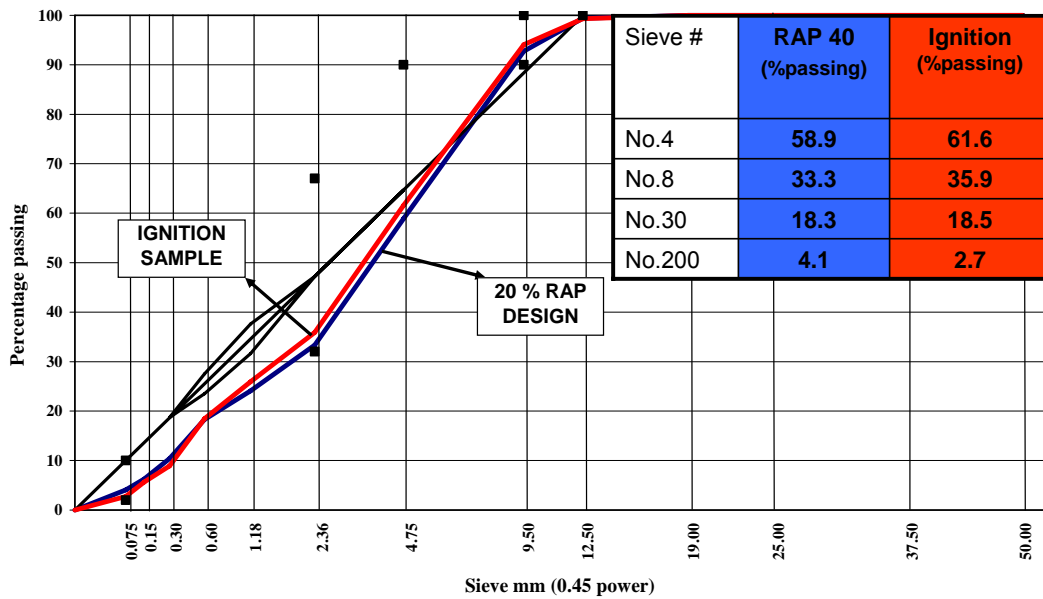


Figure 12. Blend check of District 4 design with 20% RAP.

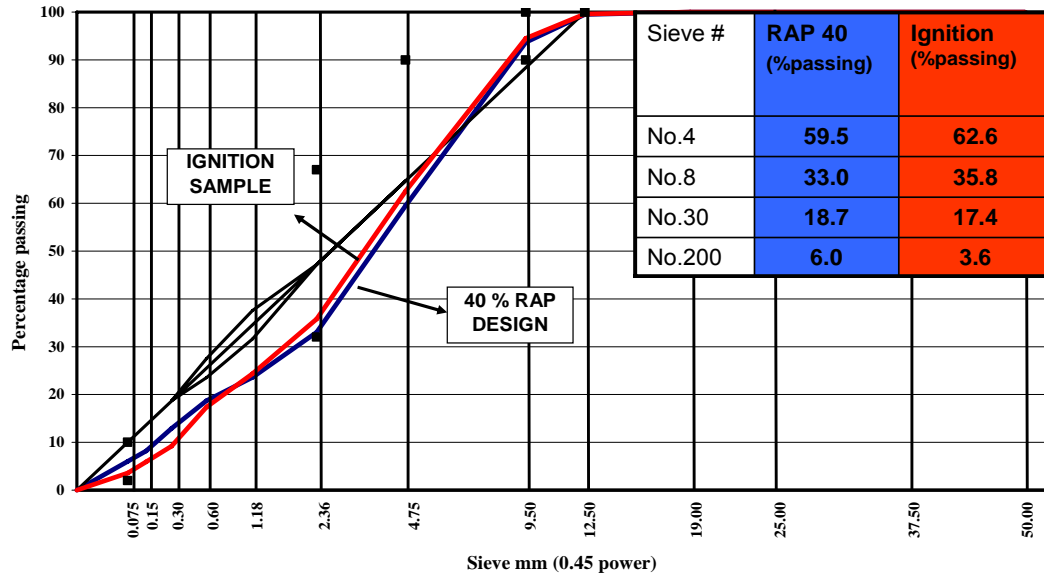


Figure 13. Blend check of District 4 design with 40 % RAP .

#### 2.4.2.4 Test Specimens

Once the design was finalized for each mixture type, gyratory test specimens were prepared at 4.0 % air voids. The specimens were compacted to 50 gyrations and air voids were controlled by adjusting mixture weight. The specimens were cored and sawed to the proper diameter and length for dynamic modulus testing following compaction.

## 2.5 SPECIMEN CHARACTERIZATION

### 2.5.1 Dynamic Modulus Testing

Dynamic modulus testing was performed on each specimen set. Because the residual binder is aged, the effect of the residual binder is expected to increase the modulus of binder mastic; hence, the modulus of the composite mixture will increase as well. The specimen sets introduced in the preceding sections were designed to investigate the effect of stiff RAP binder on dynamic modulus and determine the working binder in RAP.

Specimens were prepared using Districts 1 and 4 materials with 20 and 40% RAP blends. Specimen identification used in this report is illustrated in the following.

**Di-SETj-AA**  
 where  
 i: District 1 or 4  
 j: Specimen sets 1, 2, 3, and 4  
 AA: 00, 20 or 40% RAP  
 EX:  
 D1-SET1-20 is District 1, SET 1 (field practice), and 20% RAP  
 D4-SET1-00 is District 4, SET 1 (field practice), and 0% RAP

The following testing parameters were used in this study. An additional low frequency (0.01 Hz), not called for in the AASHTO procedure was added to the testing sequence to investigate the effect of binder which is more pronounced at low frequencies. A summary of the testing suite can be found in Table 6.

Table 6. Dynamic Modulus Testing Suite

Test Temperature (°C)	Frequency (Hz)	Load Amplitude (kN)	Contact Load (kN)
-10	25, 10, 5, 1, 0.5, 0.1, and 0.01	7	0.3
4	25, 10, 5, 1, 0.5, 0.1, and 0.01	6	0.2
20	25, 10, 5, 1, 0.5, 0.1, and 0.01	2	0.1

Testing began at the lowest temperature and highest frequency. The total number of loading cycles is shown in Table 7. The analysis software based on AASHTO TP 62-03 collects only the recordings from the last 10 cycles and then fits a sinusoid curve to the load and deformation data.

Table 7. Number of Cycles for Test Sequence

Frequency (Hz)	Number of cycles
25	200
10	200
5	100
1	20
0.5	15
0.1	15
0.01	11

Phase angle and dynamic moduli are calculated at each frequency using the following formulas:

$$|E^*(\omega)| = \frac{|\sigma^*|}{|\varepsilon^*|} \text{ and } \theta(\omega) = \overline{\theta_\varepsilon} - \theta_\sigma \quad (1)$$

where:

$\theta(\omega)$  = Phase angle between applied stress and strain for frequency  $\omega$ , degrees

$|E^*(\omega)|$  = Dynamic modulus for frequency  $\omega$ , kPa (psi)

$\overline{\theta_\varepsilon}$  = Average phase angle for all strain transducers, degrees

$\theta_\sigma$  = Stress phase angle, degrees

$|\sigma^*|$  = Stress magnitude, kPa (psi)

$|\varepsilon^*|$  = Average strain magnitude

## 2.5.2 Stripping Evaluation

The moisture susceptibility of RAP mixtures was also evaluated. Illinois modified AASHTO T 283-02 was followed to determine resistance of HMA with RAP to moisture induced damage. The procedure followed during this study is as follows:

1. Preparation of compacted specimens at 7% air voids (+/- 0.5%), 6 in (150 mm) diameter, and 95 +/- 5 mm 3.75 +/- 0.20 in thick.
2. Specimens were grouped into dry and conditioned sets.
3. Conditioned specimens were saturated to 70-80%.
4. Conditioned specimens were placed in water bath at 140 °F (60 °C) for 24 hrs.
5. Following the 24 hr conditioning, specimens were placed in a water bath at 77 °F (25 °C) for 2 hrs.
6. Conditioned specimens were tested at 77 °F (25 °C) to determine their indirect tensile strength.
7. Visual stripping inspection was conducted.
8. Dry specimens were tested for indirect tensile strength after 2 hrs conditioning at 77 °F (25 °C).

Figure 14 illustrates the sample preparation path from saturation to 70-80% through conditioning, and finally testing.

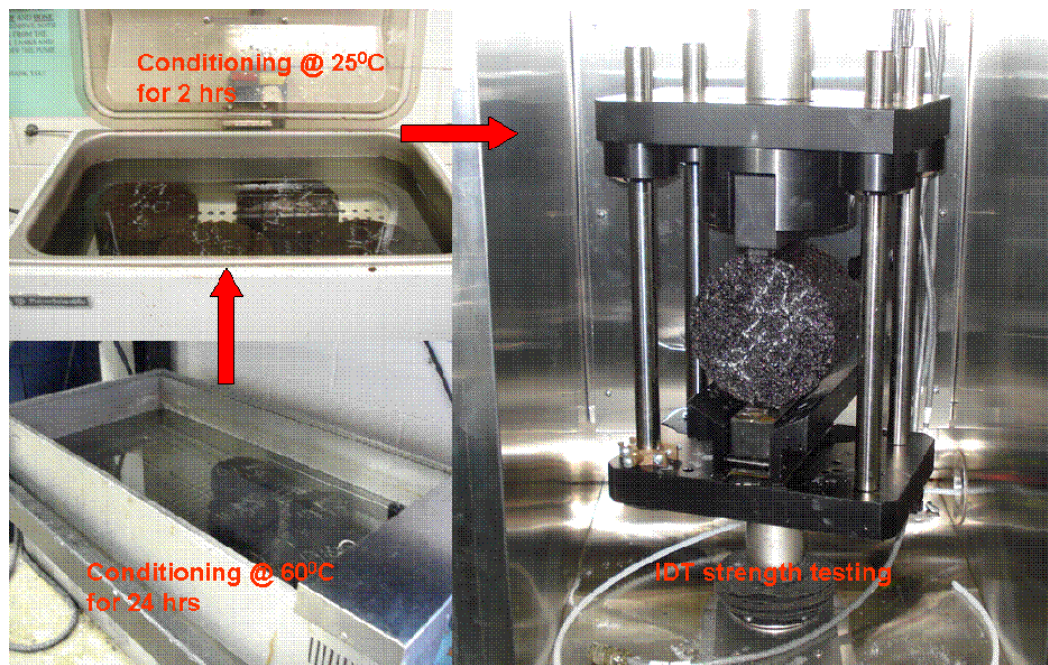


Figure 14. Moisture susceptibility procedure for conditioned specimens after saturation.

## 2.5.3 Environmental Scanning Electron Microscope Approach

The electron microscope, Philips XL30 ESEM-FEG, used in this study was a dual function SEM. It can operate as both a conventional SEM or ESEM. Although metal coating is not required in the ESEM, both coated and uncoated specimens were examined to determine resolution enhancement. The following conditions were used in the experiment. The chamber pressure of 1 tor water vapor, 5 and 7.5 kV accelerating voltage,

spot size of 3 and 4, and working distance (WD) of 7.5 were used when the specimen was observed in the wet mode (ESEM). The chamber pressure of  $1.3 \times 10^{-4}$  tor, 20 kV accelerating voltage, spot size of 4 and WD of 10 were used for SEM. The images were stored as 1,290×968 pixel TIFF files. Sample preparation started by coring a 25 mm specimen from the 100 mm core obtained from a gyratory specimen. To obtain a 3 mm deep specimen, the sample was cut through its depth. The sample was then cleaned and dried at 104 °F (40 °C) in the oven. A spot of interest was then marked on the 25 mm specimen and was magnified repetitively using ESEM and SEM to reveal different surface features of the specimen. A photo summary of this process is shown in Figure 15.

The spots of interest were determined by visual observation of the specimen. The researchers observed the cross section of the samples and noticed that certain particles appeared discolored with respect to the remaining particles. These were assumed to be the RAP particles since the discolored particles occurred at approximately the same frequency as the percentage of RAP added to the mix. These discolored particles were then assumed to be RAP, and the particle-mastic interface was investigated with the SEM.

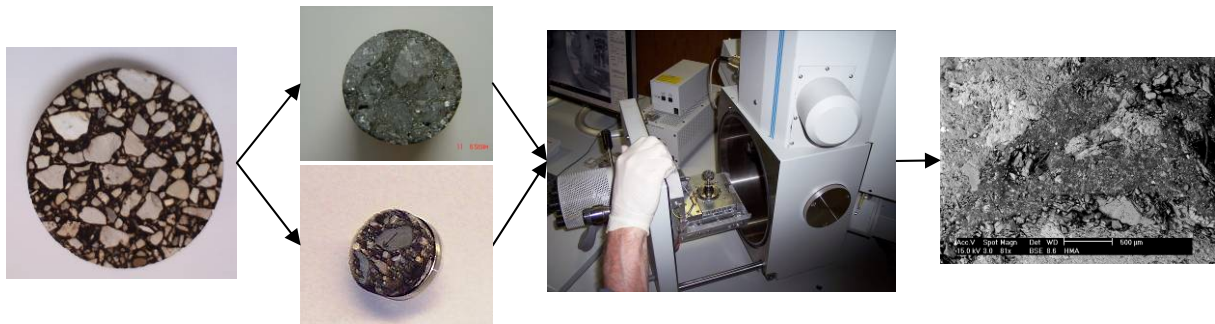


Figure 15. Sample preparation and capture of high-resolution images using scanning electron microscopy.

#### 2.5.4 Fracture Characterization

Fracture energy characterization of the HMA with RAP is necessary to illustrate the potential for low temperature cracking. Two fracture tests were selected to determine the fracture energy of the mixes in this study. The SCB test and DCT test were used for HMA fracture energy characterization. Figures 16 through 18 show the specimens tested in the SCB and DCT.

For the DCT, test specimens are easily prepared from standard 6in gyratory specimens. Preparation of the DCT test specimens was in accordance of the ASTM 7313 standard. Three replicates of each mix were tested at 10.4 °F (-12 °C) and 32°F (0 °C). Preparation of the SCB specimens was in accordance with the approach outlined by Li (2005). As with the DCT testing, the SCB testing was conducted at 10.4 °F (-12 °C) and 32 °F (0 °C.) Three test replicates of each HMA with RAP content and testing temperature were performed. Table 8 illustrates the test matrix used for the fracture testing utilizing both the DCT and SCB testing. The numbers in Table 8 are the number of replicate tests run.



Figure 16. SCB and DCT test specimens.

The fracture tests were both crack mouth opening displacement (CMOD) controlled. The loading rate of the test was 0.7 mm/min CMOD displacement for the SCB test, and 0.1 mm/min for the DCT. These loading rates are typical of the loading rates used in the respective tests. The fracture energy for both testing methods was determined by calculating the area under the load vs. CMOD curve. These calculations were performed in MATLAB.



Figure 17. SCB test.



Figure 18. DCT test.

Table 8. Fracture Energy Evaluation Test Matrix

Temperature (°C)	RAP (0%)	RAP (20%)	RAP (40%)	Total
0	3	3	3	9
-12	3	3	3	9
Total	6	6	6	18

## CHAPTER 3 RESULTS AND ANALYSIS

### 3. 1 DYNAMIC MODULUS TEST RESULTS

Dynamic modulus tests were performed on the gyratory compacted specimens prepared at the target 4.0% air voids. The results are presented in the form of master curves at a reference temperature of 68 °F (20 °C).

#### 3.1.1 District 1 HMA with 20% RAP Scenario

The specimen volumetric properties are presented in Table 9 including air voids, VMA, and VFA of each specimen. As expected significant changes in air voids, VMA and VFA were observed after cutting and coring specimens. The results in Table 9, show some variation in VMA values. It is believed that these variations do not significantly affect the dynamic modulus results in a manner that would affect the comparisons between the various specimen sets.

Dynamic modulus test results are reported as master curves, shown in Figure 19. Master curves were constructed using time-temperature superposition with the reference temperature of 68 °F (20°C). As illustrated in the figure, there is no significant difference between the results of all four specimen sets. Recall that Sets 2, 3, and 4 were prepared with recovered aggregates and binder. The proportion of recovered RAP binder to total binder content is 0, 8, and 16% for Sets 2, 3, and 4, respectively. The stiff binder effect should be most observable in the results of Sets 2, 3, and 4. However, insignificant differences exist between the HMA dynamic moduli at this percentage of RAP in the mix. Hence, it is concluded that the addition of 20% RAP to a mixture does not significantly alter the mixture dynamic modulus.

Table 9. District 1 Mix with 20% RAP

	Before cutting & coring			After cutting & coring		
	Air Voids	VMA	VFA	Air Voids	VMA	VFA
D1-SET1-20-1	4.4	15.4	71.6	3.4	14.5	76.8
D1-SET1-20-2	4.3	15.3	71.7	3.1	14.3	78.0
D1-SET1-20-3	4.6	15.6	70.5	3.4	14.5	76.4
<b>Average</b>	<b>4.4</b>	<b>15.4</b>	<b>71.3</b>	<b>3.3</b>	<b>14.4</b>	<b>77.1</b>
D1-SET2-20-1	4.3	15.2	71.5	3.4	14.4	76.6
D1-SET2-20-2	4.3	15.2	71.8	3.4	14.4	76.4
D1-SET2-20-3	4.3	15.3	72.0	3.2	14.3	77.7
<b>Average</b>	<b>4.3</b>	<b>15.2</b>	<b>71.8</b>	<b>3.3</b>	<b>14.4</b>	<b>76.9</b>
D1-SET3-20-1	4.8	15.6	69.3	3.3	14.3	77.1
D1-SET3-20-2	4.4	15.3	71.3	3.2	14.2	77.5
D1-SET3-20-3	4.5	15.4	70.7	3.2	14.2	77.7
<b>Average</b>	<b>4.6</b>	<b>15.4</b>	<b>70.4</b>	<b>3.2</b>	<b>14.2</b>	<b>77.4</b>
D1-SET4-20-1	4.8	15.6	69.3	3.4	14.4	76.3
D1-SET4-20-2	4.4	15.3	71.3	3.1	14.1	78.3
D1-SET4-20-3	4.7	15.5	69.9	3.3	14.3	77.2
<b>Average</b>	<b>4.6</b>	<b>15.5</b>	<b>70.2</b>	<b>3.2</b>	<b>14.3</b>	<b>77.3</b>

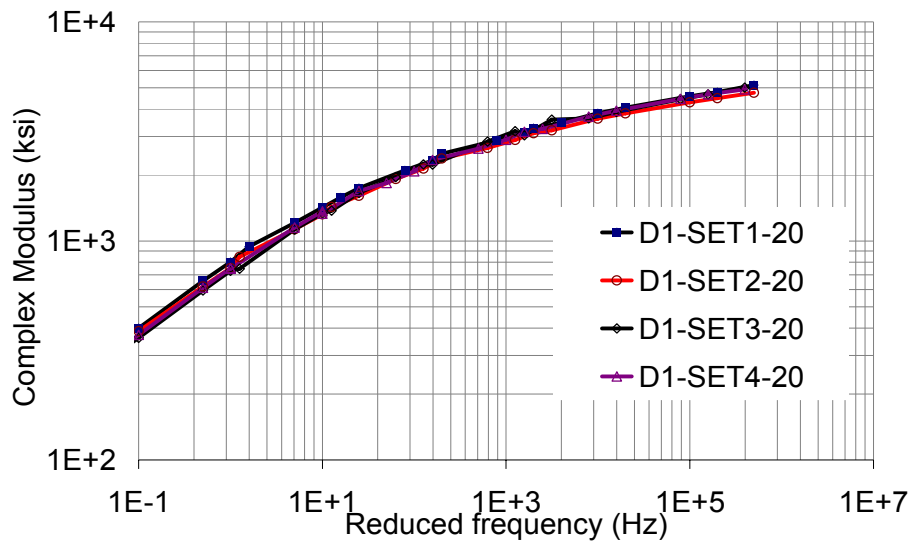


Figure 19. District 1 mix with 20% RAP master curves.

Similarly, phase angle master curves were constructed. Figure 20 presents the phase angle master curve for the four specimen sets. Similar to modulus results, phase angle results do not exhibit significant differences between the four mixes at this percentage of RAP. The differences between the mixtures are within the experimental variations.

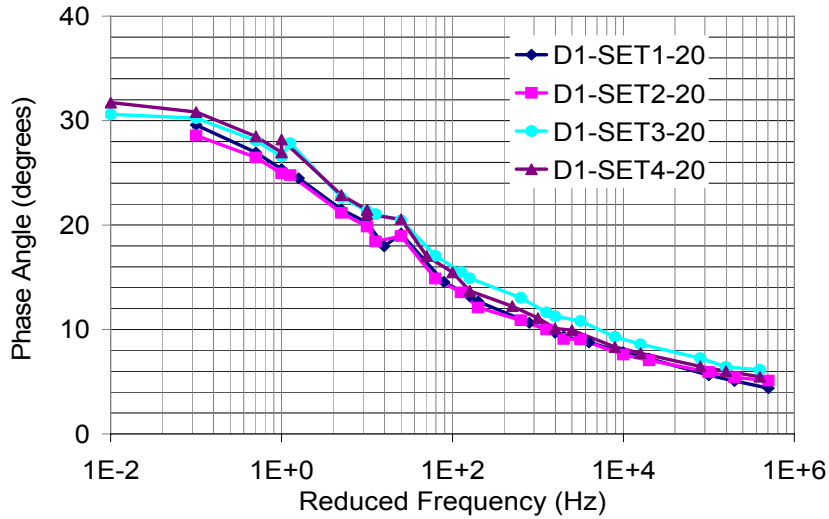


Figure 20. District 1 mix with 20% RAP phase angle.

### 3.1.2 District 1 Mix with 40% RAP scenario

Table 10 presents the volumetric characteristics of the specimens prepared with 40% RAP. For these test sets, only two specimens were tested. The resulting coefficient of variation was low (under 10%), hence, testing a third specimen was deemed unnecessary. As in the case of mixes with 20% RAP, some variations in the VMA results exist. These variations are considered acceptable and may not bias the outcome.

Table 10. District 1 Mix with 40% RAP

	Before cutting & coring			After cutting & coring		
	Air Voids	VMA	VFA	Air Voids	VMA	VFA
D1-SET1-40-1	4.2	14.4	70.9	2.8	13.2	78.6
D1-SET1-40-2	3.5	13.8	74.5	2.5	12.8	80.8
<b>Average</b>	<b>3.9</b>	<b>14.1</b>	<b>72.7</b>	<b>2.6</b>	<b>13.0</b>	<b>79.7</b>
D1-SET2-40-1	4.1	14.7	72.3	2.8	13.5	79.5
D1-SET2-40-2	3.6	14.3	74.6	2.7	13.5	79.9
<b>Average</b>	<b>3.8</b>	<b>14.5</b>	<b>73.4</b>	<b>2.7</b>	<b>13.5</b>	<b>79.7</b>
D1-SET3-40-1	3.8	14.4	73.9	3.3	13.5	75.6
D1-SET3-40-2	3.4	14.1	75.8	2.9	13.1	78.1
<b>Average</b>	<b>3.6</b>	<b>14.2</b>	<b>74.9</b>	<b>3.1</b>	<b>13.3</b>	<b>76.9</b>
D1-SET4-40-1	3.5	14.2	75.3	3.1	13.3	76.9
D1-SET4-40-2	3.5	14.1	75.5	2.9	13.2	77.7
<b>Average</b>	<b>3.5</b>	<b>14.2</b>	<b>75.4</b>	<b>3.0</b>	<b>13.2</b>	<b>77.3</b>

Figure 21 presents the master curves for each set of specimens prepared with 40% RAP. As the proportion of RAP binder increases among Sets 2, 3, and 4, the modulus also increases. This effect of the RAP binder is more pronounced at high temperature and low

frequency. The stiff RAP binder effect is likely driving the majority of the differences observed in the dynamic modulus results. The differences observed in the mixes having 40% RAP are believed to be occurring in the mixes with 20% RAP, but the effect is so small that it is masked by experimental variability. Set 1, which was prepared with actual field RAP materials and virgin materials (binder and aggregate), has a significantly higher modulus than the other sets. For the assumption of 100% working RAP binder to be valid, Sets 1 and 4 should have performed similarly if stiff RAP binder was the only variable contributing to the dynamic modulus of mixtures with RAP.

The unexpected results could be due to the variations in aggregate selective absorption of binder between the two sets. Selective absorption is a process in which the lighter fractions of the asphalt binder are absorbed into the aggregates. In the case of a fresh mix, binder on the aggregate surface will not have enough time to be sufficiently absorbed; hence, the effective binder is not as stiff. On the other hand, RAP particles already have a stiff layer of binder that may be strongly bonded to the aggregate and better absorbed into the aggregate over the service years.

The change in total effective binder, and aggregate gradation as well as the incomplete binder blending affected the HMA dynamic modulus results. This may explain the increase in the dynamic modulus of Set 1 specimens compared to Sets 2, 3, and 4 specimens in addition to the stiff RAP binder effect.

Phase angle variation is presented in Figure 22. Similar trends, as were observed in the dynamic modulus data, between Set 1 and other Sets were noted. Set 1 exhibits a less viscous response due to the possible presence of aged binder or less working binder in the mix. Sets 2, 3, and 4 reveal the effects of stiff binder; there were insignificant differences in aggregate structure and volumetric characteristics between the three Sets' specimens. The amount of RAP binder with respect to total binder is 0, 16% and 32% for Sets 2, 3, and 4, respectively. The effect of increasing the amount of stiff binder is clearly manifested in the phase angle results; especially in the intermediate and low frequency ranges. Again, Set 1 specimens show lower phase angle values compared to other sets.

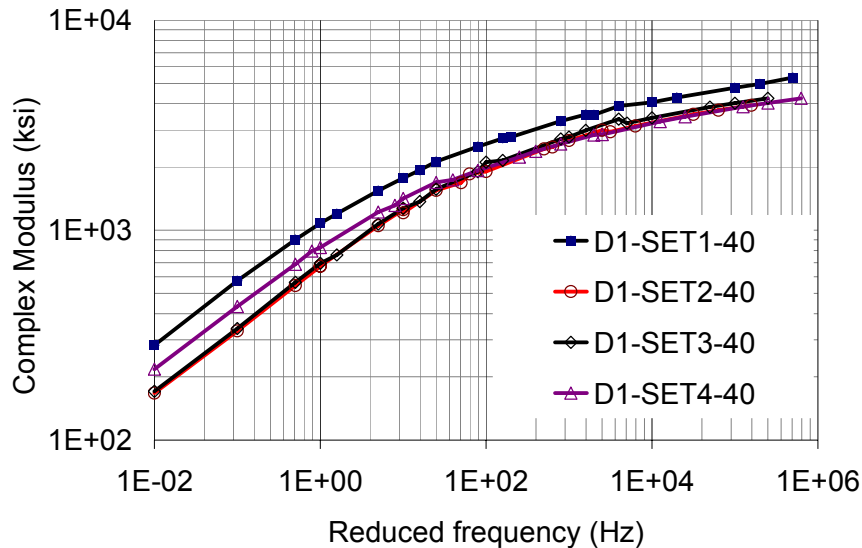


Figure 21. District 1 mix with 40% RAP master curves.

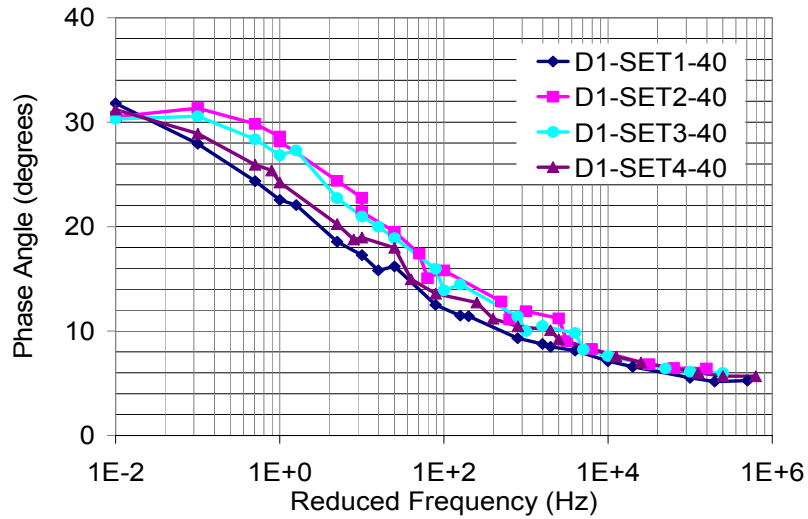


Figure 22. District 1 mix with 40% RAP phase angle.

### 3.1.3 Comparison of District 1- 0, 20, and 40% RAP Cases

To assess the effect of increased percentage of RAP with respect to a mixture without RAP, specimens containing no RAP materials were prepared. Dynamic moduli of specimen sets prepared with 0, 20, and 40% RAP are presented in Figure 23. As the RAP percentage in the mix increases, the dynamic modulus increases. Similar observations can be made with phase angle comparisons. Phase angle results are shown in Figure 24. As RAP percentage increases in the mix, phase angle decreases; demonstrating the effect of stiff RAP binder, change in HMA volumetric properties, namely VMA differences, and aggregate structure, such as the increase in fines in the mixes with RAP.

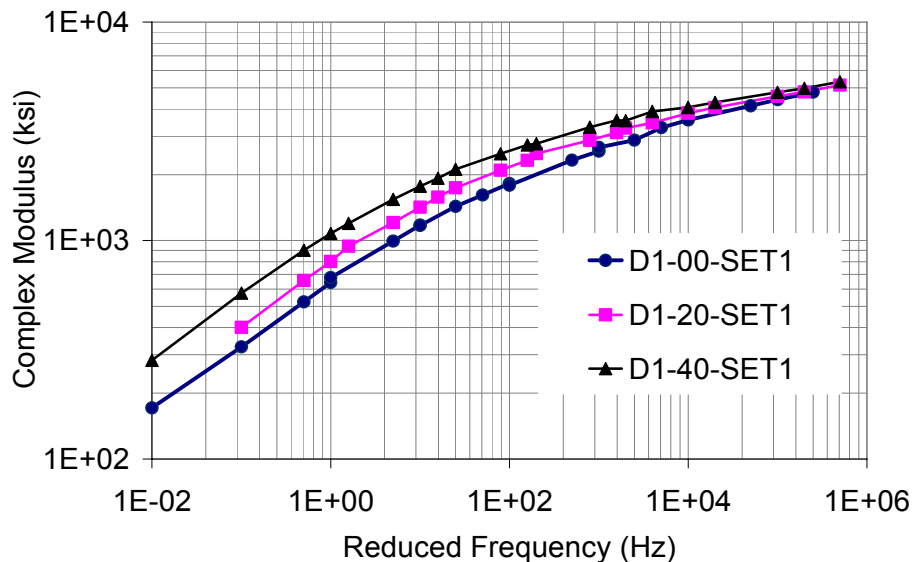


Figure 23. Dynamic modulus comparison of Set1 specimens with 0, 20, and 40% RAP.

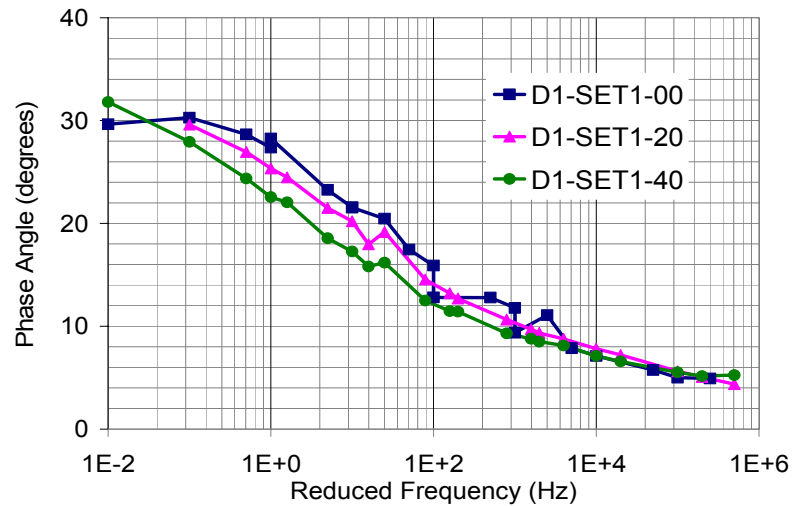


Figure 24. Phase angle comparison of Set1 specimens with 0, 20, and 40% RAP.

### 3.1.4 Statistics and Goodness of Dynamic Modulus Data

Repeatability and statistical analyses were conducted on the dynamic modulus and phase angle results. Each specimen set (Sets 1, 2, 3, and 4) master curve was constructed from a minimum of two replicates. Table 11 shows the standard deviation and coefficient of variation of dynamic modulus and phase angle results for District 1 specimens. Standard deviations and coefficients of variation for the tests at various frequencies (25, 10, 5, 1, 0.5, 0.1, and 0.01 Hz) were averaged to obtain a single value for each temperature. The coefficient of variation for the dynamic modulus and phase angle is generally less than 10%. This suggests that data reported herein exhibits good level of repeatability. A complete list of dynamic modulus test data statistics can be found in APPENDIX C.

### 3.1.5 District 4 Mix 20% RAP Scenario

District 4 materials were prepared similar to those of District 1. The objective of using different materials and mix design was to check for consistency in the findings. Not only the materials but also the mix design changed between the two District materials. The same comparisons which were made with the District 1 results were also made with the District 4 results. Volumetric properties of each specimen are shown in Table 12.

The HMA dynamic modulus master curves for specimens' Sets 1, 2, 3, and 4 are presented in Figure 25. The dynamic modulus results for HMA specimens with 20% RAP for District 4 are similar to those of District 1 specimens. Again, this indicates that the effect of RAP at this particular blending level is insignificant. Sets 2, 3, and 4 specimens were the control sets and contained 0, 8, and 16% stiff RAP binder (with respect to the total binder in the mix). On the other hand, Set 1 was prepared with actual RAP materials. Similar to the findings from District 1 materials and mixture design, the modulus results at this percentage of RAP do not display significant differences.

Table 11. District 1 Dynamic Modulus and Phase Angle Statistics

	Temp (°C)	Complex Modulus		Phase Angle	
		STDEV (ksi)	COVAR	STDEV (deg)	COVAR
<b>D1-SET1-00</b>	-10	30.7	0.9	0.3	4.6
	4	57.1	2.8	0.4	1.7
	20	19.5	3.7	1.1	6.6
<b>D1-SET1-20</b>	-10	164.0	4.2	1.2	19.4
	4	106.4	4.5	0.6	6.0
	20	125.9	12.8	0.7	5.7
<b>D1-SET2-20</b>	-10	658.1	17.3	0.5	5.8
	4	261.2	5.9	0.7	4.4
	20	99.3	5.4	0.4	1.8
<b>D1-SET3-20</b>	-10	175.5	5.9	2.2	23.5
	4	68.2	2.9	0.4	3.8
	20	33.6	4.3	0.5	2.2
<b>D1-SET4-20</b>	-10	109.0	2.8	0.3	4.7
	4	36.6	2.1	0.9	5.4
	20	56.9	7.1	1.0	4.1
<b>D1-SET1-40</b>	-10	101.9	3.7	0.2	2.8
	4	139.9	5.0	0.5	5.0
	20	102.7	7.6	0.3	1.8
<b>D1-SET2-40</b>	-10	296.8	9.7	0.2	1.8
	4	341.1	6.4	0.3	2.8
	20	80.4	5.3	1.0	3.9
<b>D1-SET3-40</b>	-10	48.8	1.5	0.1	1.3
	4	248.5	12.0	0.4	1.5
	20	91.5	4.3	1.0	4.5
<b>D1-SET4-40</b>	-10	174.6	5.2	0.1	0.8
	4	96.0	4.7	0.0	1.5
	20	65.8	6.4	0.1	1.3
<b>D1-SET1-40 w/ PG58-28</b>	-10	No statistics exist for this set. Only one good specimen.			
	4				
	20				

Table 12. District 4 HMA with 20% RAP

	Before cutting & coring			After cutting & coring		
	Air Voids	VMA	VFA	Air Voids	VMA	VFA
D4-SET1-20-1	5.0	15.0	66.8	3.9	14.1	72.2
D4-SET1-20-2	4.4	14.7	70.1	3.3	13.7	76.1
D4-SET1-20-3	4.8	15.0	68.1	3.9	14.2	72.5
D4-SET1-20-4	4.7	14.9	68.7	3.7	14.0	73.8
<b>Average</b>	<b>4.7</b>	<b>14.9</b>	<b>68.4</b>	<b>3.7</b>	<b>14.0</b>	<b>73.6</b>
D4-SET2-20-1	4.8	15.3	68.3	3.5	14.1	74.9
D4-SET2-20-2	3.9	14.4	73.2	2.7	13.4	79.8
D4-SET2-20-3						
<b>Average</b>	<b>4.3</b>	<b>14.8</b>	<b>70.8</b>	<b>2.6</b>	<b>13.3</b>	<b>80.3</b>
D4-SET3-20-1	3.8	14.3	73.6	2.6	13.3	80.3
D4-SET3-20-2	3.9	14.4	73.1	2.8	13.4	79.4
D4-SET3-20-3						
<b>Average</b>	<b>3.8</b>	<b>14.4</b>	<b>73.4</b>	<b>2.7</b>	<b>13.4</b>	<b>79.9</b>
D4-SET4-20-1	3.6	14.1	74.8	2.5	13.2	81.0
D4-SET4-20-2	3.6	14.2	74.6	2.5	13.2	81.2
D4-SET4-20-3						
<b>Average</b>	<b>3.6</b>	<b>14.1</b>	<b>74.7</b>	<b>2.5</b>	<b>13.2</b>	<b>81.1</b>

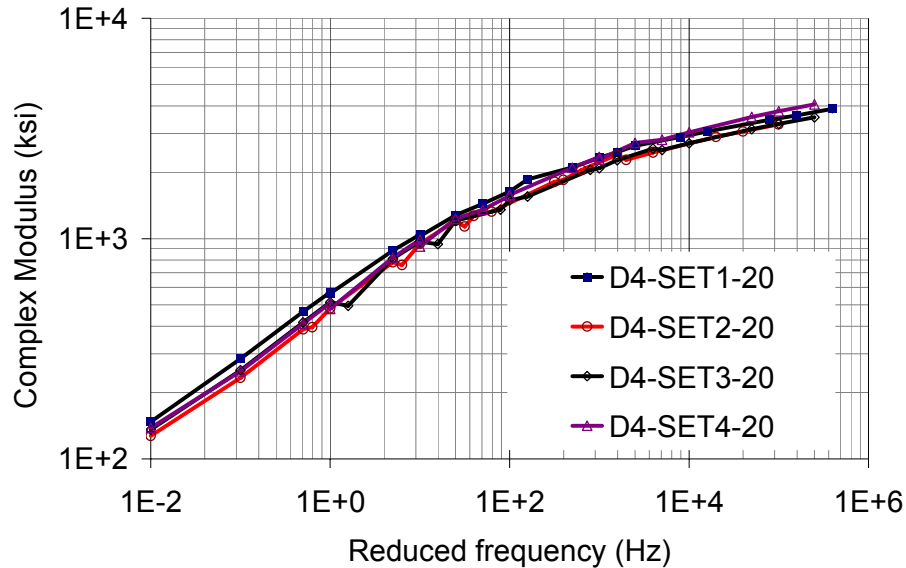


Figure 25. District 4 HMA with 20% RAP dynamic modulus master curves.

The phase angle master curves for Sets 1, 2, 3, and 4 are presented in Figure 26. Similar to phase angle results from District 1 specimens, at 20% RAP, phase angle master curves do not exhibit noticeable effects due to the RAP inclusion in the mix. Variations in the data are within experimental variability. The dynamic modulus and phase angle master curves of HMA with 20% RAP support the findings from the testing of District 1 specimens at the same level of RAP in HMA.

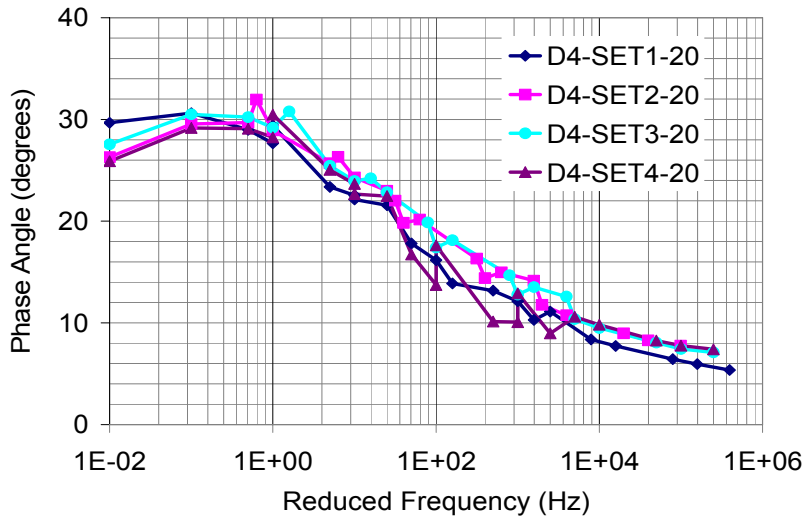


Figure 26. District 4 HMA with 20% RAP phase angles.

### 3.1.6 District 4 Mix with 40% RAP Scenario

The volumetric characteristics of the District 4 HMA sets are presented in Table 13.

Table 13. District 4 HMA with 40% RAP

	Before cutting & coring			After cutting & coring		
	Air Voids	VMA	VFA	Air Voids	VMA	VFA
D4-SET1-40-1	4.8	15.1	68.4	3.4	13.8	75.7
D4-SET1-40-2	4.6	14.9	69.4	3.2	13.7	76.3
D4-SET1-40-3	5.0	15.3	67.3	3.9	14.3	72.6
D4-SET1-40-4	4.9	15.2	67.9	3.9	14.3	72.9
<b>Average</b>	<b>4.8</b>	<b>15.1</b>	<b>68.3</b>	<b>3.6</b>	<b>14.0</b>	<b>74.4</b>
D4-SET2-40-1	4.5	15.0	70.3	3.2	13.8	77.2
D4-SET2-40-2	3.0	13.7	78.2	2.0	12.8	84.5
D4-SET2-40-3	4.0	14.6	72.6	3.0	13.7	78.3
<b>Average</b>	<b>3.8</b>	<b>14.4</b>	<b>73.7</b>	<b>2.7</b>	<b>13.5</b>	<b>79.7</b>
D4-SET3-40-1	2.9	13.6	79.0	2.0	12.8	84.3
D4-SET3-40-2	3.4	14.0	76.1	2.4	13.2	81.6
D4-SET3-40-3	4.0	14.6	72.5	2.9	13.6	78.5
<b>Average</b>	<b>3.4</b>	<b>14.1</b>	<b>75.9</b>	<b>2.5</b>	<b>13.2</b>	<b>81.5</b>
D4-SET4-40-1	2.7	13.5	79.7	1.7	12.6	86.5
D4-SET4-40-2	3.2	13.9	76.7	2.2	13.0	83.4
D4-SET4-40-3	4.1	14.7	71.8	2.9	13.7	78.4
<b>Average</b>	<b>3.4</b>	<b>14.0</b>	<b>76.1</b>	<b>2.3</b>	<b>13.1</b>	<b>82.8</b>

Figure 27 shows the dynamic modulus results for the District 4 40% RAP mixes. As the RAP percentage increases, the modulus difference in dynamic moduli between set specimens becomes more apparent. Set 1 has the highest dynamic modulus, compared to the control specimens. The effect of RAP binder on the dynamic modulus of the control specimens (Sets 2, 3, and 4) is evident. Similar to the District 1 HMA dynamic modulus

results, the high HMA dynamic modulus of Set 1 specimens suggests the possible presence of factors other than RAP content affecting the results. These factors may include changes in aggregate structure with special considerations given to the fines content of the mix, variation in degree of working binder, and volumetric characteristics as well as the selective absorption of binder into aggregate over time.

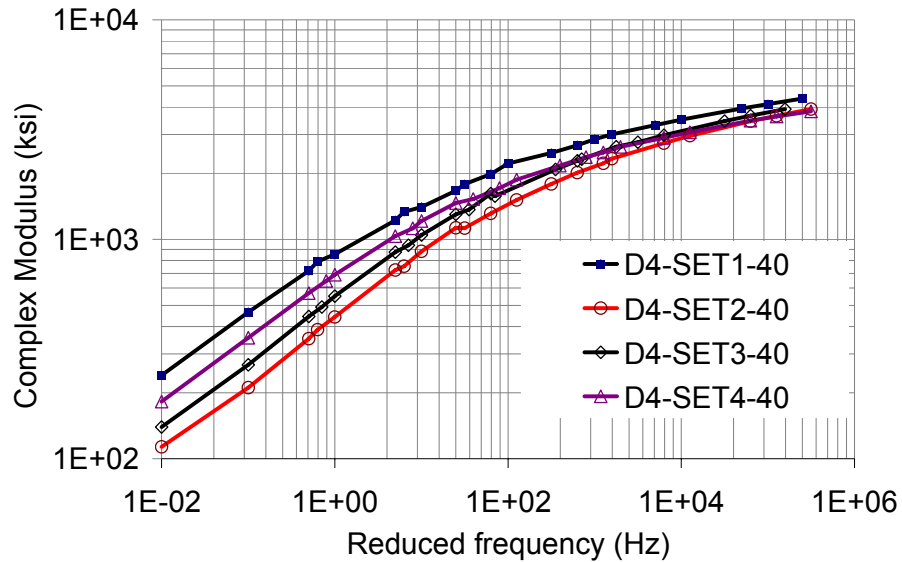


Figure 27. District 4 HMA with 40% RAP dynamic modulus master curves.

Similar observations are apparent from phase angle comparisons as well. Figure 28 contains phase angle plots. As the percentage of RAP increases from 20 to 40%, the phase angle master curves begin to separate from one another, which relates to the effect of RAP in the mix. Among the control specimens, Set 4 has the lowest phase angle compared to Set 2 and 3. This is an indication of the stiff binder effect since all other variables were held constant in these specimen sets. On the other hand, the phase angle of Set 1 is the lowest. Similar arguments can be made for the reduction in phase angle of Set 1 in terms of the potential changes in a mix with RAP addition. The viscous component of an HMA sample is binder and mastic. In a Set 1 specimen, depending on the mechanism present in RAP mixing, the mastic properties can change significantly. If RAP is not releasing binder to the mix, the fines are remaining bonded to the surface of the RAP during the mixing process. This lack of fines alters the viscous properties of the mastic and volume fraction of binder in the final mix. This may explain why the phase angle of Set 1 is lower than the others.

### 3.1.7 Comparison of District 4 HMA with 0, 20, and 40% RAP

Figure 29 presents a comparison of dynamic modulus curves for HMA with 0, 20, and 40% RAP. The increase in dynamic modulus between the 20 to 40% RAP content is significant; whereas HMA specimens with 20% RAP do not exhibit significant difference in dynamic modulus from that of specimens without RAP.

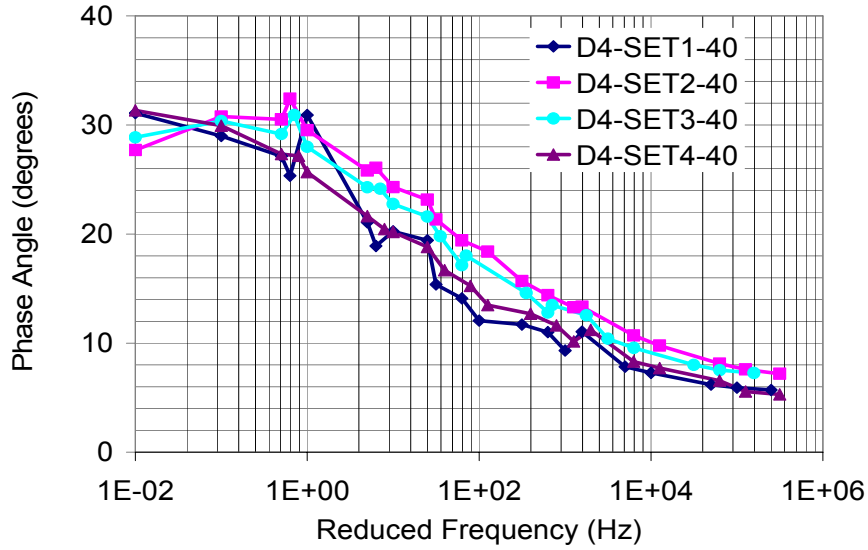


Figure 28. District 4 HMA with 40% RAP phase angles.

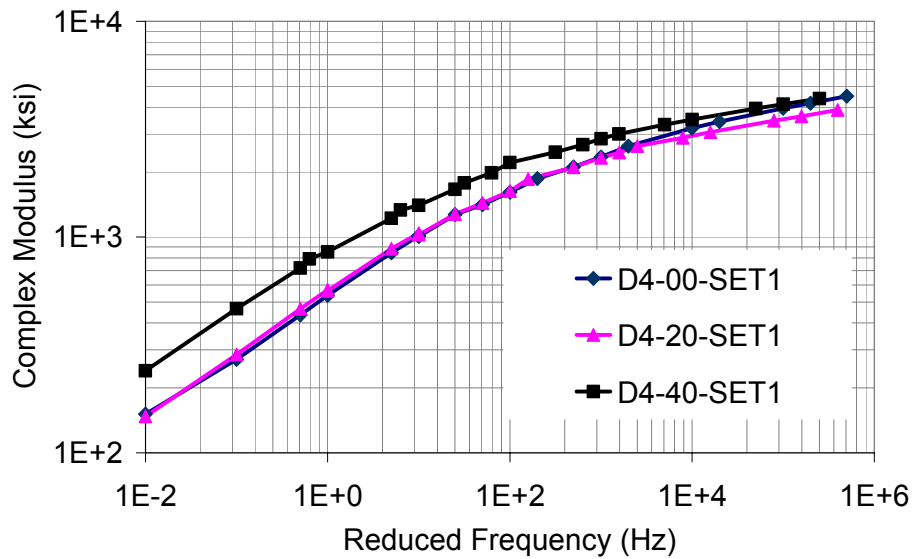


Figure 29. Dynamic modulus comparison of District 4 Set 1 HMA with 0, 20, and 40% RAP.

Figure 30 presents phase angle master curves for District 4 material, actual practice RAP percentages. As opposed to HMA dynamic modulus results, the phase angle results of 0 and 20% RAP specimens are now distinguishable. As the RAP percentage increases to 40%, the phase angle decreases further. It has to be noted that the variation in phase angle results is generally high and may mask the effect of RAP on phase angle results; particularly at high temperatures and low frequencies.

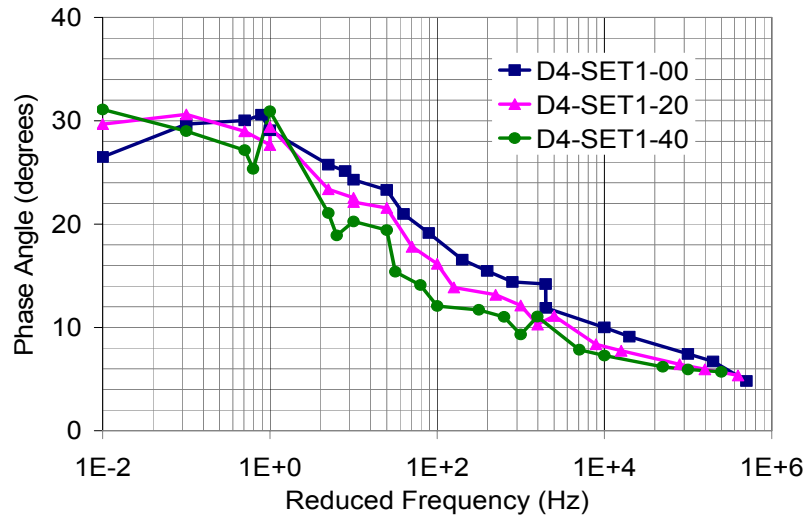


Figure 30. Phase angle comparison of 0, 20, and 40% District 4 Set 1 specimens.

### 3.1.8 Statistics of HMA Dynamic Modulus Data (District 4)

Standard deviation and coefficient of variation of HMA phase angle and dynamic modulus data are shown in Table 14. Similar to District 1 results, the statistics for District 4's HMA demonstrate a good level of repeatability, even for actual practice specimens (Set 1) where RAP mixtures can show a high coefficient of variation.

### 3.1.9 Comparison of Mixes Prepared with PG58-28 and PG64-22

The bumping of a binder grade, that is, lowering both the low and high temperature grade, called “double bumping”, of HMA containing RAP is required for mixtures having more than 20% RAP as standard practice. The objective is to compensate for the additional stiffness or brittleness of the mixture, which results from the stiff RAP binder by softening the virgin binder. To examine bumping effects, new sets of HMA specimens with 40% RAP were prepared with PG 58-28 binder and tested for HMA dynamic modulus. The results were compared to the results obtained from the same set of specimens with standard binder (PG 64-22) and also to the specimen set with no RAP. Figure 31 shows this comparison for District 1 mixes. Reduction in dynamic modulus values due to the use of double bumping binder is apparent.

Table 14. Statistics of Phase Angle and Dynamic Modulus Measurements (District 4)

	Temp (°C)	Complex Modulus		Phase Angle	
		STDEV (ksi)	COVAR	STDEV (deg)	COVAR
D4-SET1-00	-10	223.3	6.3	0.4	5.4
	4	48.9	3.0	0.3	3.0
	20	20.9	3.7	1.1	3.9
D4-SET1-20	-10	89.3	3.1	0.6	7.3
	4	110.4	6.6	0.5	3.0
	20	38.1	6.7	0.7	2.9
D4-SET2-20	-10	58.6	2.4	0.3	2.6
	4	75.8	6.0	0.9	3.0
	20	24.9	4.7	0.8	2.9
D4-SET3-20	-10	111.2	4.2	0.1	2.6
	4	21.4	1.1	0.1	3.0
	20	26.4	4.5	0.2	2.9
D4-SET4-20	-10	No statistics exist for this set. Only one good specimen.			
	4				
	20				
D4-SET1-40	-10	427.0	12.0	0.3	4.0
	4	209.1	10.3	0.3	2.0
	20	66.1	6.6	4.3	16.2
D4-SET2-40	-10	203.3	7.2	1.0	11.5
	4	219.2	15.2	0.5	2.0
	20	53.8	10.7	0.8	16.2
D4-SET3-40	-10	46.6	1.4	0.4	11.5
	4	51.7	3.9	1.0	2.0
	20	11.0	2.5	0.2	16.2
D4-SET4-40	-10	253.9	8.6	0.7	9.5
	4	205.7	12.3	0.6	8.0
	20	81.7	11.0	0.9	12.5
D4-SET1-40 w/ PG58-28	-10	46.6	1.4	1.1	9.4
	4	51.7	3.9	0.2	1.0
	20	11.0	2.5	0.5	2.1

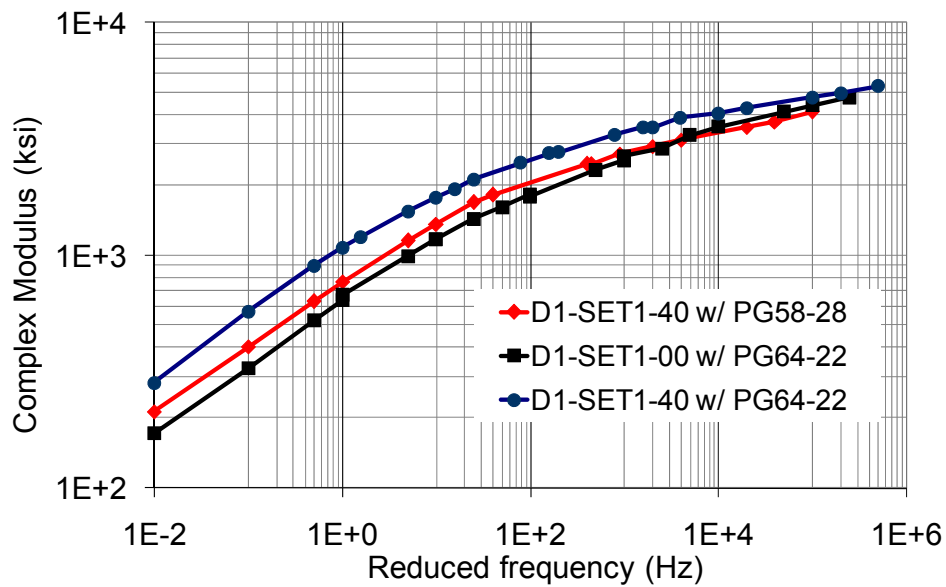


Figure 31. HMA dynamic modulus comparison when PG 58-28 binder is used (District 1 design).

The effect of softer binder grade on District 4 HMA dynamic modulus results is shown in Figure 32. The dynamic moduli of actual practice specimens (with 40% RAP) prepared with standard binder (PG 64-22) and softer binder (PG 58-28) and HMA without RAP are compared in this figure. These results are consistent with the findings from District 1 tests. Softer binder significantly reduced the HMA dynamic modulus. It can be concluded that bumping the binder grade may have the potential to reduce brittleness and premature cracking problems in HMA with high RAP. However, this observation must be supported by fracture and/or fatigue tests. Bumping the low temperature grade may reduce the modulus at intermediate temperatures as well. This effect can clearly be noted in the District 4 HMA results (Figure 32). From the dynamic modulus results, one can conclude that high temperature bumping significantly affected the stiffness of the mix. However, the effect on performance resulting from bumping the low temperature grade cannot be isolated by the dynamic modulus test. As would be expected, no conclusions could be made on the effect of low temperature bumping on the mix stiffness from the available dynamic modulus result analyses.

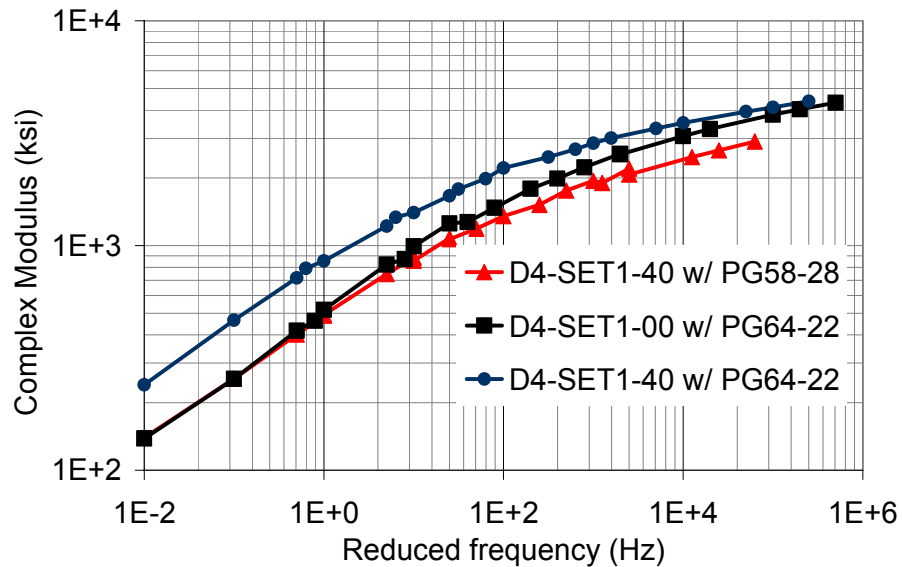


Figure 32. HMA dynamic modulus comparison when PG 58-28 binder is used (District 4 design).

### 3.1.10 Statistical Analysis of HMA Dynamic Modulus Results

In order to establish the test repeatability and the effect of various RAP percentages, a statistical analysis was conducted for the dynamic modulus test results. The first step was to verify the test repeatability. The same analysis procedure is used to examine the effect of the different RAP percentages. It can also be used to test between different sets of mixture.

First, a model shown in equation 1 was used to fit the dynamic modulus data. It was assumed that the dynamic modulus,  $G^*$ , is a function of frequency,  $f$ , and a dummy variable,  $D$ .

$$\text{Log}(G) = a + b \cdot D + c \cdot \text{Log}(f) \quad (1)$$

where,

$G$  = dynamic modulus;

D = dummy variable (=0 for G from specimen 1 group; =1 for G from specimen 2 group; =2 for G from specimen 3 group);  
 f = frequency; and  
 a, b, c = fitted regression coefficients.

The regression analysis with 95% confidence level was then performed on the selected data sets. The null hypothesis is  $b=0$  which means that there is no significant difference between the selected data sets. An example data set for the repeatability of the 0% case from District 4 between two specimens is given below in Table 15. The data were reorganized as shown in Table 16 and a dummy variable D was assigned as 0 and 1 for each data set. Table 17 shows the strength of the data correlation to the model. The  $R^2$  value of 0.954 suggests a strong correlation between the measured data with model. Table 18 shows the inference of the model coefficients. The test statistics (t stat) or the p-values of the coefficient b were used to determine whether two sets of measured data are statistically the same. As shown in Table 18, at the 5% level, the coefficient b is insignificantly different from zero since the p-value is greater than 0.05. If the  $b=0$ , there is no statistical difference between the two data sets.

Table 15. Dynamic Modulus of Two Replicate Specimens with no RAP (District 4)

Specimen 1		Specimen 2	
Red. F (Hz)	G (ksi)	Red. F (Hz)	G (ksi)
0.010	145.499	0.010	157.094
0.100	263.782	0.100	277.953
0.500	425.264	0.500	446.189
1.000	524.735	0.794	558.776
1.585	576.060	1.000	549.647
5.000	827.347	5.000	861.717
10.000	992.540	7.943	975.289
15.849	1034.586	10.000	1035.277
25.000	1243.355	25.000	1301.359
79.261	1452.456	39.724	1371.149
158.489	1655.507	79.433	1570.972
316.228	1918.662	100.000	1810.367
792.447	2159.479	397.164	2065.831
1584.893	2394.729	794.328	2310.910
3162.278	2737.256	1000.000	2540.185
3962.249	2725.185	1985.829	2660.720
15814.551	3330.011	5001.000	3058.775
31622.777	3590.093	10000.000	3271.010
158113.883	4144.552	50000.000	3750.503
316227.766	4390.748	100000.000	3952.806

The summarized regression analyses of all Districts 1 and 4 data sets are presented in Tables 19 and 20, respectively. While checking for test repeatability, it was found that, generally, the test had very good repeatability because the p-values are all greater than 0.05. However, Set 1 mix with 20% had a value of 0.05.

Table 16. Data for Fitting the Statistical Model

Log (G)	D	Log (f)	Log (G)	D	Log (f)
2.163	0	-2	2.196	1	-2
2.421	0	-1	2.444	1	-1
2.629	0	-0.301	2.65	1	-0.301
2.72	0	0	2.747	1	-0.1
2.76	0	0.2	2.74	1	0
2.918	0	0.699	2.935	1	0.699
2.997	0	1	2.989	1	0.9
3.015	0	1.2	3.015	1	1
3.095	0	1.398	3.114	1	1.398
3.162	0	1.899	3.137	1	1.599
3.219	0	2.2	3.196	1	1.9
3.283	0	2.5	3.258	1	2
3.334	0	2.899	3.315	1	2.599
3.379	0	3.2	3.364	1	2.9
3.437	0	3.5	3.405	1	3
3.435	0	3.598	3.425	1	3.298
3.522	0	4.199	3.486	1	3.699
3.555	0	4.5	3.515	1	4
3.617	0	5.199	3.574	1	4.699
3.643	0	5.5	3.597	1	5
3.675	0	5.898	3.629	1	5.398

Table 17. Measures of the Strength of Association of the Model

Regression Statistics	
Multiple R	0.9767
R <sup>2</sup>	0.9540
Adjusted R <sup>2</sup>	0.9516
Standard Error	0.0887
Observations	42

Table 18. Inferences about the Individual Coefficients of the Model

	Coefficients	Standard Error	t stat	P-value
a	2.725	0.024	112.201	0.000
b	0.039	0.027	1.405	0.168
c	0.189	0.007	28.443	0.000

The results show that for District 1 materials, at a 95% confidence level, there is a statistically significant difference between when 0% and 20% and also between 0% and 40% RAP in the mix. In addition, at 20% RAP, the results also show that there is a statistically significant difference between each mix set. This contradicts the findings reported in NCHRP 9-12, which suggests low percentages of RAP such as 20% do not significantly affect the HMA stiffness (McDaniel 2000). The significant difference between actual practice and other sets could be explained as the relative amount of working binder being different due to incomplete blending and differences in the aging of the binder in the various RAP materials used. The same observation was found, but more pronounced, when the 40% RAP was used due to the presence of stiffer binder. For HMA with 40% RAP, the effect of increased fine content and lower VMA become more pronounced, hence, may contribute to the increase in the HMA dynamic modulus..

Statistical analysis of dynamic modulus results for the HMA with District 4 materials showed that mixes with 20% RAP were not significantly different than those for mixes with no RAP. However, dynamic moduli of the mixes with 40% RAP were significantly different than those of mixes with no RAP. The only District 4 test which did not have good repeatability was the Set 2 mixture with 40% RAP. The difference in RAP effect on HMA between the districts could be due to the difference in the RAP binder stiffness of each District.

Table 19. p-value of Coefficient b for District 1

	0% Set 1	20% Set 1	20% Set 2	20% Set 3	20% Set 4	40% Set 1	40% Set 2	40% Set 3	40% Set 4
0% Set 1	0.394	0.001				5.8E-06			
20% Set 1		0.050	0.004	0.050	0.014				
20% Set 2			0.655						
20% Set 3				0.914					
20% Set 4					0.444				
40% Set 1						0.346	0.001	0.003	0.001
40% Set 2							0.015		
40% Set 3								0.095	
40% Set 4									0.260

Table 20. p-value of Coefficient b for District 4

	0% Set 1	20% Set 1	20% Set 2	20% Set 3	20% Set 4	40% Set 1	40% Set 2	40% Set 3	40% Set 4
0% Set 1	0.168	0.966				4.1E-05			
20% Set 1		0.552	0.550	0.570	0.842				
20% Set 2			0.144						
20% Set 3				0.950					
20% Set 4					0.599				
40% Set 1						0.574	1.2E-04	4.0E-05	0.038
40% Set 2							0.018		
40% Set 3								0.998	
40% Set 4									0.017

### 3.1.11 Application of Hirsch Model to RAP Mixture Volumetrics.

Some of the major factors that can cause the difference in dynamic modulus values between Set 1 and other sets with recovered aggregates are related to volumetric characteristics, binder stiffness, selective absorption, and aggregate gradation. A combination of all four factors can also influence mixture behavior. The Hirsch model allows these factors to be studied in the model to evaluate their individual impact on the resulting dynamic modulus of the HMA. It is apparent from the magnitude of the dynamic modulus increase when RAP was added that the change in binder stiffness only may not explain the magnitude of the difference.

The extent of the binder stiffness effect can be determined from a comparison between Sets 2, 3, and 4; where all variables were held constant, except binder stiffness. Sets 2, 3, and 4 mixtures were designed with similar aggregate gradations with the same RAP content. However, aggregate gradation of the actual practice specimens, Set 1, can deviate from target gradation if RAP is not dispersing fines similar to Sets 2, 3 and 4. Additionally, the batching aggregate gradation may be skewed as Set 1 is using actual practice RAP and the other mixes are using recovered aggregate. Volumetric characteristics can be quantified by air voids, VMA, or VFA. VMA involves information about both air voids and binder volume fraction. The average VMA of each specimen tested for dynamic modulus is shown in Figure 33. The VMA of Set 1 was calculated based on the assumption of 100% working binder. There are minor variations in specimen VMA that can be related to specimen preparation process. Therefore, it is safe to compare the dynamic modulus values of these specimens.

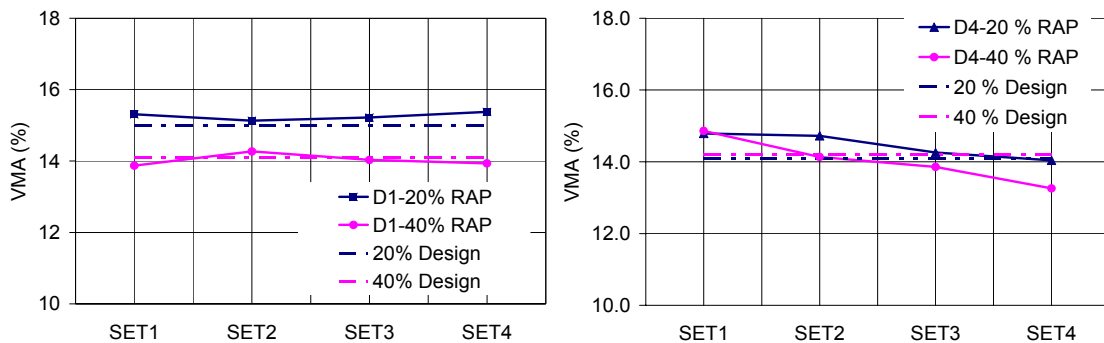


Figure 33. Specimen's VMA variation (Districts 1 and 4).

VMA is believed to influence the overall HMA behavior. Hence, accurate calculation of VMA, especially with high RAP mixes, is essential. The relatively high dynamic modulus of actual practice specimens could not be explained by the increase in RAP binder stiffness only. It was apparent that an additional mechanism may be contributing to that increase. One of these mechanisms could be the changes in HMA volumetric characteristics when RAP was added as compared to using recovered aggregates. Figure 33 presents VMA values for each specimen set. Calculating VMA for HMA without RAP is straightforward, VMA is the volume ratio of the sum of effective binder and air voids to the total volume of the mix. However, the calculated effective binder can be ambiguous. When RAP is used, it is unclear how much RAP binder is working effectively in the mix. If RAP binder does not blend with additional virgin binder, the volume of effective binder decreases. In addition, the presence of RAP binder affects the mixing and the compaction processes, and hence, the overall mixture stiffness. These hypothetical volumetric relationships are shown in Figure 34.

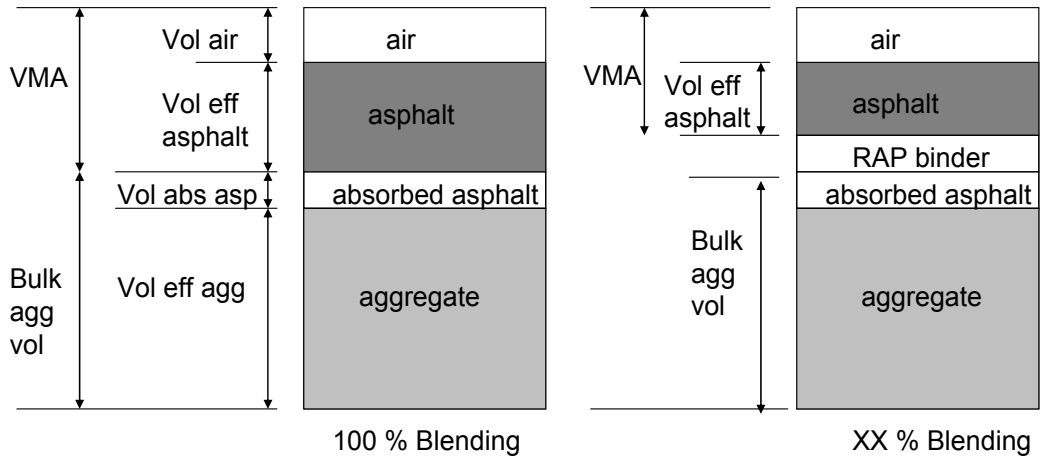


Figure 34. Volumetric relationships for different blending scenarios.

Accounting for the effect of non-blended RAP binder on the volumetric characteristics of RAP particles and total binder content, VMA was recalculated for various blending scenarios. Figure 35 shows the variation of VMA with various assumptions of RAP binder blending for Districts 1 and 4 designs. As shown in the figure, VMA and actual binder content deviate further from the design value as different working binder assumptions are made. The reduction rate is more rapid for the HMA with 40% RAP as RAP binder contributes more to the effective binder content and bulk aggregate volume. VMA decrease in actual practice specimens (Set 1) is shown with a hypothetical method of calculation that can partly explain the significant increase in the dynamic moduli of these specimens.

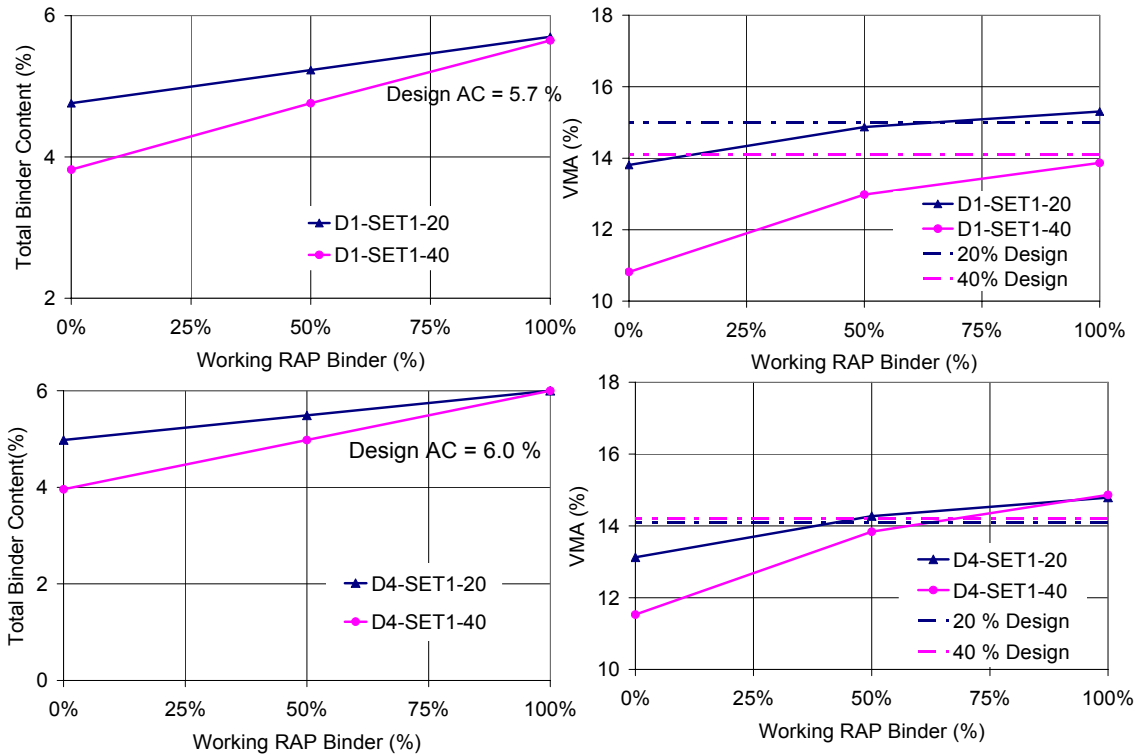


Figure 35. VMA variation with varying RAP binder blending assumptions for Districts 1 and 4 designs.

### 3. 2 RESIDUAL BINDER EVALUATION

In addition to the HMA dynamic modulus measurements, the complex modulus of the binder itself was also measured. The binder modulus values were compared to the modulus values of the HMA dynamic modulus specimens using the Hirsch model. The binder characterization was conducted at the North Central States SuperPave Center at Purdue University.

The binders blends that were prepared represented the various binder blending conditions that are assumed to occur during mixing in this research. The binders tested include the following: PG 64-22 binder, which represents the black rock or 0% blending case; binders recovered utilizing the rotovapor extraction process; binders from both Districts 1 and 4 RAP sources; and blended binders. The recovered Districts 1 and 4 binders were blended at 20% and 40% with PG 64-22 binder. The blending at 20% and 40% are not directly comparable to the amount of binder actually present in the mix. In order to resolve this issue, the 20% and 40% values were averaged to create a 30% blend which is closer to the amount of stiff RAP binder assumed to be working in a 40% RAP mix. The PG 64-22 binder, 20% and 40% blended District 1 binder, and 20% and 40% blended District 4 binder were also aged using the rolling thin film oven (RTFO) prior to testing. The non-blended recovered binders were not aged using the RTFO. The complex moduli of the RTFO aged binders represent that in the HMA after mixing, short term aging, and compaction.

Binder complex modulus testing was conducted in accordance with the following testing suite: Testing temperature ranges from 60.8 °F (16°C) to 147.2 °F (64°C) at 10.8 °F (6°C) increments; and testing frequency ranges from 0.1 Hz to 27.3 Hz at the following frequency values, 0.1, 0.2, 0.4, 0.8, 1.6, 3.2, 6.4, 13, and 27.3 Hz. Figure 36 shows the complex shear modulus master curves for original PG 64-22 (subjected to RTFO aging) and RAP binder blends. To supplement the data collected on the 20% and 40% RAP binder blends, a curve representing a 30% blend data was interpolated by averaging the 20% and 40% binder blend data. The 30% RAP binder blend is closer to the actual percentage of RAP binder in a 40% RAP mixture. From the master curves, RAP binder blends are much stiffer than PG 64-22 for both Districts' binders. The effect of increasing the RAP binder is evident in the case of District 1 RAP binder; whereas for the District 4's RAP, the 20% and 40% RAP binder blends did not show a significant difference in complex modulus. This may raise a question as to the compatibility between District 4 recovered binder and the PG 64-22 binder that may affect the resulting homogeneity in the binder.

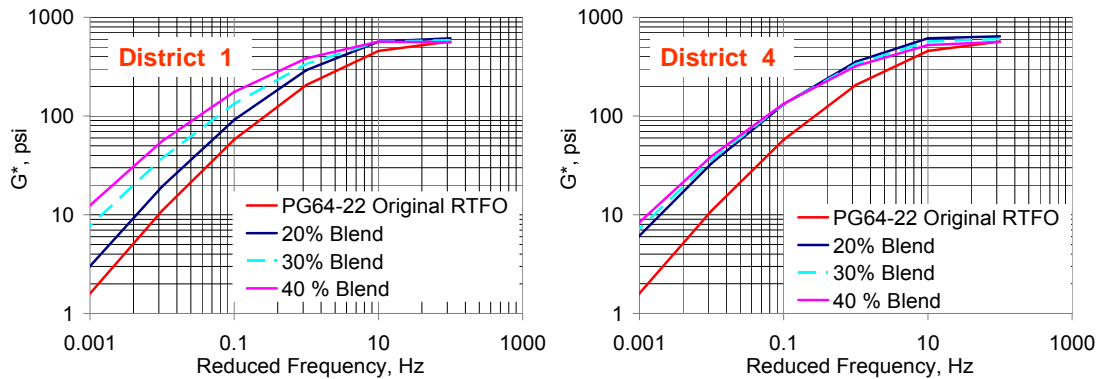


Figure 36. Complex modulus of PG 64-22 and RAP binder blends (20, 30, and 40%).

The measured binder complex shear moduli may be compared to the backcalculated values from the HMA dynamic moduli. There are numerous techniques to perform backcalculation, one of which is the Hirsch model. The Hirsch model is the simplest micromechanical model relying on law of mixtures and is commonly used for HMA modulus predictions. It is based on series and parallel configurations of different states of materials in a composite material such as HMA. These materials, or states, in our case, are aggregate, binder, and voids. The attractiveness of this method comes not only from its simplicity; but also consideration of very commonly and easily measured HMA volumetric parameters such as VMA and VFA. The final form of the Hirsch model for HMA is given in equations 2 and 3. The objective is to determine the binder shear modulus for the HMA modulus measured at each frequency and temperature; VMA and VFA are known. Details of the model development and use in HMA are described in the work by Christensen et al. (2003).

$$|E^*|_{mix} = P_c [4,200,000(1 - VMA/100) + 3 \times |G^*|_{binder} \left(\frac{VFA \times VMA}{10,000}\right)] + (1 - P_c) \left[ \frac{1 - VMA/100}{4,200,000} + \frac{VMA}{VFA \times 3 \times |G^*|_{binder}} \right]^{-1} \quad (2)$$

$$P_c = \frac{(20 + \frac{VFA \times 3 \times |G^*|_{binder}}{VMA})^{0.58}}{650 + (\frac{VFA \times 3 \times |G^*|_{binder}}{VMA})^{0.58}} \quad (3)$$

where,

$|E^*|$  = mixture compressive dynamic modulus (ksi)

$|G^*|$  = binder shear complex modulus (psi)

$P_c$  = Aggregate contact volume.

Backcalculation was performed using HMA dynamic moduli obtained for Districts 1 and 4 specimens with 40% RAP only. The effect of RAP binder is expected to be more pronounced at this percentage of RAP. Backcalculated binder moduli for Sets 1, 2, 3, and 4 are presented in Figure 37 for Districts 1 and 4. In addition to backcalculated values, measured binder shear modulus values were also plotted in the same figure as solid data points. Due to problems encountered during DSR testing, only four measured data points were selected. The authors believe that the DSR values measured at frequencies greater than 1Hz were not accurate due to device capacity limitations. Within the valid data range, a match between measured and backcalculated binder moduli were sought. As seen in the figures, there is a good match for District 1 blends for PG 64-22 and Set 2, and 30% binder blend and Set 4 pairs. Sets 2 and 4 were the control specimens with 0 and 30% RAP binder. However, District 4 blends exhibited a poor match between the measured and backcalculated modulus values. The Hirsch model is not overly sensitive to VMA variations. A 1% variation in VMA did not significantly alter the backcalculation results.

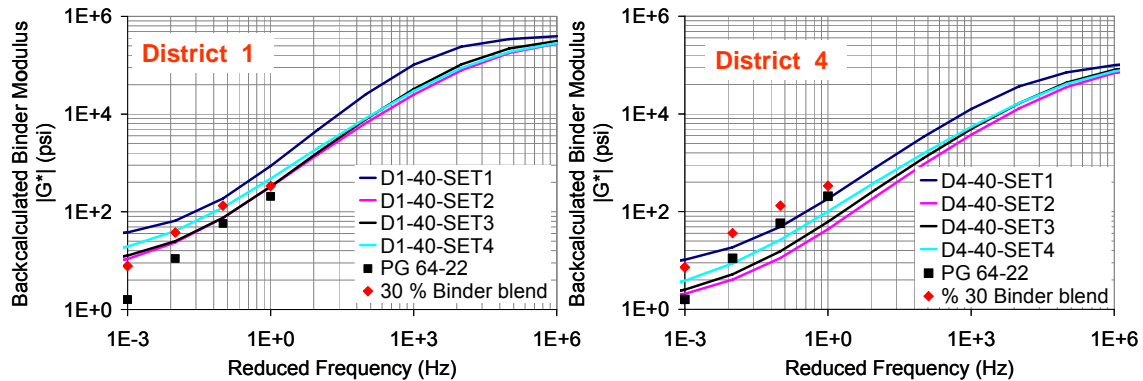


Figure 37. Comparison of backcalculated and measured binder modulus.

It is worthwhile to note some of the shortcomings of the Hirsch model when it is used for the purpose of this study, which is evaluating the complex shear modulus of RAP and virgin materials. Firstly, although it has been shown to provide good matches to  $E^*$  data, it is the simplest micromechanical model available. Secondly, and most importantly, the calculation of two of the three parameters used in the model, VMA and VFA, is ambiguous for HMA containing RAP; the percent of blending and percent of “black rock” binder are unknown. Finally, the model makes an assumption for the calculation of compressive (or extensional) modulus from shear modulus using linear elastic theory and a constant Poisson’s ratio. In the formula, the extensional modulus is replaced by  $3|G^*|$ ; assuming a Poisson’s ratio of 0.5 (for incompressible materials). This assumption, used for linear elastic materials, may not necessarily be true for binder. A linear elastic relationship may not necessarily hold for time dependent materials such as HMA and binder. This could induce some error into the Hirsch model calculation; however the level of error is not known. For these reasons, and the possible compatibility issue with the District 4 binder, the reliability of the Hirsch model calculation is unknown. It cannot be supported that the District 1 match, which supports complete binder blending, is a more accurate representation than the District 4 data, which indicates the original PG 64-22 to be stiffer than the binder in the HMA. This is not possible unless there are binder compatibility issues, which are beyond the scope of this research. For these reasons, the modulus backcalculations using the Hirsch model cannot indicate with any certainty what blending was achieved in the HMA.

### 3. 3 EVALUATION OF STRIPPING SUSCEPTIBILITY

Stripping resistance of the HMA containing RAP (specimen Set 1 only) was evaluated in accordance with the Illinois modified AASHTO T 283-02 specifications. Indirect tensile strength of dry and conditioned specimens was measured and a visual stripping inspection was conducted on cracked specimens. Figure 38 depicts the extent of stripping on some of the dry and conditioned specimens.

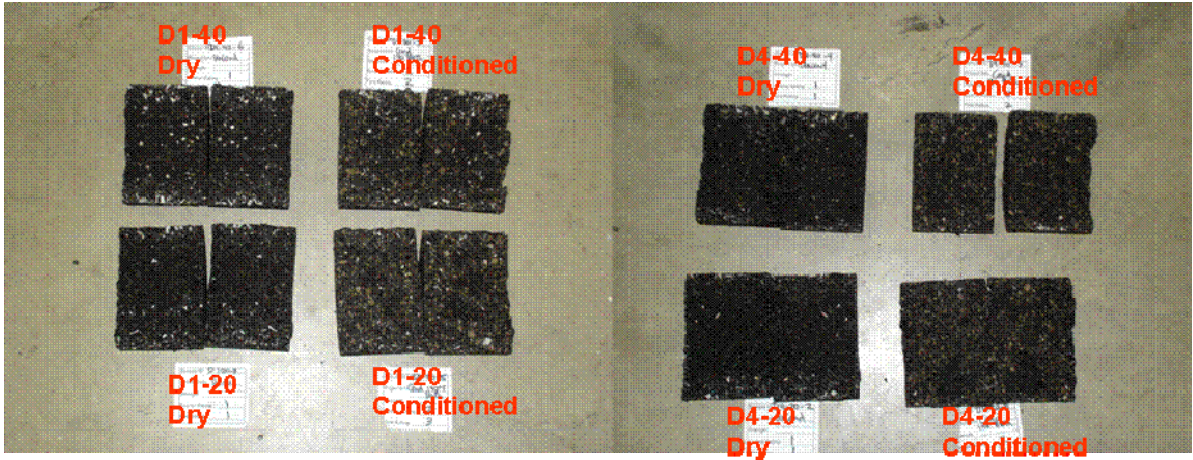


Figure 38. Fractured dry and conditioned specimens illustrating the extent of stripping.

A summary of tensile strength ratio and the stripping rating of specimens tested in this study is given in Table 21. The results show that the HMA specimens tested in this study exhibited moderate to severe stripping potential. This resulted in significant tensile strength reduction of conditioned specimens. This effect is more pronounced with District 1 materials.

The stripping rating of dry and conditioned specimens indicates the relative amount of stripping occurring in HMA specimens. The stripping scale is between 1 and 3; where 1 indicates no stripping or slight stripping, 2 indicates moderate stripping, and 3 indicates severe stripping. The fine and coarse aggregates in the stripping samples were evaluated separately and results were reported for both portions of the mix.

Table 21. Tensile Strength Ratio (TSR) and Stripping Rating of HMA containing RAP

Specimen SET	Tensile Strength Ratio (TSR)	Dry Stripping Rating (fine/coarse)	Conditioned Stripping Rating (fine/coarse)
D1-SET1-00	59.3	1/1	2/3
D1-SET1-20	73.3	1/1	2/3
D1-SET1-40	67.6	1/1	2/2
D4-SET1-00	75.8	1/1	2/3
D4-SET1-20	83.2	1/1	2/3
D4-SET1-40	80.7	1/1	2/2

Figure 39 shows the tensile strength of dry and conditioned specimens tested at room temperature. It was noted that the tensile strength of both dry and conditioned specimens increase as a function of RAP percentage. As was previously discussed with the dynamic modulus results, this increase can be attributed to several factors. One of these factors would be the HMA strength gain due to the presence of aged binder. As the percentage of aged binder increases, strength increases. Although aggregate gradation may have an effect on indirect tensile strength results as HMA with RAP could be coarser; it is well documented that indirect tensile strength test depends significantly on the binder

used in the mix. More details about indirect tensile strength test results and specimens (volumetric characteristics, saturation ratios, etc.) are presented in APPENDIX D.

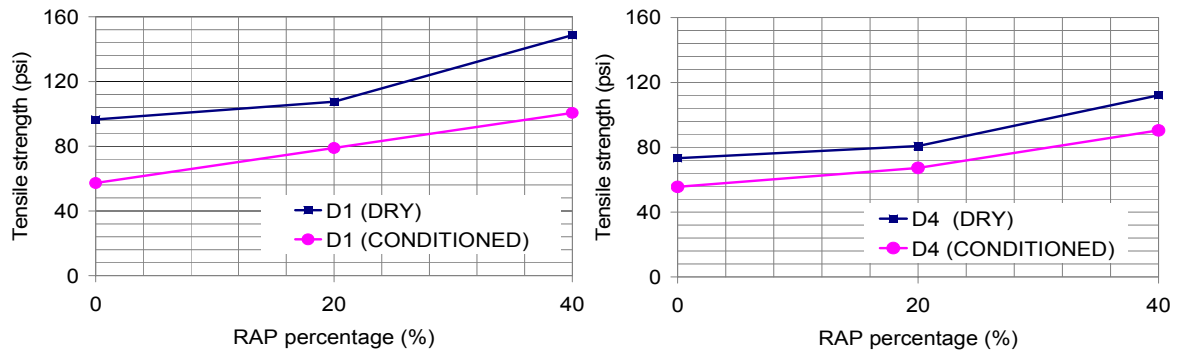


Figure 39. Tensile strength of dry and conditioned HMA with RAP.

Limited test results may suggest it was evident that the tensile strength ratio increases for mixtures containing RAP (Figure 40). However, Tensile strength ratio shows some fluctuations for specimens with 20% and 40% RAP. This may be due to the fact that these mixtures vary in volumetrics and aggregate gradation. In addition, there is experimental variation within the tensile strength tests. Although the limited data suggests that RAP particles may be more resistant to moisture damage than the virgin materials in the mixture, a valid comparison may not be made for mixtures containing RAP at this point. Selective absorption of binder into the aggregate may produce a bond, which helps in resisting stripping. It is also possible that incomplete blending of the binders is occurring which would cause double coating of the RAP particles during mixing. This would improve the stripping susceptibility of the RAP particles. Because selective absorption does not take place immediately, freshly mixed virgin aggregates and binder is expected to have a weaker bond than RAP materials; and thus could result in greater stripping susceptibility.

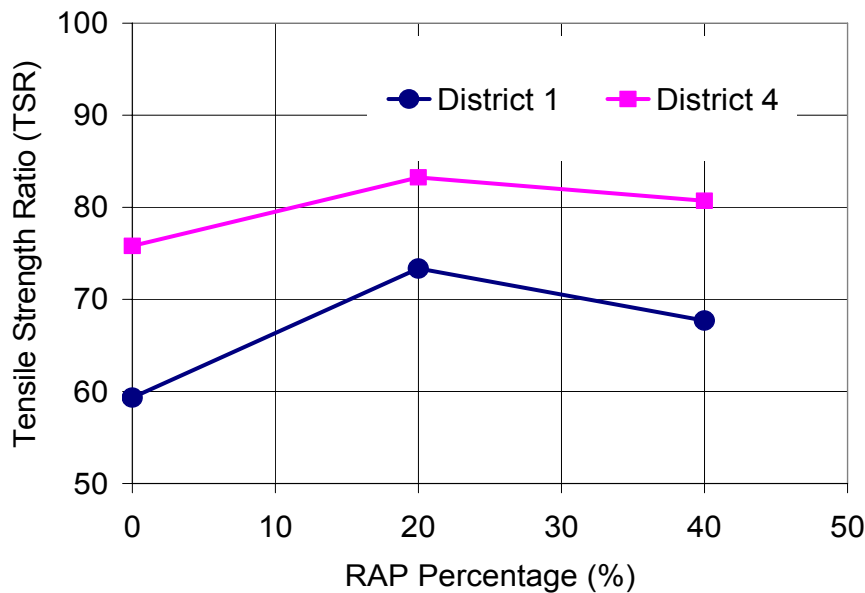


Figure 40. Tensile strength ratio of HMA with varying RAP percentages.

### 3. 4 RAP PARTICLE-MASTIC BONDING AND BLENDING: ESEM ANALYSIS

As part of the investigation of working binder, electron microscopy was utilized to determine the mechanisms visibly occurring with the mixing of RAP binder and virgin binder. The first step in determining the mechanisms of binder mixing was to determine the binder film thickness on aggregate particles. Next, further SEM images were studied to investigate if the virgin and RAP binder could be uniquely identified.

To investigate the binder film thickness within the HMA composite system, the images were captured at a low magnification and at subsequently higher levels of magnification. Figures 41a through c show the images obtained using the wet mode of ESEM (ESEM). Figure 41a presents an image of a 1.2mm by 1mm area. The darker color represents the asphalt binder and the lighter color represents the aggregate. As shown in the figure, a mastic strip was surrounded by two larger size aggregates. The image was further zoomed in to a 300 $\mu$ m to 250 $\mu$ m area, Figure 41 b, in the center of the mastic strip. This shows that the mastic was composed of binder and different sizes of fine material. Figure 41c shows further zooming into the image to a 60 $\mu$ m by 50 $\mu$ m area. The scale bar present in the image represents the length of 10 $\mu$ m, which is the theoretical film thickness. However, there is no clear boundary between binder and fines. The bright color that appears in the figure is due to overcharging by the electron beam on the specimen. This typically occurs when the highly accelerated voltage electron beam scans over the non-conducting sample.

Although the image obtained from the ESEM reveals that the HMA is a composite material composed of larger size aggregate and mastic, there is no direct evidence to show the material structure between fines and binder. To further investigate the microstructure between fines and binder requires higher quality images that ESEM could not produce. Therefore, the same specimen was coated with a thin 4nm film of gold-palladium to create a conductive surface. This metal layer is thin enough that all the micro-texture at the surface of HMA is preserved and observed under the conventional SEM.

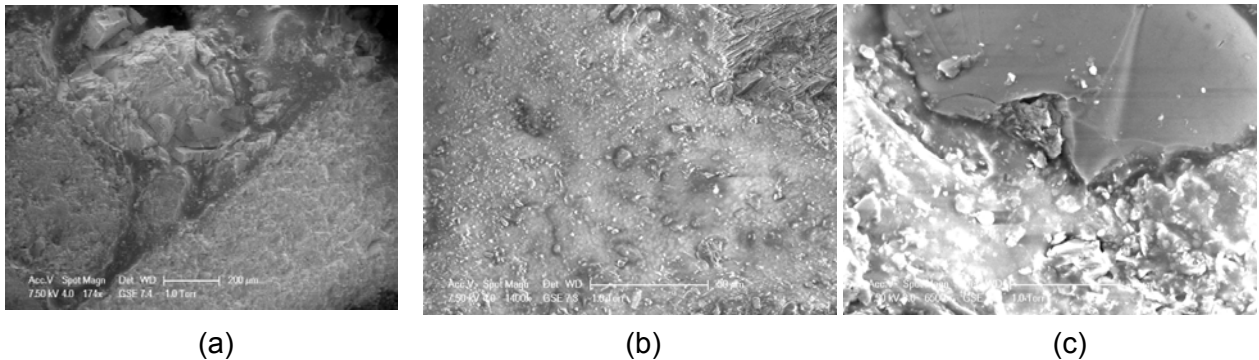


Figure 41. SEM images showing surface morphology.

When the microscope is operated at high vacuum mode, two types of electrons which produce different images of the sample can be collected. The two electron imaging methods are secondary electron (SE) and backscattered electron (BSE) imaging. The secondary electron image is most useful for examining surface structure and gives the best image resolution. Depending on the initial size of the primary beam and other conditions such as the composition of the sample, accelerating voltage, position of specimen relative to the detector, a SE signal can resolve surface structures to the order of 10nm or finer. This signal will show the topographical image of the specimen. Additionally, the BSE image arises due to different atomic numbers within a material. That is, if a sample is composed of

two or more different elements with significantly different atomic numbers, it will produce an image that shows differential contrast of the elements despite a uniform topology. Elements that are of a higher atomic number will produce more backscattered electrons and will therefore appear brighter than other elements with smaller atomic numbers. Using the advantages of these two types of images, it is possible to perform a better investigation of the microstructure of HMA samples.

An illustration showing both types of images can be found in Figure 42. Figure 42a shows the SE image of the HMA surface morphology. The image shows a darker binder strip embedded between two larger aggregate which exhibit a lighter color; and air voids can be observed. Figure 42b presents a BSE image. This image reveals even more detail of the composition of the specimen structure. This increased detail is due to the fact that the binder is composed of hydrocarbons. The aggregates are composed of calcium, silicon, magnesium, etc., which have a larger atomic number compared to binder elements which is manifested as a different brightness. The air voids have a small atomic number as well, which also appear differently from the binder and aggregate. Therefore, the aggregate appears as the lightest color in the image, the binder shows darker color, and the air voids show the darkest color. However, because air voids and binder are both shown in black, in backscattered images sometimes the edge of air voids cannot be distinguished from the binder. If one combines both secondary and backscattered electron images, the air voids and binder can easily be differentiated.

Figure 43 presents the microstructure image of HMA specimen using conventional SEM. The secondary and backscattered electron images are presented side by side from low to high magnification. Figures 43a, c, e, and g show the image of SE evolution from low magnification (2400 $\mu\text{m}$  by 1800 $\mu\text{m}$ ) to high magnification (48 $\mu\text{m}$  by 36 $\mu\text{m}$ ). In addition, BSE images (Figure 43b, d, f, and h) were also presented. From both image types, it clearly shows that up to the resolution of 10 $\mu\text{m}$ , the morphology of HMA still presents a combination of aggregate and mastic. Furthermore, the lens was focused to the right side of the image in Figure 43h where the density of fines was higher and further magnified to investigate the film thickness of the HMA. This result shows the current film thickness assumption is not accurate to assess the true film thickness in the HMA composite system.

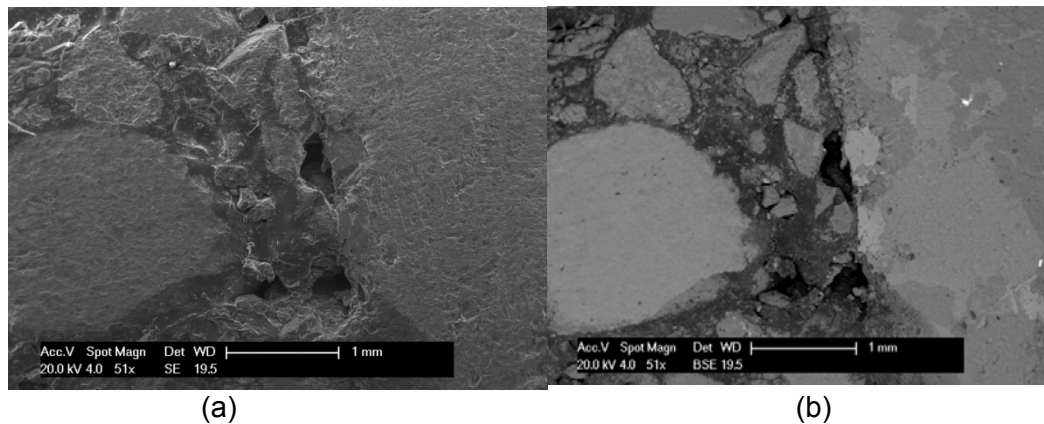
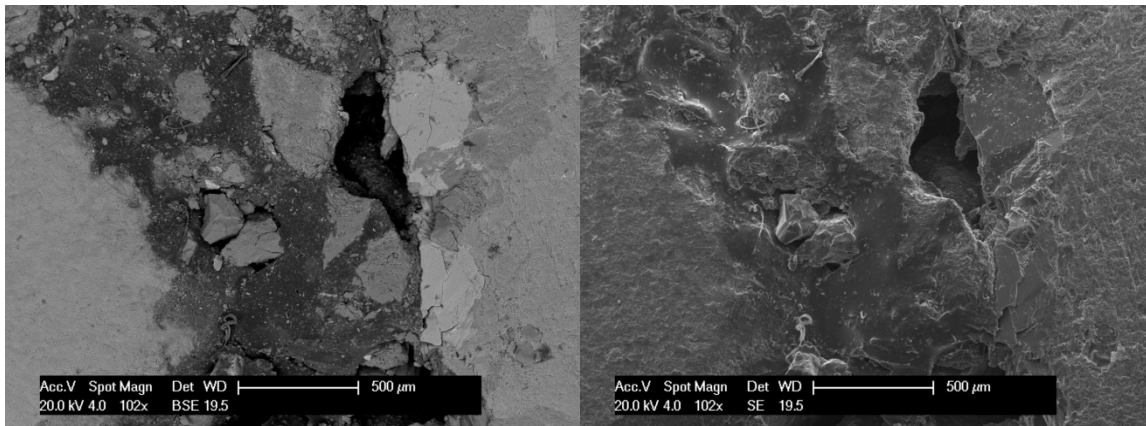
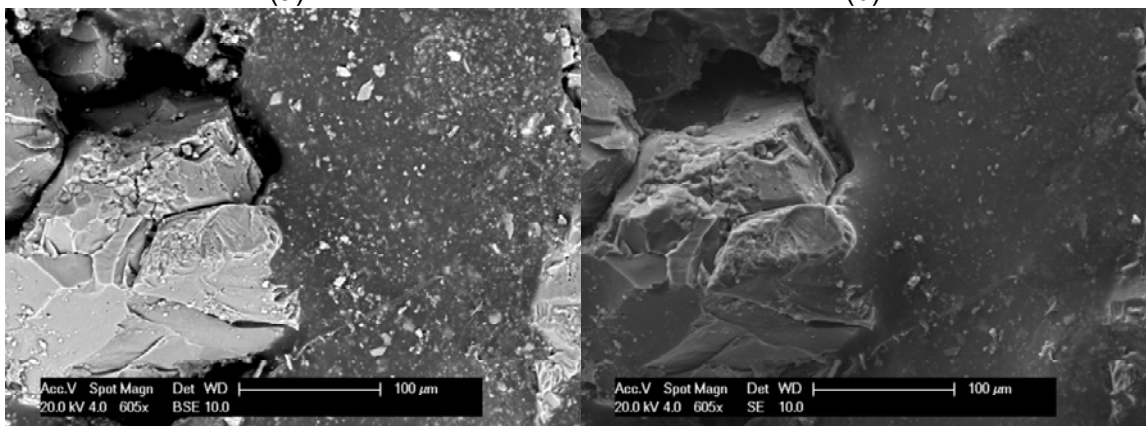


Figure 42. Image of HMA surface.



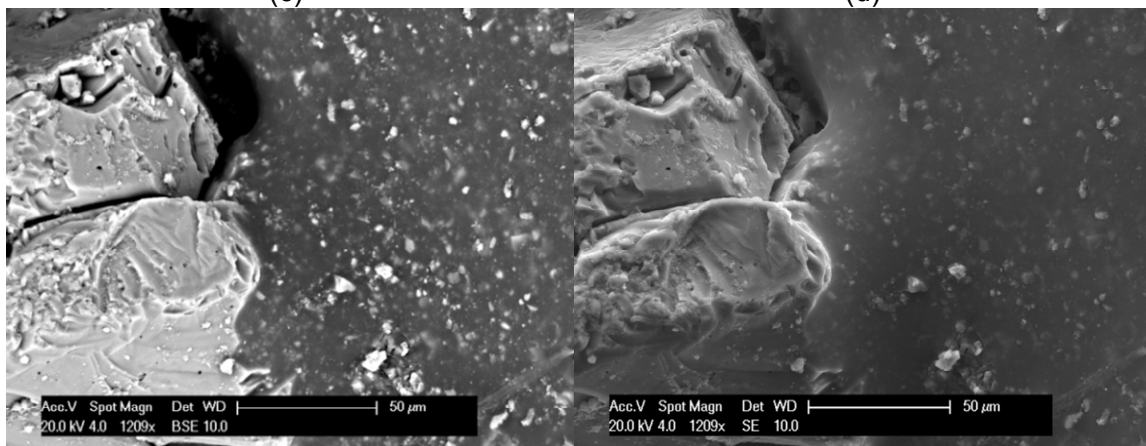
(a)

(b)



(c)

(d)



(e)

(f)

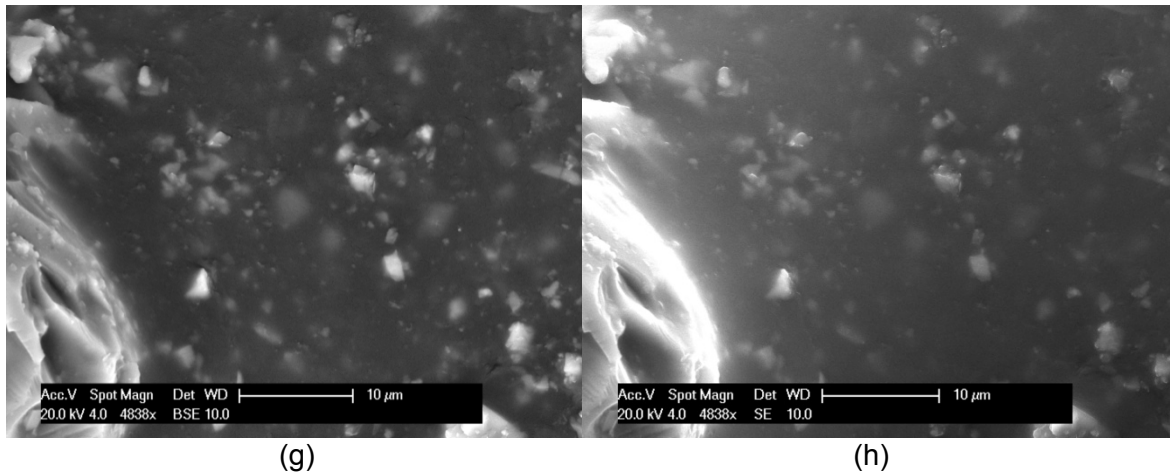
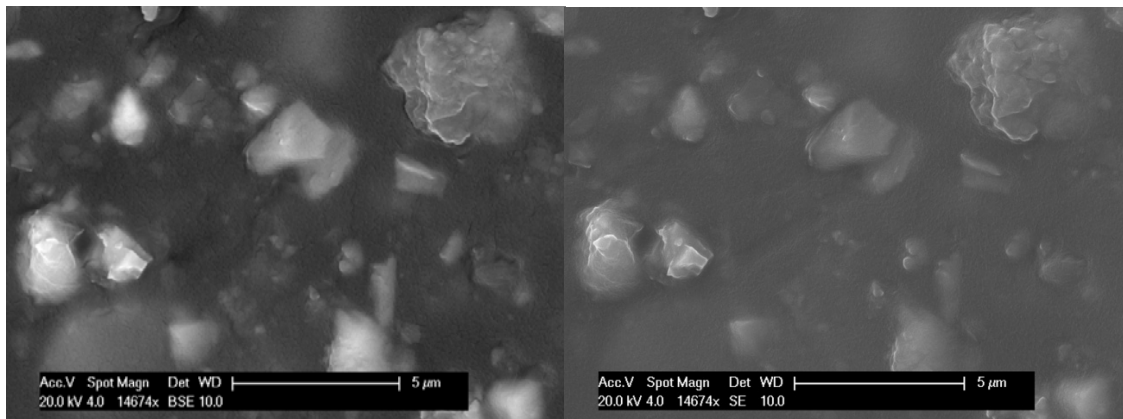


Figure 43. Image of HMA surface binder film.

Figure 44 shows the resolution from  $5\mu\text{m}$  up to  $500\text{nm}$ , the images at  $5\mu\text{m}$  start showing a clear two phase structure. Again, the images on the left are SE and those on the right are BSE. The fines were shown as a substrate embedded in the binder matrix. The benefit of using BSE detector is clear at such a small scale. In Figure 44b, more fine particles were revealed than images taken using SE in Figure 44a. From these two figures, it appears that there is no direct contact between the fine particles. With further zooming into the area where two fine particles appear to have direct contact, Figures 44c and d, the two fine particles actually do not have direct contact. The film thickness which was assumed in the aforementioned work can now be calculated. The distance between two particles is less than or equal to  $2\mu\text{m}$ . This value is five times less than the theoretical calculation, unless the size of filler is defined and considered as part of the mastic.

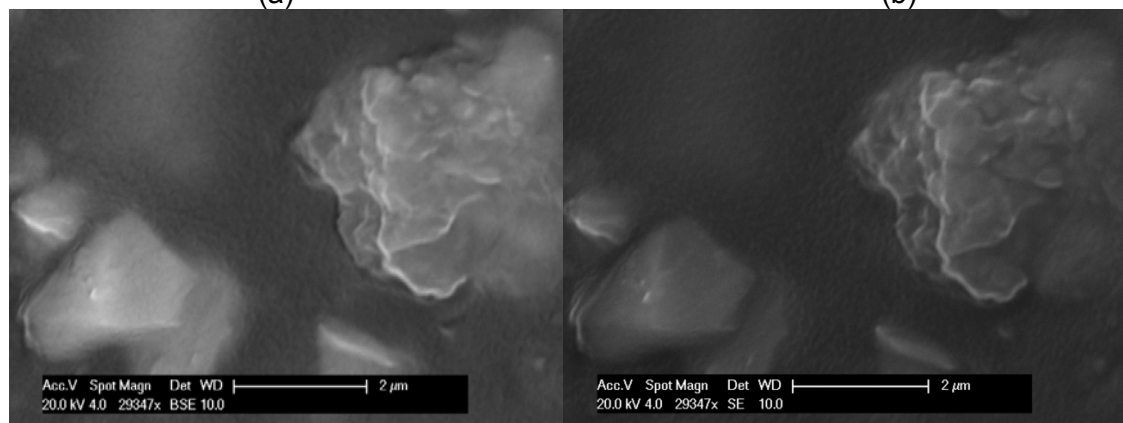
From the SEM procedures, the meaning of “film thickness” can be discussed in terms of what is seen in the mixtures. If film thickness is defined as the binder between any aggregates then the film thickness would be  $2\mu\text{m}$ . However, if the film thickness is defined as the binder between any two particles retained on a specific sieve the film thickness value becomes a moving target. If the second definition is applied to film thickness then a completely different value is obtained. An alternative to film thickness is to rename what has classically been referred to as film thickness. As has been shown in the SEM images the distance of the theoretical value of film thickness contains fine materials. Thus it may be wiser to refer to this as a ‘mastic thickness’ while reserving the term film thickness for the binder between the two fine particles.

Microscopy images were initially captured and evaluated to determine the amount of blending occurring between RAP particles and the virgin binder added to the mix. The amount of blending was not observable in the SEM images. Once it was deemed not possible to determine the blending from the initial SEM images, an alternative SEM method was investigated to determine if this method was promising for future work in identifying the film thickness of the coated aggregate, determining aggregate absorption/ binder penetration depth, and verifying the virgin/ aged binder intermixing phenomena.



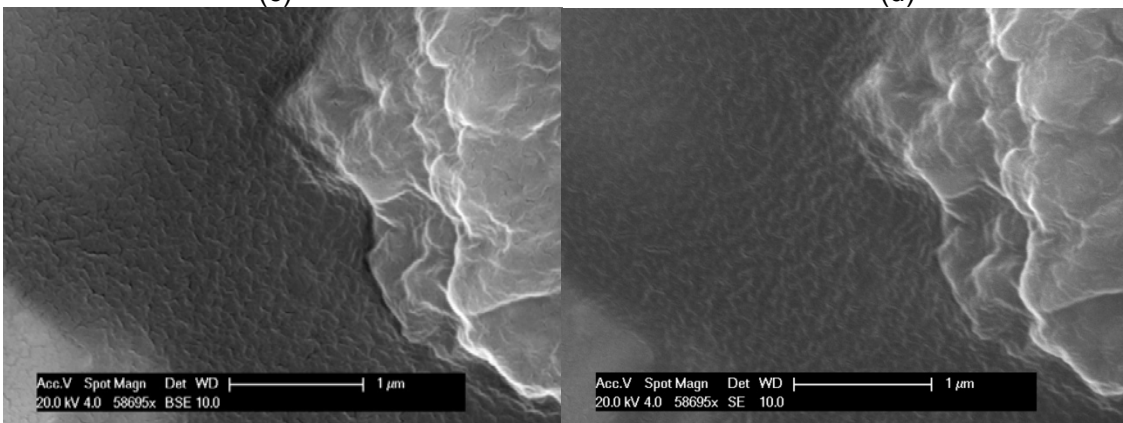
(a)

(b)



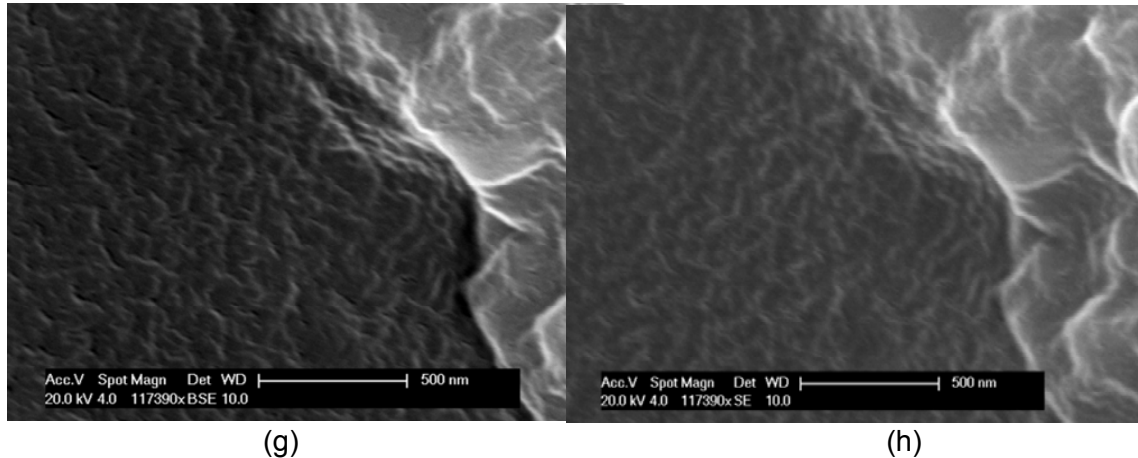
(c)

(d)



(e)

(f)



(g) (h)  
Figure 44. Image of HMA surface at high resolution.

To detect binder blending, Lee et al. (1983) used trace amounts of titanium incorporated with an AR-2000 paving grade asphalt binder before mixing with RAP material. The resulting SEM image and the corresponding Energy Dispersive X-Ray Spectroscopy (EDS) scan showed a clear interlayer of virgin binder and aged asphalt. It was concluded that the method had significant potential for verifying the micro scale interaction between virgin binder and RAP material.

The rationale of using SEM to study bitumen-aggregate interface relies on the different elements which constitute asphalt binder and aggregate. As the electron beam of the SEM is scanned across the sample surface, it generates X-ray fluorescence from the atoms in its path. The energy of each X-ray photon is characteristic of the element which produced it. The EDS microanalysis system collects the X-rays, sorts and plots them by energy, and automatically identifies and labels the elements responsible for the peaks in this energy distribution. The EDS data are typically compared with computer-generated standards to produce a full quantitative analysis showing the sample composition. Therefore, if the chemical composition of the asphalt and aggregate are known, the EDS can be used to map those elements and determine the configuration of asphalt and aggregate. Some representative petroleum elemental analysis is presented in Table 22 (Plancher et al. 1976). It shows that the major component of the asphalt binder is carbon. Table 23 shows the typical chemical composition of sandstone and limestone. The main composition of sandstone and limestone are silicon (Si) and calcium (Ca), respectively. The data output from the EDS analysis plots the original spectrum showing the number of X-rays collected at each energy level. Maps of element distributions over the areas of interest and quantitative composition tables can also be provided as necessary.

As part of a preliminary study, two aggregate types (limestone and sandstone) and a PG 64-22 virgin binder were investigated. The virgin binder and virgin aggregate were first heated to 155°C for one hr. Then, the aggregate was thoroughly mixed with heated binder. The coated aggregates were then placed on a steel sieve and allowed to drip the excess binder in the oven for an additional two hrs. The coated aggregates were then held at room temperature for 24 hrs to allow adhesion and binder absorption into aggregate. After 24 hrs, the coated aggregates were placed in liquid nitrogen, cooled, and then cut to expose the interface at the perimeter of the specimen. Figures 45a and b show the SEM image of sandstone in BSE and SE mode, respectively. Figure 45a clearly shows the binder absorption into the pores of the sandstone. The X-Ray analysis using EDS was employed to closely investigate these regions and map the chemical elements. As shown in Figure

46, the silicon and carbon element distribution was detected and the results were mapped with original SE image and shown in Figure 47.

Table 22. Elemental Analysis of Representative Petroleum Asphalts

Element	Mexican	Ark-La.	Boscam	Calif.
Carbon (%)	83.77	85.78	82.90	86.77
Hydrogen (%)	9.91	10.19	10.45	10.94
Nitrogen (%)	0.28	0.26	0.78	1.10
Sulfur (%)	5.25	3.41	5.43	0.99
Oxygen (%)	0.77	0.36	0.29	0.20
Vanadium (ppm)	180.0	7.0	1380.0	4.0
Nickel (ppm)	22.0	0.4	109.0	6.0

Table 23. Chemical Composition of Sandstone and Limestone

Sandstone		Limestone	
Chemical Composition	(%)	Chemical Composition	(%)
SiO <sub>2</sub>	93-94	CaCO <sub>3</sub>	97.30
Fe <sub>2</sub> O <sub>3</sub>	1.5-1.6	MgCO <sub>3</sub>	0.40
Al <sub>2</sub> O <sub>3</sub>	1.4-1.5	Al <sub>2</sub> O <sub>3</sub>	0.50
Na <sub>2</sub> O & Kro	1.0-1.2	SiO <sub>2</sub>	1.70
CaO	0.8-0.9		
MgO	0.2-0.25		
Loss On Ignition (LOI)	1.0-1.2%		

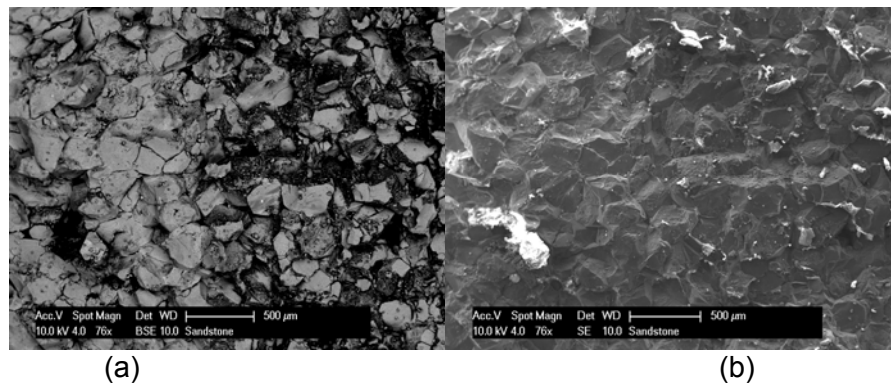
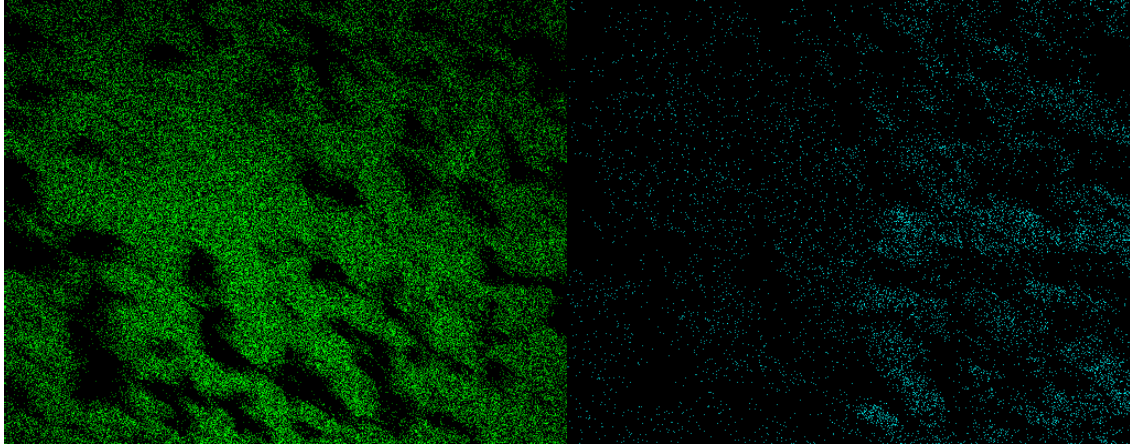
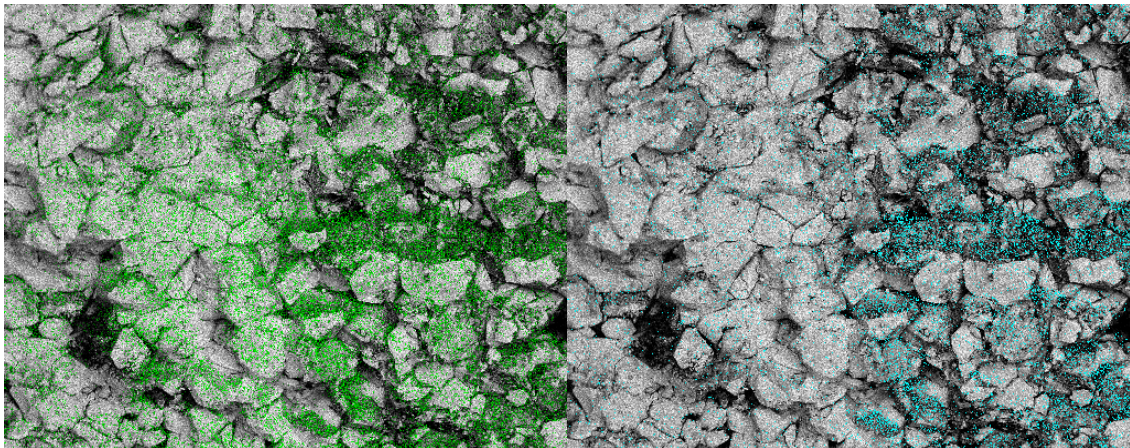


Figure 45. SEM view of PG 64-22 absorption into sandstone in (a) BSE mode and (b) in SE mode.



(a) (b)  
 Figure 46. EDS x-ray scan of PG 64-22 coated sandstone cross-section (a) silicon element distribution and (b) carbon element distribution.



(a) (b)  
 Figure 47. Mapping EDS element distribution results on the SE image for sandstone (a) silicon element distribution and (b) carbon element distribution.

The same observation was performed with coated limestone. In this case, a much denser structure was observed in the limestone compared to that of sandstone. No distinct absorption phenomenon was observed. Figure 48 shows the asphalt binder coating the outside aggregate surface. The EDS analysis, Figures 49 and 50, shows the distribution of carbon and calcium in the area of interest. From the EDS data plot, the carbon elements mainly concentrate at the upper part of the picture (asphalt film) and calcium elements have a high concentration in the lower part of the picture (limestone). In Figure 50a, some carbon elements were detected at the bottom part of the specimen and this could be caused by the absorption of the binder. Alternatively the limestone used in the study has minor carbon compound that was also measured by the EDS and appears as “noise” in the measurements. The carbon in the limestone makes it difficult to accurately determine the absorption depth. This technique has potential to detect the film thickness outside the aggregate.



Figure 48. SEM view of PG 64-22 absorption into limestone in SE mode.

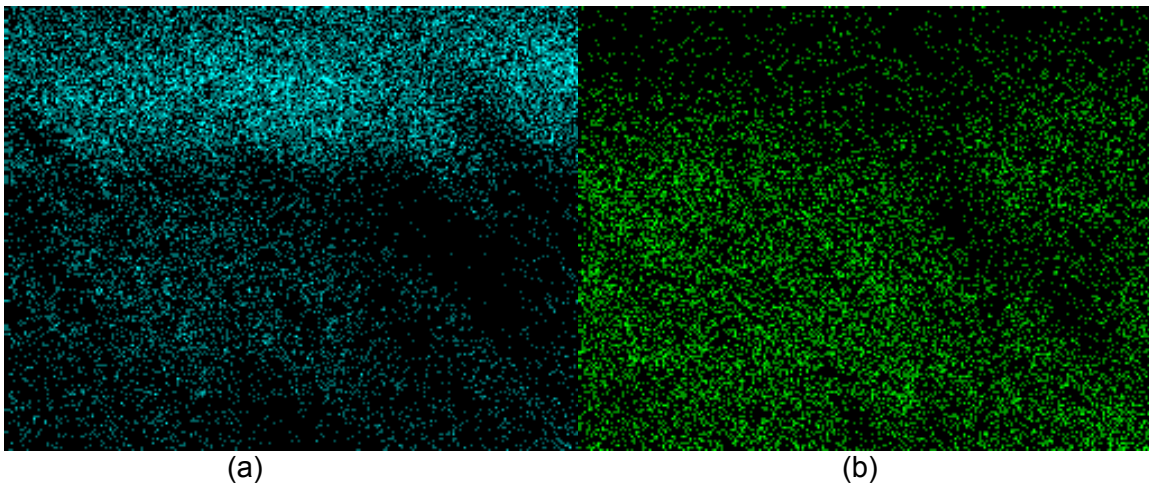


Figure 49. EDS x-ray scan of PG 64-22 coated limestone cross-section (a) silicon element distribution and (b) carbon element distribution.

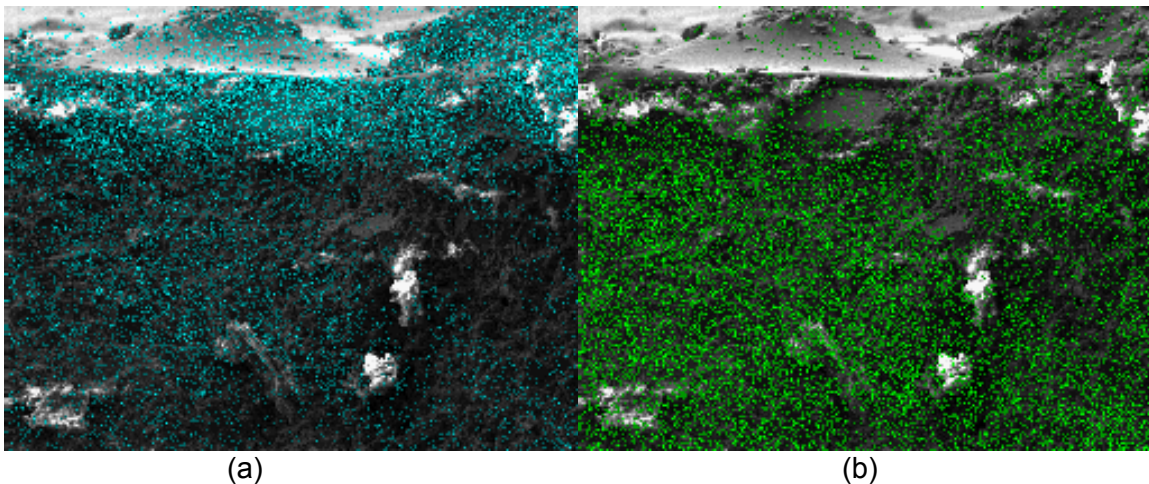


Figure 50. Mapping EDS element distribution SE image for limestone (a) silicon element distribution and (b) carbon element distribution.

### 3. 5 FRACTURE ENERGY ANALYSIS

In addition to the dynamic modulus testing, fracture tests were performed to investigate the RAP effect on HMA low temperature behavior. The fracture energy testing results can be used to characterize the thermal cracking characteristics of the mix. Only District 1 materials were tested for fracture energy.

The fracture energy was first tested with the SCB test due to the more fundamental nature of the test compared to the DCT test. The effect of double bumping was only investigated using the SCB test. It was found that as the RAP content in the HMA increases, the fracture energy of the mix decreases. Although some variations in VMA and percent passing the #200 sieve exist between various mixtures tested herein. However, these variations were not significant enough to alter the comparative findings of the fracture energy analysis. This finding was in agreement with the work reported by Li, et al. (2008). A summary of the PG 64-22 SCB results is presented in Table 24.

Table 24. SCB Fracture Energy Results (PG 64-22)

Temperature (°C)	RAP (%)	Fracture Energy (J/m <sup>2</sup> )	Average Fracture Energy (J/m <sup>2</sup> )	Binder RAP/Total (%)
0	0	1925.4	1620.5	0
		1516		
		1420.1		
	20	1202.6	1243.0	16
		1283.4		
		1199.6		
	40	702.8	750.2	32
		797.6		
		762.5		
-12	0	805.7	986.2	0
		1036.3		
		1116.6		
	20	795.7	915.7	16
		895.5		
		1055.9		
	40	892	651.6	32
		635.2		
		427.7		

Graphs comparing the average values of the load (kN) vs. CMOD (mm) for the SCB tests are presented in Figures 51 and 52 for 0°C and -12°C, respectively. These graphs indicate a noticeable difference in the fracture energy depending on the RAP content of the mix. Therefore, the effect of double bumping the binder grade to offset the lack of fracture energy was investigated.

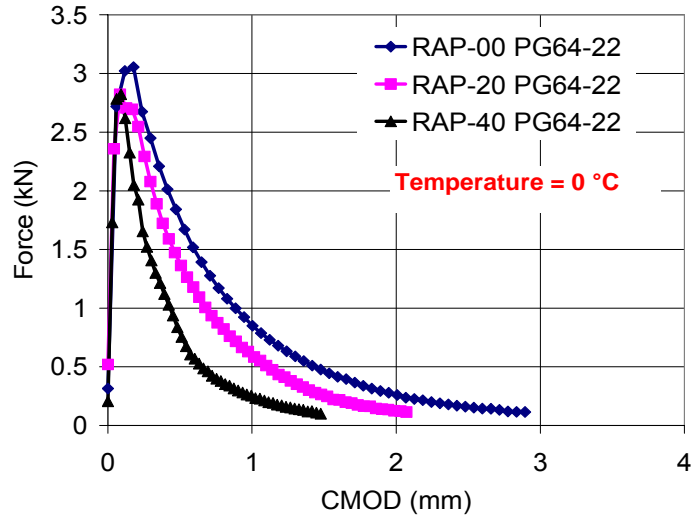


Figure 51. Average load vs. CMOD curves for 0 °C SCB test.

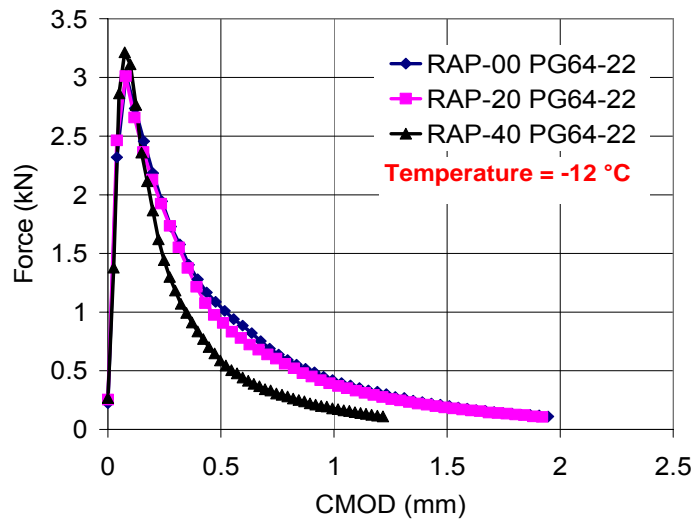


Figure 52. Average load vs. CMOD curves for -12 °C SCB test.

In addition to the SCB tests, DCT tests were conducted to check the consistency of the results. Similar trends were observed between the two fracture test methods. Table 25 presents the DCT fracture energy results. The average fracture energy results of the DCT testing were slightly higher than those of the SCB tests at 0°C. However, the results were slightly lower at -12°C. The average Load vs. CMOD curves for the 0°C and -12°C DCT tests are presented in Figures 53 and 54, respectively.

Since the test results are comparable and follow the same trends, the effect of RAP on HMA is evident. However, due to the limited number of specimens tested, conducting an extensive fracture energy testing is recommended.

Table 25. DCT Fracture Energy Results (PG 64-22)

Temperature (°C)	RAP (%)	Fracture Energy (J/m <sup>2</sup> )	Average Fracture Energy (J/m <sup>2</sup> )	Binder RAP/Total (%)
0	0	1631.2	1639.8	0
		1648.4		
	20	1009.5	1332.5	16
		1514		
		1474		
	40	781.9	843.4	32
767.9				
980.4				
-12	0	551.1	596.7	0
		600.9		
		638.2		
	20	588.5	532.5	16
		576.3		
		432.6		
	40	449.3	437.7	32
		432.1		
		431.7		

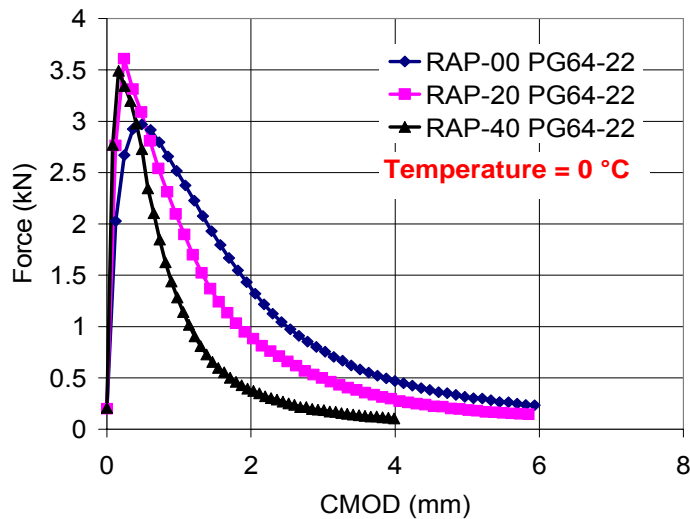


Figure 53. Average load vs. CMOD curves for DCT testing at 0°C.

The effect of double bumping on fracture energy was also studied. The double bumping investigation was conducted using only SCB specimens. Greater fracture energy values were observed in the specimens containing PG 58-28 than in the specimens containing PG 64-22, Table 26. These results are expected as the softer PG 58-28 binder allows the HMA specimen to distort more (or to provide for greater flexibility to absorb more energy thus reducing crack occurrence.) under loading; hence, absorbing more energy during crack propagation.

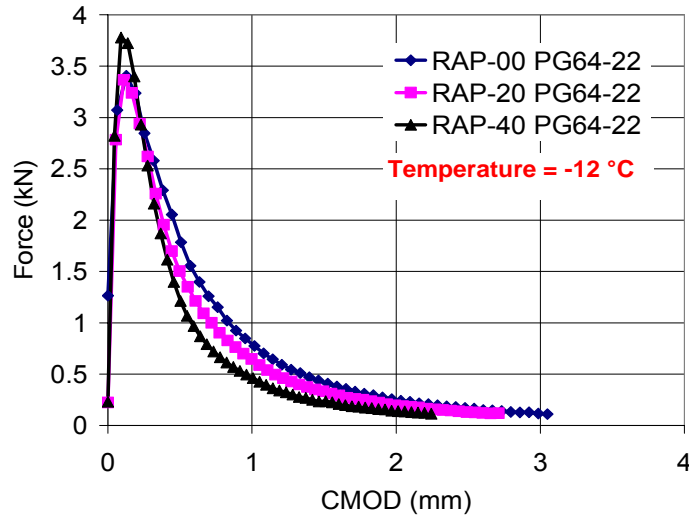


Figure 54. Average load vs. CMOD curves for DCT testing at -12°C.

Table 26. SCB Fracture Energy Results (PG 58-28)

Temperature (°C)	RAP (%)	Fracture Energy (J/m <sup>2</sup> )	Average Fracture Energy (J/m <sup>2</sup> )	Binder RAP/Total (%)
0	0	2581.3	2845.3	0
		2344.5		
		2530		
	20	2063.5	1787.7	16
		1490.3		
		1809.4		
	40	1466.7	1364.7	32
		1541.4		
		1086.1		
-12	0	878.6	1097.7	0
		1071.9		
		1342.7		
	20	899.5	988.2	16
		1038.5		
		1026.5		
	40	686.9	638.8	32
		522.2		
		707.2		

To compare the fracture energy results between HMA with PG 64-22 binder to that with PG 58-28 binder using 40% RAP in the mix, the effect of double bumping can be determined. At testing temperatures, -12 °C and 0 °C, the HMA specimens with PG 58-28 and 40% RAP exhibited lower fracture energy than the HMA specimens with PG 64-22 and 0% RAP. Table 27 presents the average SCB fracture energies. The results indicate that double bumping offsets the impact of RAP at 0 °C; the SCB fracture energy was 1365 J/m<sup>2</sup>, for 40% RAP, which is higher than the fracture energy of mixes with 20% RAP and

unbumped binder (1243 J/m<sup>2</sup>). However, the impact of double bumping was not as effective at the lower temperature of -12 °C where one would anticipate greater thermal cracking susceptibility. Below glassy transition temperature (T<sub>g</sub>) the viscoelastic nature of the binder is minimized and the binder becomes brittle. This should not imply that the low temperature binder grade should or should not be changed. Before any strong conclusions or design recommendations can be made, more extensive fracture testing is recommended. The testing may require fracture testing of specimens prepared with a PG 58-22 binder in order to determine if double bumping or only single bumping is needed. Additionally, testing at lower temperatures such as -30, and -24 °C will also be beneficial to determining if double bumping is required.

Table 27. SCB Fracture Energy Comparison

Temperature (°C)	RAP (%)	Average Fracture Energy PG 64-22 Samples (J/m <sup>2</sup> )	Average Fracture Energy PG 58-28 Samples (J/m <sup>2</sup> )	Binder RAP/Total (%)
0	0	1620.5	2845.3	0
	20	1243.0	1787.7	16
	40	750.2	1364.7	32
-12	0	986.2	1097.7	0
	20	915.7	988.2	16
	40	651.6	638.8	32

## CHAPTER 4 SUMMARY AND CONCLUSIONS

The main objective of this research was to investigate procedures that had the potential to indicate the amount of working binder contributed by RAP to HMA during mixing. To accomplish this, six various mixture formulas were prepared according to current practice for two RAP sources at 0, 20, and 40% RAP in the HMA. One set of samples was prepared in accordance with current mix design practice. Three sets of samples, prepared with recovered RAP materials (binder and aggregate) and virgin materials, were designed to represent differing amounts of working binder in the RAP. No RAP materials were used in stockpile form in these control samples. The proportion of recovered RAP binder in the control samples was adjusted in an attempt to simulate the effect produced when the RAP used in an actual practice mix provided different amounts of working RAP binder in a mixture. The control samples were mixed with recovered RAP binder at 0, 50, and 100% working RAP binder blends. These three values represent the variation from the “black

rock” case where 0% of the RAP binder is released from the RAP to combine with the virgin binder, to the completely working case where 100% of the effective RAP binder combines with the added virgin binder.

The mix design procedure produced an important and practical outcome that provides insight into the consideration of working binder in RAP. None of the mix designs with RAP, specifically the HMA with 40% RAP mix designs, required additional total binder content (RAP binder plus virgin binder added) to achieve the same density of HMA with no RAP. The asphalt binder content of the virgin HMA design was reproduced for the HMA with RAP. If the RAP binder was not working, the total asphalt content would have significantly increased with higher amounts of RAP in the HMA. The fact that the total asphalt content did not significantly increase indicates that the RAP binder was combined with the virgin binder to a very high extent.

The dynamic modulus test was selected to investigate the amount of working binder in the HMA. It was felt that comparisons of the dynamic modulus results between the actual practice mix and those of the control samples with a known amount of working binder would provide comparative results. Such results would show which blending assumption most closely matched actual practice.

The dynamic modulus results clearly show a consistent RAP effect. As the percentage of RAP increases, dynamic modulus values increase. These results are consistent for all materials and job mix formulae used in this research study. However, comparison of the individual results for the four different mixture sets did not produce definitive indication as to the working binder quantitatively. The generally held belief is that modulus increases as RAP percentages increase because of the increased amount of RAP's aged binder that blends with the virgin binder being added. The dynamic modulus values for HMA with 20% RAP did not change significantly, which indicated that the RAP binder has little effect on mixture properties at this low percentage of RAP.

Given that the mix design considerations indicate a rather near complete blending of the effective RAP binder, it would be expected that the dynamic modulus values from actual practice would match the values obtained from the 100% working binder samples. If less than complete blending were occurring, the dynamic modulus of actual practice specimens would be less stiff than those of specimens having 100% working binder. However, the test results consistently showed that the dynamic modulus values for the specimens with 100% working binder were significantly lower than those of actual practice specimens.

The VMA of all mixes either meets the IDOT minimum requirement, or is at most 0.3% below the minimum requirement. In addition, there was variation in the amount of material passing the # 200 sieve. Although the passing #200 and VMA can have an effect on the HMA dynamic modulus, fracture energy, and moisture susceptibility results, however, these variations may not affect the overall behavior trend of the mixes.

The causes for the actual practice mixtures to have higher dynamic modulus values than those of the control specimens could include the following:

- Although the JMF aggregate gradation is similar for all sample sets, actual aggregate structure may not be the same for all mixes. Design blends are prepared with a tacit assumption that RAP binder is fully released during the mixing process. Variations will result from differing amounts of fines being released with various amounts of blending of the RAP binder. If complete blending does not occur, the aggregate structure will be altered significantly in favor of larger fractions.
- The differing amounts of fines released during blending will alter the mastic properties of the binder in the final mixture.

- Alterations in volumetric characteristics resulting from differing VMA calculations when various amounts of binder blend with the virgin binder, i.e. the relative amount of black rock changes.
- The asphalt-aggregate interface is not well-defined. This produces an asphalt material at this interface that is significantly stiffer than the remaining binder due to selective absorption of components of the binder into the aggregate. This selective absorption changes the aggregate binder interaction over time and forms a stiff layer of binder on the aggregate surface. This composite binder structure on the aggregate surface increases the mixture modulus. The HMA with aged RAP already contains this stiff binder layer at the aggregate surface, a condition not present in the control specimens.

The current practice that assumes 100% working binder is considered acceptable; but may not be explicitly supported utilizing the data collected herein. However, it is clear that 100% of the RAP binder is not working because of the absorbed binder portion.

In addition to the HMA dynamic modulus, the binder shear complex modulus was tested. A comparison of blended binders' complex shear modulus,  $G^*$ , prepared using recovered and virgin binder illustrated that the blended binder stiffness increased when aged RAP binder percent increased. Increasing District 1 RAP binder in the blend (20 and 40% blends) showed consistent increase in the  $G^*$  of the blended binder with respect to the standard PG64-22 binder. On the other hand, 20 and 40% blends of District 4 RAP binder did not show significant difference in the  $G^*$  values. This raises a question as to the compatibility between District 4 recovered binder and the PG 64-22 binder combination; incompatibility may have prevented homogeneous blending. This could alter the interpretation of the dynamic modulus  $E^*$  test data for the HMA; however, the exact nature is not known. The comparison between the binder backcalculated and measured  $G^*$  values showed a good match for District 1 HMA with 40% RAP; suggesting nearly complete blending. However, the contradictory data for District 4 HMA does not allow a conclusion to be drawn at this time.

The stripping of the HMA containing RAP was determined in accordance with the IDOT procedures. Visual inspection of the specimens that failed in indirect tension testing was also conducted. The tensile strength ratio (TSR) of the specimens was calculated to determine the stripping susceptibility. The TSR increased as the amount of RAP in HMA increased when compared to HMA with no RAP. There appears to be some variations in the TSR results for the mixes with 20 and 40% RAP. These variations could be related to testing as well as the low number of valid tested specimens. Moisture susceptibility test results suggest that mixes containing RAP are less susceptible to moisture damage than virgin HMA. The District 4 materials had greater TSR values than those of District 1 materials. The reduction in stripping potential of HMA with RAP may be attributed to the strong binder-aggregate bonds of RAP materials that formed over time.

While the testing conducted here showed that increased RAP percentages in HMA reduce stripping potential, the two HMA with RAP investigated in this study should not be accepted as being indicative for all HMA with RAP. If the RAP source used in mixing had stripping problems prior to recycling, the stripping properties may not be improved. One might expect the mix to be more likely to strip although this has not been investigated in this study.

The amount of blending occurring between virgin and RAP binders was evaluated using SEM images. The film thickness was found to be significantly less than the theoretically calculated film thickness if film thickness is defined as the binder thickness between any two aggregate particles. Hence, an accurate definition of binder film thickness is needed. This method could not accurately determine the amount of binder blending. An

alternative method was performed to further investigate binder blending, ESM and EDS. This method showed promising results, and a further investigation will likely determine the binder blending.

The increasing stiffness of HMA as the amount of RAP increases results in an increased brittleness of the HMA which may lead to low temperature cracking. The HMA with RAP were tested using SCB and DCT fracture tests to determine the fracture energy of HMA with RAP. The fracture energy is related to the development of thermal cracking in the field. Preliminary results showed that as RAP content increases, fracture energy decreases and the mix becomes more susceptible to low-temperature cracking. Double bumping the binder grade had a positive effect on fracture energy results.

The research outcome supports the following conclusions:

- While data suggests complete blending is not occurring, an accurate determination of actual blending percentages could not be obtained. However, a high percentage of blending can be interpreted from the various testing results.
- The current mix design for HMA with RAP that assumes 100% working binder may be considered acceptable.
- Fractionation of RAP stockpiles into four fractions for mix designs of laboratory prepared specimens produced excellent quality control.
- Dynamic modulus testing,  $E^*$ , on the HMA with RAP is not sufficient to differentiate binder blending impact.
- The HMA with 20% RAP did not indicate the need for changing the virgin binder grade to achieve similar dynamic modulus of HMA with no RAP. However, the fracture energy did show an increase in potential thermal cracking in these mixtures.
- At 40% RAP in HMA, double bumping the binder grade appears to be needed. Although preliminary tests suggested the potential need for low temperature binder grade bumping, more tests are required to verify that.
- The Hirsch model may not be appropriate to backcalculate binder complex shear modulus from HMA with RAP because of the complex nature of HMA with RAP. Binder compatibility could produce a four phase system rather than the three phase system assumed in the model development.

## CHAPTER 5 RECOMMENDATIONS

Based upon the findings of this study, the following points summarize the recommendations for practical applications and future research:

- Fractionating RAP into four sizes for laboratory mix design allowed preparation of repeatable laboratory specimens. Field practice using fractionated RAP in order to avoid potential non homogenous gradations due to stockpiling and agglomeration of RAP particles has been recommended by IDOT for years and should be performed for quality control in the field. Studies into the degree of fractionation and the impact on quality control should be undertaken.
- No change in current mix design procedures for high RAP mixtures is supported by this study. However, mixes containing high RAP require special attention to ensure minimum VMA is met and the aggregate gradation is not significantly altered by the addition of fines associated with RAP materials.

- The dynamic modulus may not be an appropriate test to examine performance differences in HMA arising from binder effects due to its reliance on compressive aggregate to aggregate contact which minimizes binder effects.
- Further study into SEM imaging using the EDS technique is recommended to verify the potential ability of the systems to provide visual indications of RAP and virgin binder blending.
- Preliminary study showed that RAP may increase HMA susceptibility to low-temperature cracking. However, a more thorough investigation into grade bumping and the impact on low-temperature thermal cracking should be undertaken.
- An extensive performance testing program is recommended to investigate fatigue cracking, rutting, and thermal cracking for HMA with high RAP percentages. Analyzing distress related parameters should consider mixtures that meet VMA requirements and those that are 1% below current minimum VMA threshold.
- A testing program is recommended to investigate the effect of compaction temperature on mixes containing high RAP percentages.

## REFERENCES

Al-Qadi, I. L., M. Elseifi, S. H. Carpenter, *Reclaimed Asphalt Pavement – A Literature Review*. FHWA-ICT-07-001. Illinois Center for Transportation, University of Illinois at Urbana-Champaign, Urbana, IL, 2007.

Christensen, D. W., T. K. Pellinen, and R. F. Bonaquist, “Hirsch Model for Estimating the Modulus of Asphalt Concrete.” *Proceedings of the Association of Asphalt Paving Technologists*, Vol. 72, 2003, pp. 97-121.

Huang, B., G. Li, D. Vukosavljevic, X. Shu, X., and B. K. Egan, “Laboratory Investigation of Mixing Hot-Mix Asphalt with Reclaimed Asphalt Pavement,” *Transportation Research Record: Journal of the Transportation Research Board*, No. 1929, Washington, D.C., 2005, pp. 37-45.

Kemp, G. R. and N. H. Predoehl, “A Comparison of Field and Laboratory Environments on Asphalt Durability,” *Proceedings of the Association of Asphalt Paving Technologists*, Vol. 50, 1981, pp. 492-537.

Kennedy, T. W., W. O. Tam, and M. Solaimanian, “Optimizing Use of Reclaimed Asphalt Pavement with the SuperPave System,” *Journal of the Association of Asphalt Paving Technologists*, Vol. 67, 1998, pp. 311-333.

Lee, T. C., R. L. Terrel, and J. P. Mahoney, “Test for Efficiency of Mixing of Recycled Asphalt Paving Material,” *Transportation Research Record: Journal of the Transportation Research Board*, No. 911, Washington D.C., 1983, pp. 51-60.

Li, X., Investigation of the Fracture Resistance of Asphalt Mixtures at Low Temperature with a Semi Circular Bend (SCB) Test. Ph.D. Thesis, University of Minnesota, August 2005.

McDaniel, R. S., H. Soleymani, R. M. Anderson, P. Turner, and R. Peterson, *Recommended Use of Reclaimed Asphalt Pavement in the SuperPave Mixture Design Method*, NCHRP Final Report (9-12), TRB, Washington, D.C., 2000.

McMillan, C., and D. Palsat, "Alberta's Experience in Asphalt Recycling," *Proceedings of the Canadian Technical Asphalt Association*, Vol. 30, 1985, pp. 148-167.

Murphy, T. Personal Communication. 2008.

Plancher, H., E. L. Green, and J. C. Petersen. "Reduction of Oxidative Hardening of Asphalts by Treatment with Hydrated Lime—A Mechanistic Study," *Proceedings of Association of Asphalt Paving Technologists*, Vol. 45, 1976, pp.1-24.

Smiljanic, M., J. Stefanovic, H.-J. Neumann, I. Rahimaian, and J. Jovanovic, "Aging of Asphalt on Paved Roads — Characterization of Asphalt Extracted from the Wearing Courses of the Belgrade-Nis Highway," *Journal of Erdol and Kohl*, Vol. 46, No. 6, Hamburg, Germany, 1993.

## **APPENDIX A BATCHING EXAMPLES FOR MIXES WITH RAP**

**SET 1 (ACTUAL PRACTICE 100 % BLENDING CASE)**

This mixture set assumes 100 % residual binder mobilization from RAP aggregates. Mixture preparation step for this set is shown with the following example of 4700 g sample size.

Table A-1. SET1 Batching Example

<b>SET 1-ACTUAL PRACTICE (100 % BLENDING)</b>			
<i>Design AC %</i>		5.7	
<i>AC in RAP %</i>		4.7	
<i>Sample Size</i>		4700 g	
	<b>Total Mix %</b>	<b>Agg %</b>	<b>Weight (g)</b>
<b>CM16</b>	50.7	51.2	2383
<b>FM20</b>	15.9	16.1	747
<b>FM02</b>	11.9	12.0	559
<b>RAP</b>	<b>20.0</b>	<b>19.2</b>	<b>940</b>
<b>MFM</b>	1.5	1.5	71
<b>total</b>	100.0	100.0	4700
<b>STEP 1</b>			
Determine AC and Agg weight in RAP			
	AC	$\frac{940 \times 4.7}{100} =$	<u><u>44</u></u> g
	Agg	$\frac{940 - 9.4}{100} =$	<u><u>896</u></u> g
<b>STEP 2</b>			
Determine new aggregate batch size			
		$2383 + 747 + 559 + 940 + 71 =$	<u><u>4656</u></u> g
<b>STEP 3</b>			
Determine total AC content			
		$4656 / (1 - 5.7/100) - 4656 =$	<u><u>281</u></u> g
<b>STEP 4</b>			
Determine virgin AC to add			
		$281 - 44 =$	<u><u>237</u></u> g
<b>STEP 5</b>			
Total mix			
		$4656 + 281 =$	<u><u>4937</u></u> g

**SET 2 (BLACK ROCK 0 % BLENDING CASE)**

This mixture set uses recovered RAP aggregates in addition to virgin aggregates and binder. Since we assume no blending occurs, there is no need for recovered binder. Blending example is as follows;

Table A-2. SET2 Batching Example

<b>SET 2-BLACK ROCK (0 % BLENDING)</b>			
<i>Design AC %</i>	5.7		
<i>AC in RAP %</i>	0		
<i>Sample Size</i>	4700 g		
	<b>Total Mix %</b>	<b>Agg %</b>	<b>Weight (g)</b>
<i>CM16</i>	50.7	50.7	2383
<i>FM20</i>	15.9	15.9	747
<i>FM02</i>	11.9	11.9	559
<i>RAP</i>	<b>20.0</b>	<b>20.0</b>	<b>940</b>
<i>MFM</i>	1.5	1.5	71
<i>total</i>	100.0	100.0	4700
<b>STEP 1</b>			
Determine AC and Agg weight in RAP			
	AC	$\frac{940 \times 0.0}{100} =$	<u><u>0</u></u> g
<b>STEP 2</b>			
Determine new batch size			
		$2383 + 747 + 559 + 940 + 71 =$	<u><u>4700</u></u> g
<b>STEP 3</b>			
Determine total AC content			
		$4700 / (1 - 5.7/100) - 4700 =$	<u><u>284</u></u> g
<b>STEP 4</b>			
Determine virgin and recovered AC to add			
Virgin	$284 - 0 =$		<u><u>284</u></u> g
Recovered			<u><u>0</u></u> g
<b>STEP 5</b>			
Total mix			
		$4700 + 284 =$	<u><u>4984</u></u> g

**SET 3 (BLACK ROCK 50 % BLENDING CASE)**

Table A-3. SET3 Batching Example

<b>SET 3-BLACK ROCK (50 % BLENDING)</b>			
<i>Design AC %</i>		5.7	
<i>AC in RAP %</i>		4.7	
<i>Sample Size</i>		4700 g	
	<b>Total Mix %</b>	<b>Agg %</b>	<b>Weight (gr)</b>
<b>CM16</b>	50.7	50.7	2383
<b>FM20</b>	15.9	15.9	747
<b>FM02</b>	11.9	11.9	559
<b>RAP</b>	<b>20.0</b>	<b>20.0</b>	<b>940</b>
<b>MFM</b>	1.5	1.5	71
<b>total</b>	100.0	100.0	1000
<b>STEP 1</b>			
Determine equivalent recovered AC			
	AC	$\frac{940 \times 2.35}{100} =$	<u><u>22</u></u> g
<b>STEP 2</b>			
Determine batch size (no change this due to recovered RAP)			
		$2383 + 747 + 559 + 940 + 71 =$	<u><u>4700</u></u> g
<b>STEP 3</b>			
Determine total AC content			
		$4700 / (1 - 5.7/100) - 4700 =$	<u><u>284</u></u> g
<b>STEP 4</b>			
Determine virgin and recovered AC to add			
Virgin		$284 - 22 =$	<u><u>262</u></u> g
Recovered			<u><u>22</u></u> g
<b>STEP 5</b>			
Total mix			
		$4700 + 284 =$	<u><u>4984</u></u> g

**SET 4 (BLACK ROCK 100 % BLENDING CASE)**

Table A-4. SET4 Batching Example

<b>SET 4-BLACK ROCK (100 % BLENDING)</b>			
<i>Design AC %</i>		5.7	
<i>AC in RAP %</i>		4.7	
<i>Sample Size</i>		4700 g	
	<b>Total Mix %</b>	<b>Agg %</b>	<b>Weight (g)</b>
<b>CM16</b>	50.7	50.7	2383
<b>FM20</b>	15.9	15.9	747
<b>FM02</b>	11.9	11.9	559
<b>RAP</b>	<b>20.0</b>	<b>20.0</b>	<b>940</b>
<b>MFM</b>	1.5	1.5	71
<b>total</b>	100.0	100.0	1000
<b>STEP 1</b>			
Determine equivalent recovered AC and RAP			
	AC	$\frac{940 \times 4.7}{100} =$	<u><u>44 g</u></u>
		<u><u>                    </u></u>	<u><u>                    </u></u>
<b>STEP 2</b>			
Determine batch size (no change this due to recovered RAP)			
		$2383 + 747 + 559 + 940 + 71 =$	<u><u>4700 g</u></u>
<b>STEP 3</b>			
Determine total AC content			
		$4700 / (1 - 5.7/100) - 4700 =$	<u><u>284 g</u></u>
<b>STEP 4</b>			
Determine virgin AC to add			
Virgin		$284 - 44 =$	<u><u>240 g</u></u>
Recovered			<u><u>44 g</u></u>
<b>STEP 5</b>			
Total mix			
		$4700 + 284 =$	<u><u>4984 g</u></u>

## APPENDIX B MIXTURE DESIGN

Table A-5. District 1 RAP 0% Job Mix Formula  
**DISTRICT 1-RAP 0 % DESIGN**

<b>Design Number</b>	District 1 RAP 0 %						
<b>Agg No</b>		<b>CM16</b>	<b>FM20</b>	<b>FM02</b>	<b>MFM</b>	<b>RAP</b>	<b>% AC</b>
<b>Agg Blend %</b>		57.5	23.0	18.0	1.5	0.0	

100.0 total

Sieve Size (No.)	Sieve Size (No.)	Sieve Size (mm)	Stockpile 1 (%)	Stockpile 2 (%)	Stockpile 3 (%)	Stockpile 4 (%)	Stockpile 5 (%)	Blend (%)
2 inches	2 inches	50.00	100.0	100.0	100.0	100.0	100.0	100.0
1 1/2 inches	1 1/2 inches	37.50	100.0	100.0	100.0	100.0	100.0	100.0
1 inch	1 inch	25.00	100.0	100.0	100.0	100.0	100.0	100.0
3/4 inch	3/4 inch	19.00	100.0	100.0	100.0	100.0	100.0	100.0
1/2 inch	1/2 inch	12.50	100.0	100.0	100.0	100.0	100.0	100.0
3/8 inch	3/8 inch	9.50	97.0	100.0	100.0	100.0	98.0	98.3
No. 4	No. 4	4.75	29.0	97.0	97.0	100.0	71.0	57.9
No. 8	No. 8	2.36	8.0	81.0	85.0	100.0	48.0	40.0
No. 16	No. 16	1.18	4.0	50.0	65.0	100.0	36.0	27.0
No. 30	No. 30	0.60	4.0	31.0	53.0	100.0	28.0	20.5
No. 50	No. 50	0.30	4.0	19.0	20.0	100.0	21.0	11.8
No. 100	No. 100	0.15	4.0	10.0	5.0	95.0	13.0	6.9
No. 200	No. 200	0.075	3.4	4.0	1.5	90.0	9.7	4.5

	Gsb
CM16	2.664
FM20	2.670
FM02	2.597
Filler	2.900
RAP	2.660
Blend	2.656

<b>Bulk Specific Gravity</b>	2.664	2.670	2.597	2.900	2.660
<b>Apparent Specific Gravity</b>	2.790	2.766	2.681	2.900	

<i>Data for N-Design =50</i>		<i>Min 15</i>			<i>65-78</i>								
Trial Batch #	AC % (MIX)	Gmb	Gmm	VMA	VTM	VFA	Vbulk(cm3)	Veff (cm3)	Gse	Gsb	Pbe	Pba	DP
1	5.7	2.396	2.510	14.9	4.5	70	1761.0	1702.1	2.748	2.656	4.5	1.3	0.8
2	5.9	2.398	2.502	15.0	4.1	72	1756.1	1697.5	2.748	2.656	4.7	1.3	0.8
3													

<i>Data for N-Initial =6</i>							
Trial Batch #	AC % (MIX)	Gmb	Gmm	VMA	VTM	VFA	%Gmm
1	5.7	2.155	2.510	23.5	14.1	40	85.9
2	5.9	2.206	2.502	21.9	11.8	46	88.2
3							

<b>Design AC</b>	<b>Design AC %</b>	<b>Gmb</b>	<b>Gmm</b>	<b>VMA</b>	<b>VTM</b>	<b>VFA</b>
	5.9	2.398	2.502	15.0	4.1	72

Table A-6. District 1 RAP 20% Job Mix Formula

**DISTRICT 1-RAP 20 % DESIGN**

<b>Design Number</b>	District 1 RAP 20 %							
<b>Agg No</b>			<b>CM16</b>	<b>FM20</b>	<b>FM02</b>	<b>MFM</b>	<b>RAP</b>	
							4.7	% AC
<b>Agg Blend %</b>			51.2	16.1	12.0	1.5	19.2	

100.0 total

Sieve Size (No.)	Sieve Size (No.)	Sieve Size (mm)	Stockpile 1 (%)	Stockpile 2 (%)	Stockpile 3 (%)	Stockpile 4 (%)	Stockpile 5 (%)	Blend (%)
2 inches	2 inches	50.0	100.0	100.0	100.0	100.0	100.0	100.0
1 1/2 inches	1 1/2 inches	37.5	100.0	100.0	100.0	100.0	100.0	100.0
1 inch	1 inch	25.0	100.0	100.0	100.0	100.0	100.0	100.0
3/4 inch	3/4 inch	19.0	100.0	100.0	100.0	100.0	100.0	100.0
1/2 inch	1/2 inch	12.5	100.0	100.0	100.0	100.0	100.0	100.0
3/8 inch	3/8 inch	9.5	97.0	100.0	100.0	100.0	98.0	98.1
No. 4	No. 4	4.8	29.0	97.0	97.0	100.0	71.0	57.4
No. 8	No. 8	2.4	8.0	81.0	85.0	100.0	48.0	38.2
No. 16	No. 16	1.2	4.0	50.0	65.0	100.0	36.0	26.4
No. 30	No. 30	0.6	4.0	31.0	53.0	100.0	28.0	20.4
No. 50	No. 50	0.3	4.0	19.0	20.0	100.0	21.0	13.1
No. 100	No. 100	0.2	4.0	10.0	5.0	95.0	13.0	8.2
No. 200	No. 200	0.1	3.4	4.0	1.5	90.0	9.7	5.8

	Gsb
<b>CM16</b>	2.664
<b>FM20</b>	2.670
<b>FM02</b>	2.597
<b>Filler</b>	2.900
<b>RAP</b>	2.660
<b>Blend</b>	2.659

$$RAP\ Agg\ \% = \frac{20 - 20 + 4.7/100}{100 - 20 + 4.7/100} = 19.2$$

<b>Bulk Specific Gravity</b>	2.664	2.670	2.597	2.900	2.660	2.659
<b>Apparent Specific Gravity</b>						

Data for N-Design =50				Min 15		65-78							
Trial Batch #	AC % (MIX)	Gmb	Gmm	VMA	VTM	VFA	Vbulk(cm3)	Veff (cm3)	Gse	Gsb	Pbe	Pba	DP
1	5.0	2.368	2.525	15.4	6.2	60	1668.3	1622.7	2.734	2.659	4.0	1.1	1.2
2	5.5	2.386	2.505	15.2	4.8	69	1667.9	1623.1	2.733	2.659	4.5	1.0	1.1
3	6.0	2.415	2.482	14.6	2.7	82	1660.8	1619.2	2.727	2.659	5.1	1.0	1.0

Data for N-Initial =6							
Trial Batch #	AC % (MIX)	Gmb	Gmm	VMA	VTM	VFA	%Gmm
1	5.0	2.157	2.525	23.0	14.6	36	85.4
2	5.5	2.169	2.505	22.9	13.4	42	86.6
3	6.0	2.194	2.482	22.5	11.6	48	88.4

Design AC	Design AC %	Gmb	Gmm	VMA	VTM	VFA
	5.7	2.397	2.496	15.0	3.9	74
REC AGG	5.7	2.395	2.499	15.1	4.2	72

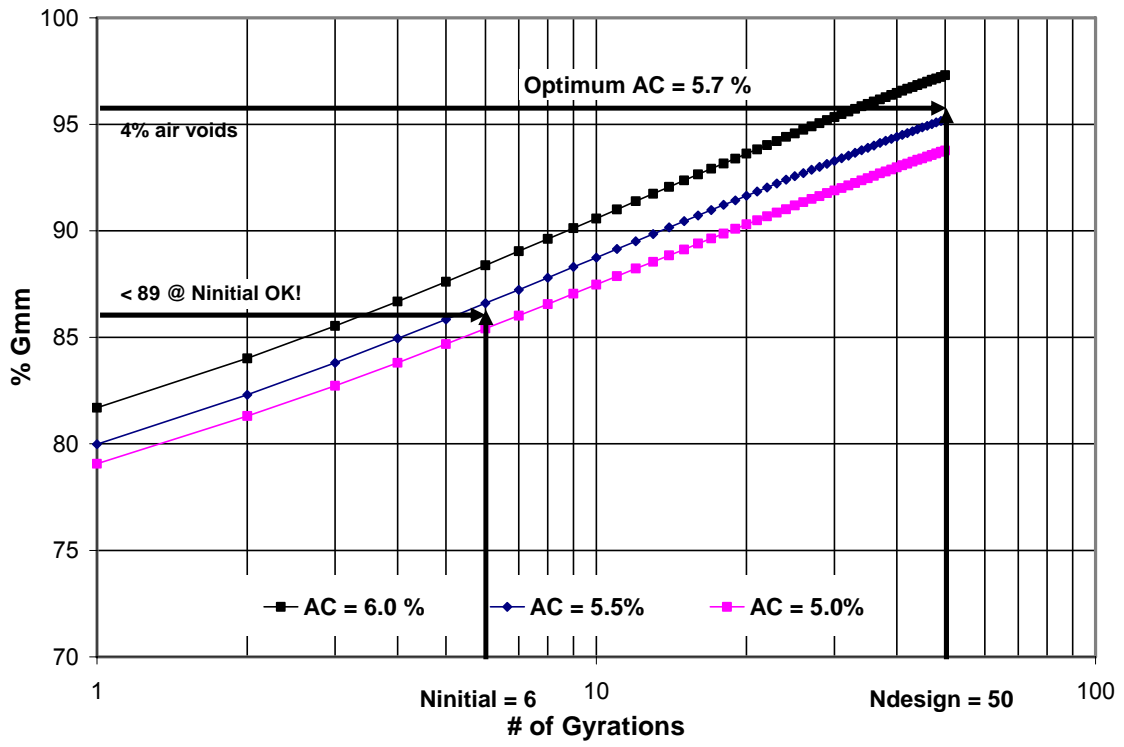


Figure A-1. Optimum AC content determination for District 1 20 % RAP design

Table A-7. District 1 RAP 40% Job Mix Formula  
DISTRICT 1-RAP 40 % DESIGN

Design Number	District 1 RAP 40 %							
Agg No			CM16	FM20	FM02	MFM	CM16 (RAP)	% AC
Agg Blend %			40.8	9.7	9.2	1.5	38.9	

100.0 total

Sieve Size (No.)	Sieve Size (No.)	Sieve Size (mm)	Stockpile 1 (%)	Stockpile 2 (%)	Stockpile 3 (%)	Stockpile 4 (%)	Stockpile 5 (%)	Blend (%)
2 inches	2 inches	50.0	100.0	100.0	100.0	100.0	100.0	100.0
1 1/2 inches	1 1/2 inches	37.5	100.0	100.0	100.0	100.0	100.0	100.0
1 inch	1 inch	25.0	100.0	100.0	100.0	100.0	100.0	100.0
3/4 inch	3/4 inch	19.0	100.0	100.0	100.0	100.0	100.0	100.0
1/2 inch	1/2 inch	12.5	100.0	100.0	100.0	100.0	100.0	100.0
3/8 inch	3/8 inch	9.5	97.0	100.0	100.0	100.0	98.0	98.0
No. 4	No. 4	4.8	29.0	97.0	97.0	100.0	71.0	59.4
No. 8	No. 8	2.4	8.0	81.0	85.0	100.0	48.0	39.2
No. 16	No. 16	1.2	4.0	50.0	65.0	100.0	36.0	28.1
No. 30	No. 30	0.6	4.0	31.0	53.0	100.0	28.0	22.0
No. 50	No. 50	0.3	4.0	19.0	20.0	100.0	21.0	15.1
No. 100	No. 100	0.2	4.0	10.0	5.0	95.0	13.0	9.6
No. 200	No. 200	0.1	3.4	4.0	1.5	90.0	9.7	7.1

	Gsb
CM16	2.664
FM20	2.670
FM02	2.597
Filler	2.900
RAP	2.660
Blend	2.660

$$RAP\ Agg\ \% = \frac{40 - 40 + 4.7/100}{100 - 40 + 4.7/100} = 88.9$$

Bulk Specific Gravity	2.664	2.670	2.597	2.900	2.660	2.660
Apparent Specific Gravity						

Data for N-Design =50				Min 15		65-78							
Trial Batch #	AC % (MIX)	Gmb	Gmm	VMA	VTM	VFA	Vbulk(cm3)	Veff (cm3)	Gse	Gsb	Pbe	Pba	DP
1	5.8	2.429	2.508	14.0	3.1	77	1727.2	1670.1	2.751	2.660	4.6	1.3	1.2
2	5.4	2.408	2.535	14.4	5.0	65	1727.5	1661.8	2.765	2.660	4.0	1.5	1.3
3 (REC AGG)	5.4	2.386	2.511	15.2	5.0	67	1726.2	1678.9	2.735	2.660	4.4	1.1	1.3
4 (REC AGG)	5.6	2.418	2.503	14.2	3.4	76	1721.7	1674.5	2.735	2.660	4.6	1.1	1.3

Data for N-Initial =6							
Trial Batch #	AC % (MIX)	Gmb	Gmm	VMA	VTM	VFA	%Gmm
1	5.8	2.215	2.508	21.6	11.7	46	88.3
2	5.4	2.151	2.535	23.5	15.1	36	84.9
3 (REC AGG)	5.4	2.139	2.511	23.9	14.8	38	85.2
4 (REC AGG)	5.6	2.169	2.503	23.0	13.4	42	86.6

Design AC	Design AC %	Gmb	Gmm	VMA	VTM	VFA
	5.6	2.418	2.521	14.2	4.1	71
	5.65	2.421	2.519	14.1	3.9	72
RECOVERED AGG	5.6	2.418	2.503	14.2	3.4	76
RECOVERED AGG	5.55	2.410	2.505	14.4	3.8	74

OPT AC = 5.65 %  
OPT AC (REC AGG) = 5.55 %

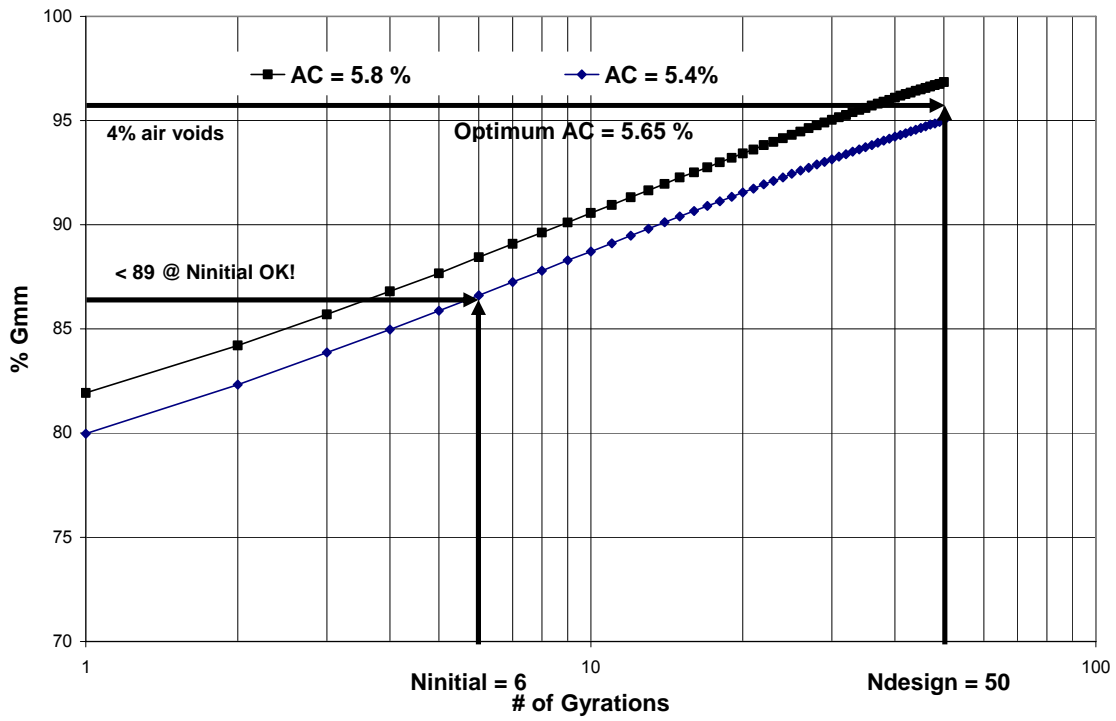


Figure A-1. Optimum AC determination for District 1 40 % RAP mixture design

Table A-8. District 4 RAP 0% Job Mix Formula

**DISTRICT 4-RAP 0 % DESIGN**

<b>Design Number</b>	District 4 RAP 0 %						
<b>Agg No</b>			<b>CM13</b>	<b>FM21</b>	<b>FM01</b>	<b>MFM</b>	<b>CM13 (RAP)</b>
							5.1
<b>Agg Blend %</b>			69.0	21.5	8.0	1.5	0.0

100.0 total

Sieve Size (No.)	Sieve Size (No.)	Sieve Size (mm)	Stockpile 1 (%)	Stockpile 2 (%)	Stockpile 3 (%)	Stockpile 4 (%)	Stockpile 5 (%)	Blend (%)
2 inches	2 inches	50.0	100.0	100.0	100.0	100.0	100.0	100.0
1 1/2 inches	1 1/2 inches	37.5	100.0	100.0	100.0	100.0	100.0	100.0
1 inch	1 inch	25.0	100.0	100.0	100.0	100.0	100.0	100.0
3/4 inch	3/4 inch	19.0	100.0	100.0	100.0	100.0	100.0	100.0
1/2 inch	1/2 inch	12.5	99.0	100.0	100.0	100.0	100.0	99.3
3/8 inch	3/8 inch	9.5	88.3	100.0	100.0	100.0	98.8	91.9
No. 4	No. 4	4.8	41.1	100.0	96.3	100.0	72.6	59.1
No. 8	No. 8	2.4	8.7	91.6	91.4	100.0	48.6	34.5
No. 16	No. 16	1.2	1.2	71.8	85.4	100.0	37.4	24.6
No. 30	No. 30	0.6	0.6	51.9	62.0	100.0	30.8	18.0
No. 50	No. 50	0.3	0.5	35.1	9.7	100.0	23.8	10.2
No. 100	No. 100	0.2	0.4	20.1	0.9	95.0	14.9	6.1
No. 200	No. 200	0.1	0.4	6.2	0.2	90.0	11.6	3.0

	Gsb
<b>CM13</b>	2.627
<b>FM21</b>	2.713
<b>FM01</b>	2.614
<b>Filler</b>	2.900
<b>RAP</b>	2.630
<b>Blend</b>	2.648

<b>Bulk Specific Gravity</b>	2.627	2.713	2.614	2.900	2.630	2.648
<b>Apparent Specific Gravity</b>						

<i>Data for N-Design =50</i>				<i>Min 15</i>		<i>65-78</i>							
<i>Trial Batch #</i>	<i>AC % (MIX)</i>	<i>Gmb</i>	<i>Gmm</i>	<i>VMA</i>	<i>VTM</i>	<i>VFA</i>	<i>Vbulk(cm3)</i>	<i>Veff (cm3)</i>	<i>Gse</i>	<i>Gsb</i>	<i>Pbe</i>	<i>Pba</i>	<i>DP</i>
1	5.9	2.429	2.524	13.7	3.8	72	1765.7	1683.5	2.777	2.648	4.2	1.8	0.5
2													
3													
4													

<i>Data for N-Initial =6</i>							
<i>Trial Batch #</i>	<i>AC % (MIX)</i>	<i>Gmb</i>	<i>Gmm</i>	<i>VMA</i>	<i>VTM</i>	<i>VFA</i>	<i>%Gmm</i>
1	5.9	2.219	2.524	21.1	12.1	43	87.9
2							
3							
4							

<b>Design AC</b>	<b>Design AC %</b>	<b>Gmb</b>	<b>Gmm</b>	<b>VMA</b>	<b>VTM</b>	<b>VFA</b>
	5.9	2.429	2.524	13.7	3.8	72

Table A-9. District 4 RAP 20% Job Mix Formula  
DISTRICT 4-RAP 20 % DESIGN

Design Number	District 4 RAP 20 %						
Agg No		CM13	FM21	FM01	MFM	CM13 (RAP)	% AC
Agg Blend %		60.6	10.1	9.1	1.0	5.1	19.2

100.0 total

Sieve Size (No.)	Sieve Size (No.)	Sieve Size (mm)	Stockpile 1 (%)	Stockpile 2 (%)	Stockpile 3 (%)	Stockpile 4 (%)	Stockpile 5 (%)	Blend (%)
2 inches	2 inches	50.0	100.0	100.0	100.0	100.0	100.0	100.0
1 1/2 inches	1 1/2 inches	37.5	100.0	100.0	100.0	100.0	100.0	100.0
1 inch	1 inch	25.0	100.0	100.0	100.0	100.0	100.0	100.0
3/4 inch	3/4 inch	19.0	100.0	100.0	100.0	100.0	100.0	100.0
1/2 inch	1/2 inch	12.5	99.0	100.0	100.0	100.0	100.0	99.4
3/8 inch	3/8 inch	9.5	88.3	100.0	100.0	100.0	98.8	92.8
No. 4	No. 4	4.8	41.1	100.0	96.3	100.0	72.6	58.9
No. 8	No. 8	2.4	8.7	91.6	91.4	100.0	48.6	33.3
No. 16	No. 16	1.2	1.2	71.8	85.4	100.0	37.4	24.1
No. 30	No. 30	0.6	0.6	51.9	62.0	100.0	30.8	18.3
No. 50	No. 50	0.3	0.5	35.1	9.7	100.0	23.8	10.4
No. 100	No. 100	0.2	0.4	20.1	0.9	95.0	14.9	6.3
No. 200	No. 200	0.1	0.4	6.2	0.2	90.0	11.6	4.1

	Gsb
CM13	2.627
FM21	2.713
FM01	2.614
Filler	2.900
RAP	2.630
Blend	2.637

$$RAP Agg \% = \frac{20 - 20 * 6.1/100}{100 - 20 * 6.1/100} = 19.2$$

Bulk Specific Gravity	2.627	2.713	2.614	2.900	2.630	2.637
Apparent Specific Gravity						

Data for N-Design =50															
Trial Batch #	AC % (MIX)	Gmb	Gmm	Min 15	VMA	VTM	65-78	VFA	Vbulk(cm3)	Veff (cm3)	Gse	Gsb	Pbe	Pba	DP
1	6.0	2.409	2.504	14.1	3.8	73	1748.7	1673.6	2.756	2.637	6.0	1.7	0.7		
2	5.5	2.380	2.523	14.7	5.7	62	1751.7	1676.6	2.755	2.637	5.5	1.7	0.7		
3	5.0	2.375	2.546	14.4	6.7	54	1758.1	1680.2	2.760	2.637	5.0	1.7	0.8		
4	4.5	2.350	2.566	14.9	8.4	44	1758.6	1680.7	2.760	2.637	4.5	1.7	0.9		

Data for N-Initial =6							
Trial Batch #	AC % (MIX)	Gmb	Gmm	VMA	VTM	VFA	%Gmm
1	6.0	2.203	2.504	21.5	12.0	44	88.0
2	5.5	2.127	2.523	23.8	15.7	34	84.3
3	5.0	2.125	2.546	23.4	16.5	30	83.5
4	4.5	2.111	2.566	23.6	17.7	25	82.3

Design AC	Design AC %	Gmb	Gmm	VMA	VTM	VFA
	5.9	2.404	2.508	14.2	4.1	71
	6.0	2.409	2.504	14.1	3.8	73
REC AGG	5.9	2.394	2.496	14.6	4.1	72

OPT AC = 6.0 %  
OPT AC (REC AGG) = 5.9 %

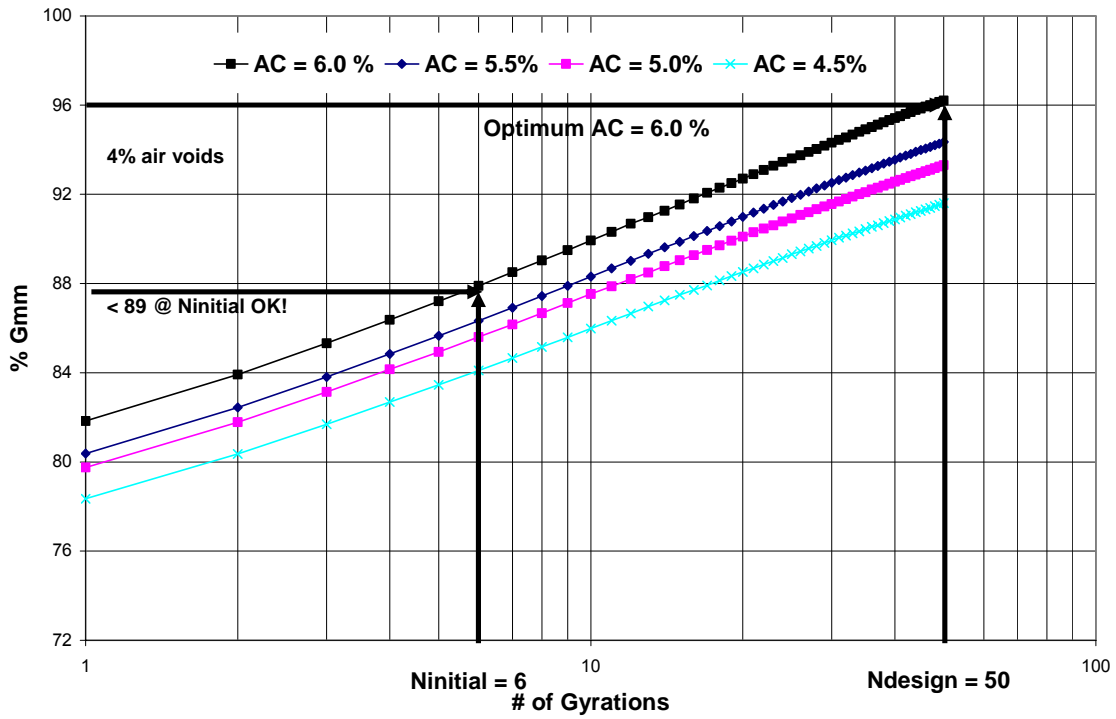


Figure A-3: District 4 20 % optimum AC

**Table A-10. District 4 RAP 40% Job Mix Formula  
DISTRICT 4-RAP 40 % DESIGN**

<b>Design Number</b>	District 4 RAP 40 %						
<b>Agg No</b>		<b>CM13</b>	<b>FM21</b>	<b>FM01</b>	<b>MFM</b>	<b>CM13 (RAP)</b>	<b>% AC</b>
<b>Agg Blend %</b>		51.0	5.1	4.1	1.0	38.8	

100.0 total

Sieve Size (No.)	Sieve Size (No.)	Sieve Size (mm)	Stockpile 1 (%)	Stockpile 2 (%)	Stockpile 3 (%)	Stockpile 4 (%)	Stockpile 5 (%)	Blend (%)
2 inches	2 inches	50.0	100.0	100.0	100.0	100.0	100.0	100.0
1 1/2 inches	1 1/2 inches	37.5	100.0	100.0	100.0	100.0	100.0	100.0
1 inch	1 inch	25.0	100.0	100.0	100.0	100.0	100.0	100.0
3/4 inch	3/4 inch	19.0	100.0	100.0	100.0	100.0	100.0	100.0
1/2 inch	1/2 inch	12.5	99.0	100.0	100.0	100.0	100.0	99.5
3/8 inch	3/8 inch	9.5	88.3	100.0	100.0	100.0	98.8	93.7
No. 4	No. 4	4.8	41.1	100.0	96.3	100.0	72.6	59.5
No. 8	No. 8	2.4	8.7	91.6	91.4	100.0	48.6	33.0
No. 16	No. 16	1.2	1.2	71.8	85.4	100.0	37.4	23.6
No. 30	No. 30	0.6	0.6	51.9	62.0	100.0	30.8	18.7
No. 50	No. 50	0.3	0.5	35.1	9.7	100.0	23.8	12.9
No. 100	No. 100	0.2	0.4	20.1	0.9	95.0	14.9	8.2
No. 200	No. 200	0.1	0.4	6.2	0.2	90.0	11.6	6.0

	Gsb
CM13	2.627
FM21	2.713
FM01	2.614
Filler	2.900
RAP	2.630
Blend	2.634

$$RAP\ Agg\ \% = \frac{40 - 40 + 6.1/100}{100 - 40 + 6.1/100} = 88.8$$

<b>Bulk Specific Gravity</b>	2.627	2.713	2.614	2.900	2.630	2.634
<b>Apparent Specific Gravity</b>						

Data for N-Design =50				Min 15		65-78							
Trial Batch #	AC % (MIX)	Gmb	Gmm	VMA	VTM	VFA	Vbulk(cm3)	Veff (cm3)	Gse	Gsb	Pbe	Pba	DP
1	6.0	2.406	2.499	14.2	3.7	73.6	1734.2	1661.5	2.750	2.634	4.5	1.6	1.0
2	5.5	2.393	2.524	14.2	5.2	63.3	1738.5	1661.5	2.756	2.634	3.9	1.7	1.1
3	5.0	2.373	2.552	14.4	7.0	51.3	1744.1	1660.5	2.767	2.634	3.2	1.9	1.2
4 (REC AGG)	5.8	2.397	2.510	14.3	4.5	68.7	1749.4	1677.0	2.748	2.634	4.1	1.6	1.0

Data for N-Initial =6							
Trial Batch #	AC % (MIX)	Gmb	Gmm	VMA	VTM	VFA	%Gmm
1	6.0	2.192	2.499	21.8	12.3	44	87.7
2	5.5	2.123	2.524	23.9	15.9	33	84.1
3	5.0	2.106	2.552	24.0	17.5	27	82.5
4 (REC AGG)	5.8	2.149	2.510	23.2	14.4	38	85.6

Design AC	Design AC %	Gmb	Gmm	VMA	VTM	VFA
	5.9	2.402	2.506	14.2	4.2	71
	6.0	2.406	2.499	14.2	3.7	74
REC AGG	5.8	2.397	2.515	14.3	4.7	67
REC AGG	5.9	2.391	2.490	14.6	4.0	73

**OPT AC = 6.0 %  
OPT AC (REC AGG) = 5.9 %**

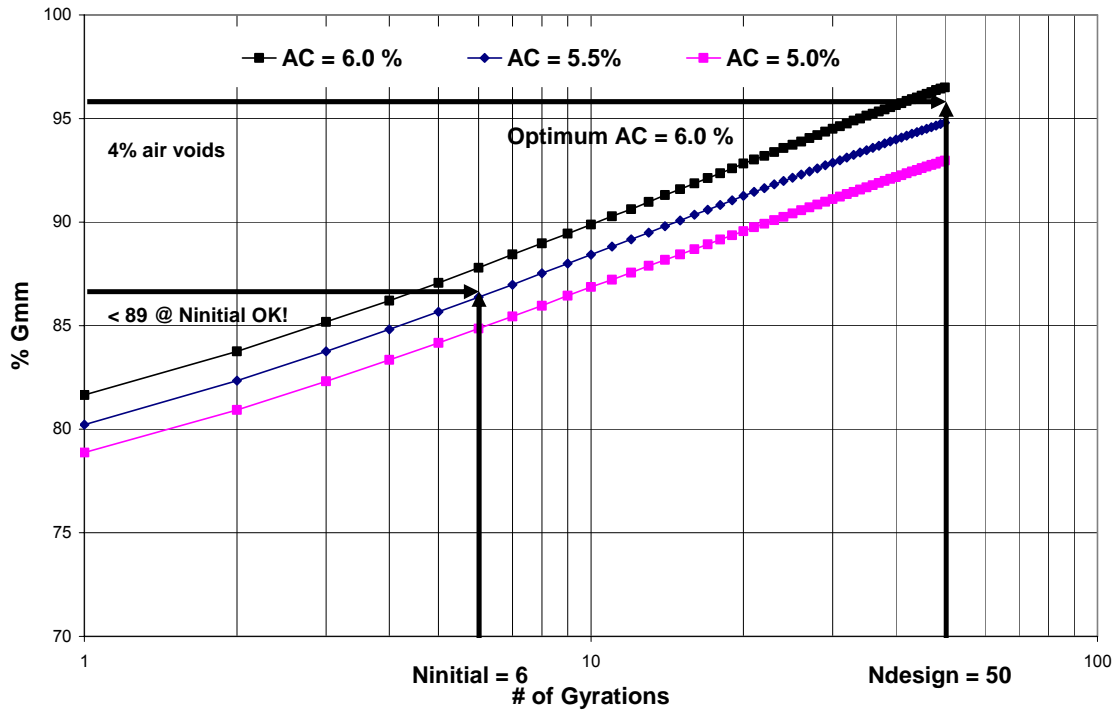


Figure A-4: District 4 40% RAP optimum AC

## APPENDIX C COMPLEX MODULUS TEST DATA STATISTICS

Table A-11. District 1 0 % RAP (5.9% AC) specimen SET 1 complex modulus test data

	Temp	Frequency (Hz)	Dynamic Modulus (ksi)	STDEV	COVAR	Phase Angle (Deg)	STDEV	COVAR
<b>D1-SET1-00 (AC = 5.9%)</b>	-10	25.00	3,905	79	2	5	0	10
		10.00	3,650	39	1	5	0	7
		5.00	3,485	29	1	6	0	8
		1.00	3,085	23	1	7	0	1
		0.50	2,907	17	1	8	0	0
		0.10	2,474	13	1	9	0	3
		0.01	1,853	16	1	13	0	3
	4	25.00	2,782	102	4	11	0	0
		10.00	2,468	88	4	12	0	0
		5.00	2,242	83	4	13	0	1
		1.00	1,744	57	3	16	0	2
		0.50	1,536	47	3	17	0	2
		0.10	1,096	21	2	22	1	3
		0.01	604	2	0	28	1	3
	20	25.00	1388	4	0	20	1	5
		10.00	1122	18	2	22	1	6
		5.00	949	28	3	23	1	4
		1.00	616	31	5	27	1	2
		0.50	503	29	6	29	1	2
		0.10	311	21	7	30	0	1
		0.01	161	6	4	30	1	2

Table A-12. District 1 0 % RAP (5.7% AC) specimen SET 1 complex modulus test data

	Temp	Frequency (Hz)	Dynamic Modulus (ksi)	STDEV	COVAR	Phase Angle (Deg)	STDEV	COVAR
<b>D1-SET1-00 (AC = 5.7%)</b>	-10	25.00	4776	281	6	6	1	9
		10.00	4408	184	4	7	1	12
		5.00	4134	84	2	7	1	12
		1.00	3563	24	1	9	1	15
		0.50	3287	110	3	10	2	16
		0.10	2670	257	10	12	2	20
		0.01	1791	488	27	17	5	29
	4	25.00	2881	124	4	11	0	2
		10.00	2563	102	4	12	0	2
		5.00	2335	93	4	13	0	2
		1.00	1825	90	5	16	0	3
		0.50	1614	82	5	17	1	3
		0.10	1172	62	5	21	1	5
		0.01	677	34	5	27	1	5
	20	25.00	1432	51	4	21	0	1
		10.00	1175	52	4	22	0	2
		5.00	993	43	4	23	0	2
		1.00	642	29	5	27	1	3
		0.50	524	24	4	28	1	4
		0.10	326	12	4	30	2	7
		0.01	171	3	2	29	3	9

Table A-13. District 1 20 % RAP specimen SET 1 case complex modulus test data

Specimen Id	Temp	Frequency (Hz)	Dynamic Modulus (ksi)	STDEV	COVAR	Phase Angle (Deg)	STDEV	COVAR
D1-SET1-20	-10	25.00	5,141	184	4	4	2	43
		10.00	4,778	209	4	5	2	31
		5.00	4,572	176	4	6	1	21
		1.00	4,058	143	4	7	1	11
		0.50	3,824	138	4	8	1	10
		0.10	3,273	143	4	9	1	10
		0.01	2,499	156	6	13	1	10
	4	25.00	3,460	178	5	9	2	18
		10.00	3,122	135	4	10	1	11
		5.00	2,878	123	4	11	1	7
		1.00	2,331	103	4	13	0	2
		0.50	2,097	94	4	15	0	2
		0.10	1,580	73	5	18	0	2
		0.01	942	38	4	24	0	1
	20	25.00	1741	187	11	19	1	4
		10.00	1421	166	12	20	1	4
		5.00	1207	147	12	21	1	4
		1.00	801	106	13	25	1	3
		0.50	657	90	14	27	1	3
		0.10	400	60	15	30	0	1
		0.01	No Data					

Table A-14. District 1 20 % RAP specimen SET 2 case complex modulus test data

Specimen Id	Temp	Frequency (Hz)	Dynamic Modulus (ksi)	STDEV	COVAR	Phase Angle (Deg)	STDEV	COVAR
D1-SET2-20	-10	25.00	4,744	869	18	6	1	14
		10.00	4,481	790	18	6	1	9
		5.00	4,287	751	18	6	1	9
		1.00	3,823	667	17	7	0	3
		0.50	3,612	624	17	8	0	3
		0.10	3,103	533	17	9	0	5
	0.01	2,378	373	16	12	1	4	
	4	25.00	3,195	363	11	9	1	13
		10.00	2,888	344	12	10	1	5
		5.00	2,657	324	12	11	0	3
		1.00	2,138	272	13	14	0	3
		0.50	1,916	245	13	15	0	3
		0.10	1,428	172	12	18	1	3
	0.01	846	108	0	24	0	1	
	20	25.00	1606	184	11	19	0	2
		10.00	1322	150	11	20	0	2
		5.00	1130	126	11	21	0	2
		1.00	752	87	12	25	0	2
0.50		619	70	11	26	0	1	
0.10		387	53	14	29	0	1	
0.01	199	26	13	29	1	3		

Table A-15. District 1 20 % RAP specimen SET 3 case complex modulus test data

Specimen Id	Temp	Frequency (Hz)	Dynamic Modulus (ksi)	STDEV	COVAR	Phase Angle (Deg)	STDEV	COVAR
D1-SET3-20	-10	25.00	5,005	51	1	6	1	21
		10.00	4,667	41	1	6	1	20
		5.00	4,431	32	1	7	2	26
		1.00	3,875	158	4	9	2	25
		0.50	3,626	219	6	9	2	25
		0.10	3,036	333	11	11	3	26
	0.01	2,231	394	18	15	3	22	
	4	25.00	3,578	116	3	11	0	3
		10.00	3,169	95	3	12	0	4
		5.00	2,842	109	4	13	0	1
		1.00	2,232	48	2	15	0	3
		0.50	1,955	47	2	17	0	3
		0.10	1,374	43	3	21	0	2
	0.01	747	20	3	28	0	2	
	20	25.00	1655	48	3	20	1	4
		10.00	1334	58	4	21	1	3
		5.00	1127	50	4	23	1	3
		1.00	730	28	4	27	1	3
0.50		594	24	4	28	1	2	
0.10		361	16	4	30	0	1	
0.01	181	11	6	31	0	0		

Table A-16. District 1 20 % RAP specimen SET 4 case complex modulus test data

Specimen Id	Temp	Frequency (Hz)	Dynamic Modulus (ksi)	STDEV	COVAR	Phase Angle (Deg)	STDEV	COVAR
D1-SET4-20	-10	25.00	4,913	157	3	5	1	10
		10.00	4,668	128	3	6	0	5
		5.00	4,448	126	3	6	0	5
		1.00	3,933	111	3	8	0	3
		0.50	3,696	105	3	8	0	3
		0.10	3,147	81	3	10	1	6
		0.01	2,342	54	2	14	0	1
	4	25.00	3,247	41	1	10	2	17
		10.00	2,894	43	1	11	1	9
		5.00	2,638	37	1	12	0	4
		1.00	2,076	36	2	15	0	2
		0.50	1,837	35	2	17	0	2
		0.10	1,331	31	2	21	0	2
	20	0.01	747	32	4	28	1	3
		25.00	1688	90	5	21	1	7
		10.00	1365	85	6	21	1	4
		5.00	1152	76	7	23	1	4
		1.00	751	54	7	27	1	4
		0.50	612	46	8	28	1	4
		0.10	373	30	8	31	1	3
	0.01	185	16	9	32	1	3	

Table A-17. District 1 40 % RAP specimen SET 1 case complex modulus test data

	Temp	Frequency (Hz)	Dynamic Modulus (ksi)	STDEV	COVAR	Phase Angle (Deg)	STDEV	COVAR
D1-SET1-40	-10	25.00	5,331	301	6	5	0	6
		10.00	4,973	216	4	5	0	5
		5.00	4,765	196	4	6	0	2
		1.00	4,285	162	4	7	0	2
		0.50	4,067	144	4	7	0	1
		0.10	3,541	101	3	8	0	1
		0.01	2,777	38	1	11	0	3
	4	25.00	3,897	187	5	8	1	12
		10.00	3,555	186	5	9	1	8
		5.00	3,305	181	5	9	1	6
		1.00	2,741	152	6	11	0	3
		0.50	2,499	132	5	12	0	3
		0.10	1,930	98	5	16	0	1
	20	0.01	1,198	42	4	22	1	3
		25.00	2121	170	8	16	0	2
		10.00	1773	142	8	17	0	0
		5.00	1542	116	8	19	0	1
		1.00	1078	81	8	23	0	1
		0.50	902	64	7	24	0	1
		0.10	575	43	7	28	0	1
	0.01	283	22	8	32	1	2	

Table A-18. District 1 40 % RAP specimen SET 2 case complex modulus test data

Specimen Id	Temp	Frequency (Hz)	Dynamic Modulus (ksi)	STDEV	COVAR	Phase Angle (Deg)	STDEV	COVAR
D1-SET2-40	-10	25.00	3,934	368	9	6	0	1
		10.00	3,727	352	9	6	0	1
		5.00	3,560	339	10	7	0	1
		1.00	3,134	293	9	8	0	1
		0.50	2,943	275	9	9	0	2
		0.10	2,488	241	10	11	0	4
		0.01	1,852	209	11	15	1	6
	4	25.00	2,996	526	18	11	0	2
		10.00	2,674	465	17	12	0	3
		5.00	2,438	422	17	13	0	3
		1.00	1,906	340	18	16	1	4
		0.50	1,682	302	18	17	1	4
		0.10	1,209	217	18	21	1	3
		0.01	674	116	17	28	0	2
	20	25.00	1546	81	5	20	1	7
		10.00	1251	126	10	23	1	4
		5.00	1049	118	11	24	1	3
		1.00	672	90	13	29	1	3
		0.50	545	77	14	30	1	2
		0.10	331	49	15	31	1	3
		0.01	167	23	14	31	1	4

Table A-19. District 1 40 % RAP specimen SET 3 case complex modulus test data

Specimen Id	Temp	Frequency (Hz)	Dynamic Modulus (ksi)	STDEV	COVAR	Phase Angle (Deg)	STDEV	COVAR
D1-SET3-40	-10	25.00	4,247	117	3	6	0	0
		10.00	4,025	63	2	6	0	1
		5.00	3,858	40	1	6	0	1
		1.00	3,427	23	1	8	0	0
		0.50	3,236	10	0	8	0	1
		0.10	2,778	30	1	10	0	2
		0.01	2,107	59	3	14	0	3
	4	25.00	3,379	329	10	10	0	1
		10.00	2,989	315	11	10	0	1
		5.00	2,719	298	11	11	0	1
		1.00	2,149	258	12	14	0	3
		0.50	1,901	242	13	16	0	3
		0.10	1,369	187	14	20	1	3
		0.01	763	110	14	27	1	3
	20	25.00	1565	167	11	19	2	13
		10.00	1271	134	11	21	1	6
		5.00	1070	114	11	23	1	4
		1.00	694	86	12	27	0	2
		0.50	564	74	13	28	0	1
		0.10	340	46	13	31	0	1
		0.01	171	20	12	30	1	4

Table 20. District 1 40 % RAP specimen SET 4 case complex modulus test data

Specimen Id	Temp	Frequency (Hz)	Dynamic Modulus (ksi)	STDEV	COVAR	Phase Angle (Deg)	STDEV	COVAR
D1-SET4-40	-10	25.00	4,244	199	5	6	0	5
		10.00	4,034	185	5	6	0	4
		5.00	3,868	185	5	6	0	2
		1.00	3,470	173	5	7	0	1
		0.50	3,291	172	5	8	0	1
		0.10	2,858	164	6	9	0	1
		0.01	2,227	143	6	13	0	1
	4	25.00	2,841	177	6	6	0	1
		10.00	2,570	138	5	6	0	1
		5.00	2,375	119	5	6	0	1
		1.00	1,923	87	5	7	0	1
		0.50	1,735	74	4	8	0	2
		0.10	1,312	47	4	9	0	3
		0.01	795	30	4	13	0	2
	20	25.00	1689	150	9	6	0	1
		10.00	1414	106	7	6	0	2
		5.00	1219	81	7	6	0	2
		1.00	828	51	6	7	0	1
		0.50	687	41	6	8	0	2
		0.10	433	22	5	9	0	1
		0.01	218	10	4	13	0	0

Table A-21. District 4 0 % RAP specimen SET 1 case complex modulus test data

	Temp	Frequency (Hz)	Dynamic Modulus (ksi)	STDEV	COVAR	Phase Angle (Deg)	STDEV	COVAR
D4-SET1-00	-10	25.00	4,494	342	8	6	1	16
		10.00	4,172	310	7	6	0	4
		5.00	3,948	279	7	7	1	11
		1.00	3,431	226	7	8	0	2
		0.50	3,194	192	6	9	0	1
		0.10	2,639	139	5	11	0	3
		0.01	1,865	77	4	15	0	1
	4	25.00	2,725	46	2	12	1	6
		10.00	2,395	59	2	13	0	3
		5.00	2,159	66	3	14	0	2
		1.00	1,656	60	4	17	0	1
		0.50	1,452	57	4	19	0	1
		0.10	1,035	42	4	23	0	0
		0.01	576	12	2	28	0	1
	20	25.00	1243	41	3	22	0	2
		10.00	993	30	3	23	0	2
		5.00	827	24	3	25	1	4
		1.00	525	18	3	28	2	7
		0.50	425	15	3	29	2	6
		0.10	264	10	4	28	1	5
		0.01	145	8	6	24	1	2

Table A-22. District 4 20 % RAP specimen SET 1 case complex modulus test data

	Temp	Frequency (Hz)	Dynamic Modulus (ksi)	STDEV	COVAR	Phase Angle (Deg)	STDEV	COVAR
D4-SET1-20	-10	25.00	3,882	115	3	5	0	9
		10.00	3,627	83	2	6	0	5
		5.00	3,466	86	2	6	0	5
		1.00	3,064	71	2	8	1	7
		0.50	2,889	75	3	8	1	8
		0.10	2,467	85	3	10	1	8
		0.01	1,855	109	6	14	1	9
	4	25.00	2,638	168	6	11	1	5
		10.00	2,330	150	6	12	0	4
		5.00	2,106	136	6	13	0	3
		1.00	1,634	113	7	16	0	3
		0.50	1,437	101	7	18	0	3
		0.10	1,025	72	7	22	0	2
	20	0.01	564	33	6	29	0	1
		25.00	1277	48	4	21	1	4
		10.00	1043	51	5	22	1	4
		5.00	883	48	5	23	1	3
		1.00	570	44	8	27	1	3
0.50		465	38	8	29	1	2	
0.10		285	26	9	31	0	1	
0.01	147	11	8	30	1	3		

Table A-23. District 4 20 % RAP specimen SET 2 case complex modulus test data

Specimen Id	Temp	Frequency (Hz)	Dynamic Modulus (ksi)	STDEV	COVAR	Phase Angle (Deg)	STDEV	COVAR
D4-SET2-20	-10	25.00	3,302	85	3	8	0	3
		10.00	3,067	67	2	8	0	2
		5.00	2,894	66	2	9	0	2
		1.00	2,462	65	3	11	0	2
		0.50	2,279	61	3	12	0	2
		0.10	1,847	41	2	14	0	2
		0.01	1,268	26	2	20	1	5
	4	25.00	2,401	121	5	14	1	5
		10.00	2,052	93	5	15	1	6
		5.00	1,812	81	4	16	1	5
		1.00	1,325	77	6	20	1	5
		0.50	1,134	70	6	22	1	5
		0.10	759	55	7	26	1	4
	20	0.01	396	33	8	32	1	2
		25.00	1205	50	4	23	1	4
		10.00	948	34	4	24	1	5
		5.00	780	28	4	26	1	4
		1.00	482	22	5	29	1	3
0.50		387	19	5	30	1	3	
0.10		233	14	6	30	0	1	
0.01	127	8	7	26	0	1		

Table A-24. District 4 20 % RAP specimen SET 3 case complex modulus test data

Specimen Id	Temp	Frequency (Hz)	Dynamic Modulus (ksi)	STDEV	COVAR	Phase Angle (Deg)	STDEV	COVAR
D4-SET3-20	-10	25.00	3,551	129	4	7	0	1
		10.00	3,318	126	4	7	0	0
		5.00	3,137	125	4	8	0	0
		1.00	2,710	118	4	10	0	1
		0.50	2,523	113	4	10	0	1
		0.10	2,086	96	5	13	0	1
		0.01	1,493	72	5	17	0	0
	4	25.00	2,558	69	3	13	0	4
		10.00	2,270	32	1	14	0	1
		5.00	2,051	21	1	15	0	1
		1.00	1,552	12	1	18	0	0
		0.50	1,353	5	0	20	0	0
		0.10	944	4	0	24	0	0
	20	0.01	495	6	1	31	0	0
		25.00	1207	50	4	23	1	2
		10.00	969	37	4	24	0	1
		5.00	811	35	4	25	0	1
		1.00	514	23	5	29	0	1
0.50		417	20	5	30	0	0	
0.10		253	13	5	31	0	0	
0.01	136	6	4	28	0	1		

Table A-25. District 4 40 % RAP specimen SET 1 case complex modulus test data

	Temp	Frequency (Hz)	Dynamic Modulus (ksi)	STDEV	COVAR	Phase Angle (Deg)	STDEV	COVAR
D4-SET1-40	-10	25.00	4,385	593	14	6	0	3
		10.00	4,125	549	13	6	0	3
		5.00	3,946	517	13	6	0	4
		1.00	3,510	418	12	7	0	4
		0.50	3,314	380	11	8	0	4
		0.10	2,857	303	11	9	0	5
		0.01	2,215	230	10	12	1	5
	4	25.00	3,006	294	10	11	0	2
		10.00	2,683	284	11	11	0	2
		5.00	2,472	267	11	12	0	2
		1.00	1,984	214	11	14	0	2
		0.50	1,783	193	11	15	0	2
		0.10	1,335	139	10	19	0	2
	20	0.01	792	72	9	25	1	3
		25.00	1664	148	9	19	3	14
		10.00	1402	105	7	20	3	14
		5.00	1221	80	7	21	2	11
		1.00	854	49	6	31	13	43
0.50		718	39	5	27	4	16	
0.10		466	24	5	29	3	10	
0.01	240	17	7	31	2	6		

Table A-26. District 4 40 % RAP specimen SET 2 case complex modulus test data

Specimen Id	Temp	Frequency (Hz)	Dynamic Modulus (ksi)	STDEV	COVAR	Phase Angle (Deg)	STDEV	COVAR
D4-SET2-40	-10	25.00	3,916	226	6	6	1	19
		10.00	3,653	243	7	7	1	17
		5.00	3,448	241	7	7	1	12
		1.00	2,961	205	7	9	1	9
		0.50	2,741	198	7	10	1	9
		0.10	2,220	182	8	13	1	8
		0.01	1,511	128	8	18	1	6
	4	25.00	2,328	404	17	14	1	5
		10.00	2,011	323	16	15	1	4
		5.00	1,787	276	15	16	1	4
		1.00	1,311	208	16	20	1	4
		0.50	1,123	172	15	22	1	3
		0.10	753	102	14	26	1	2
		0.01	388	48	13	32	0	0
	20	25.00	1,128	100	9	24	1	5
		10.00	880	78	9	25	1	3
		5.00	724	68	9	26	1	3
		1.00	442	48	11	30	1	3
		0.50	352	42	12	31	1	3
		0.10	211	27	13	31	0	0
		0.01	113	14	12	27	1	3

Table A-27. District 4 40 % RAP specimen SET 3 case complex modulus test data

Specimen Id	Temp	Frequency (Hz)	Dynamic Modulus (ksi)	STDEV	COVAR	Phase Angle (Deg)	STDEV	COVAR
D4-SET3-40	-10	25.00	3,919	80	2	7	0	0
		10.00	3,654	69	2	8	0	1
		5.00	3,457	64	2	8	0	2
		1.00	2,978	48	2	10	0	5
		0.50	2,770	39	1	10	1	5
		0.10	2,282	23	1	13	1	6
		0.01	1,617	3	0	17	1	4
	4	25.00	2,642	39	1	13	1	6
		10.00	2,316	48	2	13	1	7
		5.00	2,080	53	3	15	1	7
		1.00	1,571	68	4	18	1	7
		0.50	1,364	67	5	20	1	7
		0.10	939	58	6	24	1	5
		0.01	491	30	6	31	0	1
	20	25.00	1,299	6	0	22	0	0
		10.00	1,045	12	1	23	0	1
		5.00	873	17	2	24	0	0
		1.00	550	14	3	28	0	0
		0.50	444	13	3	29	0	0
		0.10	268	9	3	30	0	1
		0.01	139	7	5	29	0	1

Table A-28. District 4 40 % RAP specimen SET 4 case complex modulus test data

Specimen Id	Temp	Frequency (Hz)	Dynamic Modulus (ksi)	STDEV	COVAR	Phase Angle (Deg)	STDEV	COVAR
D4-SET4-40	-10	25.00	3,833	317	8	5	1	22
		10.00	3,627	287	8	6	1	11
		5.00	3,470	272	8	7	1	11
		1.00	3,070	243	8	8	0	5
		0.50	2,899	232	8	8	1	6
		0.10	2,488	219	9	10	0	3
		0.01	1,869	208	11	13	1	8
	4	25.00	2,634	259	10	6	0	4
		10.00	2,367	263	11	6	0	7
		5.00	2,165	253	12	6	1	9
		1.00	1,712	219	13	7	1	11
		0.50	1,526	203	13	8	1	11
		0.10	1,122	158	14	9	1	9
		0.01	646	85	13	13	1	5
	20	25.00	1462	130	9	6	1	12
		10.00	1212	121	10	6	0	8
		5.00	1034	109	11	6	1	13
		1.00	690	79	11	7	1	18
0.50		569	67	12	8	1	18	
0.10		356	43	12	9	1	12	
0.01		182	22	12	13	1	6	

Table A-29. District 4 40 % RAP specimen SET 1 (w/ PG58-28) case complex modulus test data

Specimen Id	Temp	Frequency (Hz)	Dynamic Modulus (ksi)	STDEV	COVAR	Phase Angle (Deg)	STDEV	COVAR
D4-SET1-40 PG 58-28	-10	25.00	2,902	80	2	8	1	7
		10.00	2,653	69	2	9	1	12
		5.00	2,475	64	2	10	1	11
		1.00	2,068	48	2	12	1	11
		0.50	1,897	39	1	12	1	10
		0.10	1,516	23	1	15	1	8
		0.01	1,068	3	0	20	1	6
	4	25.00	2,199	39	1	13	0	0
		10.00	1,940	48	2	13	0	1
		5.00	1,757	53	3	14	0	1
		1.00	1,351	68	4	17	0	2
		0.50	1,189	67	5	18	0	2
		0.10	856	58	6	22	0	1
		0.01	492	30	6	28	0	0
	20	25.00	1078	6	0	22	1	3
		10.00	883	12	1	22	1	3
		5.00	747	17	2	24	1	2
		1.00	488	14	3	27	0	1
0.50		401	13	3	28	0	1	
0.10		256	9	3	29	0	1	
0.01		140	7	5	29	1	3	

## APPENDIX D MOISTURE SUSCEPTIBILITY TESTING DATA

Table A-30. District 1 Specimens Moisture Damage Study Specimen Volumetrics and IDT Strength Results

	[1]	[2]			[3]	[2]X[3]/100	[5]	[5]-[1]	[6]	[7]	[8]	[9]	
	Mdry (g)	Volume (cm3)	VMA	VFA	Air Voids %	Air Voids (cm3)	SSD (g)	Absorbed Water (cm3)	Saturation %	Thickness (mm)	Max Load (lbs)	Tensile Strength (psi)	Notes
D1-00-1	3838	1647	17.3	58.7	7.1	118				95.9	3397	97.0	
D1-00-2	3836	1650	17.5	57.8	7.4	122	3930	94	77.4	96.0	1914	54.6	
D1-00-3	3849	1647	17.0	59.7	6.9	113				95.7	3353	95.9	
D1-00-4	3849	1636	16.5	62.1	6.2	102	3931	81.6	79.9	95.1	2211	63.7	outlier
D1-00-5	3840	1644	17.1	59.4	6.9	114	3926	86.5	75.7	95.4	2086	59.9	
D1-00-6	3844	1631	16.3	62.8	6.1	99				94.8	3456	99.8	outlier
<b>TSR</b>												<b>59.3</b>	
D1-20-1	3821	1645	18.1	61.8	6.9	114	3906	84.1	73.8	95.9	2763	78.9	
D1-20-2	3815	1651	18.6	59.9	7.5	123				96.5	3823	108.5	
D1-20-3	3820	1656	18.7	59.5	7.6	125				96.7	3850	109.0	
D1-20-4	3816	1649	18.4	60.5	7.3	120				96.4	3699	105.1	
D1-20-5	3804	1653	18.9	58.7	7.8	129	3896	91.7	71.0	96.7	2307	65.3	outlier
D1-20-6	3823	1658	18.7	59.3	7.6	126	3910	86.8	68.7	96.9	2468	69.7	outlier
<b>TSR</b>												<b>73.3</b>	
D1-40-1	3844	1654	18.6	58.2	7.8	128				96.1	4441	126.5	outlier
D1-40-2	3846	1632	17.5	62.8	6.5	106				96.3	5252	149.4	
D1-40-3	3855	1646	17.9	60.8	7.0	115	3934	79.1	68.5	96.0	3752	107.0	outlier
D1-40-4	3850	1645	18.0	60.5	7.1	117	3932	82	70.1	96.0	3599	102.7	
D1-40-5	3853	1646	18.0	60.6	7.1	116	3937	83.7	71.9	95.9	3454	98.6	
D1-40-6	3846	1640	17.8	61.3	6.9	113				96.0	5187	147.9	
<b>TSR</b>												<b>67.7</b>	

Table A-31. District 4 Specimens Moisture Damage Study Specimen Volumetrics and IDT Strength Results

	[1]	[2]			[3]	[2]X[3]/100	[5]	[5]-[1]	[6]	[7]	[8]	[9]	
	Mdry (g)	Volume (cm3)	VMA	VFA	Air Voids %	Air Voids (cm3)	SSD (g)	Absorbed Water (cm3)	Saturation %	Thickness (mm)	Max Load (lbs)	Tensile Strength (psi)	Notes
D4-00-1	3852	1648	16.9	56.2	7.4	122				95.9	2420	69.1	
D4-00-2	3851	1632	16.2	59.5	6.5	107	3930	79.1	74.0	95.4	1745	50.1	
D4-00-3	3855	1644	16.7	57.3	7.1	117	3945	89.8	76.9	96.0	2003	57.1	
D4-00-4	3849	1632	16.2	59.4	6.6	107				95.2	2691	77.4	
D4-00-5	3851	1626	15.8	60.9	6.2	101				95.0	2774	80.0	outlier
D4-00-6	3847	1630	16.1	59.6	6.5	106	3927	80	75.3	95.1	2061	59.3	
<b>TSR</b>												<b>75.8</b>	
D4-20-1	3809	1643	17.9	58.6	7.4	121	3903	94.1	77.6	96.1	2317	66.0	
D4-20-2	3812	1644	17.8	58.7	7.4	121				96.0	2833	80.8	
D4-20-3	3799	1604	16.1	66.3	5.4	87				93.9	3475	101.3	outlier
D4-20-4	3815	1631	17.2	61.5	6.6	108	3897	81.7	75.9	95.4	2387	68.5	
D4-20-5	3813	1652	18.2	57.1	7.8	129	3912	99.7	77.1	96.1	1845	52.6	outlier
D4-20-6	3813	1658	18.5	56.0	8.1	135				96.2	2803	79.8	outlier
<b>TSR</b>												<b>83.2</b>	
D4-40-1	3798	1644	18.6	59.3	7.6	124				96.0	3715	106.0	outlier
D4-40-2	3806	1630	17.7	62.8	6.6	107				96.0	3927	112.0	
D4-40-3	3804	1631	17.8	62.5	6.7	109	3884	79.9	73.4	95.5	3237	92.8	
D4-40-4	3810	1624	17.3	64.5	6.2	100				95.1	3998	115.1	outlier
D4-40-5	3806	1634	17.9	62.0	6.8	111	3887	81.5	73.3	96.0	3028	86.4	
D4-40-6	3798	1628	17.8	62.6	6.7	108	3879	80.4	74.2	95.2	3199	92.0	
<b>TSR</b>												<b>80.7</b>	

